Title
Synthesis and Biological Evaluation of Acid-Degradable Polymeric Materials for Pulmonary Gene Delivery

Author
Cohen, Jessica Lynn

Publication Date
2011

Peer reviewed|Thesis/dissertation

Synthesis and Biological Evaluation of Acid-Degradable Polymeric Materials for Pulmonary Gene Delivery

by

Jessica Lynn Cohen

A dissertation submitted in partial satisfaction of the

requirements for the degree of

Doctor of Philosophy

in

Chemistry

in the

Graduate Division

of the

University of California, Berkeley

Committee in charge:

Professor Jean M. J. Fréchet, Chair
Professor T. Don Tilley
Professor David V. Schaffer

Spring 2011

Synthesis and Biological Evaluation of Acid-Degradable Polymeric Materials for Pulmonary Gene Delivery

Jessica Lynn Cohen

Abstract

Synthesis and Biological Evaluation of Acid-Degradable Polymeric Materials for Pulmonary Gene Delivery

by

Jessica Lynn Cohen

Doctor of Philosophy in Chemistry

University of California, Berkeley

Professor Jean M. J. Fréchet, Chair

RNA interference (RNAi) represents a promising method for the treatment and prevention of disease. Due to the tremendous potential of RNAi as a therapeutic strategy, there has been significant interest in the development of delivery vehicles which could efficiently deliver siRNA and reduce the expression of a protein of interest. Unfortunately, translation of the potential of siRNA into the clinic is limited by the lack of safe and effective delivery systems. Because of their tunability and synthetic addressability, acid-degradable polymeric materials represent a promising approach for the delivery of siRNA and are the subject of this dissertation. Acid-sensitive systems have particularly desirable characteristics, as payload release can be triggered in response to endosomal acidification upon uptake. In particular, we describe the development, functionalization, and biological evaluation of biodegradable polymer systems which can efficiently deliver siRNA therapeutics to non-phagocytic cells. Specific emphasis is placed on the development of materials that have optimal physicochemical properties for pulmonary delivery.

Chapter 1 introduces various delivery strategies for siRNA therapeutics and discusses the basics of RNA interference. Additionally, the field of polymeric particulate siRNA carriers is reviewed, with an overview of relevant design criteria for materials intended for pulmonary administration. The advantages of systems capable of triggered payload release are discussed, with an emphasis on acid-sensitive carrier systems. Two acid-sensitive particle systems developed by our group are described.

In Chapter 2, the synthesis of acid-sensitive, acrylamide-based microparticles containing a cell-penetrating peptide (CPP) is discussed. Particles functionalized with a polyarginine CPP are prepared and evaluated for their ability to deliver a model therapeutic payload to non-phagocytic cells. The importance of CPP incorporation on cellular uptake *in vitro* is investigated in lung epithelial cells. The modification of the microparticles with CPPs greatly improved their uptake by non-phagocytic cells in culture without inducing any cytotoxic effects.

Chapter 3 discusses the role of particle size and functionalization with cationic CPPs on pulmonary delivery using hydrogel particles. The optimal particle design parameters for pulmonary delivery are investigated and the fate of model particles following intratracheal administration is studied by several techniques. Particles are characterized to determine their *in*

vivo behavior in terms of lung retention, localization within specific cell types, and potential for inducing inflammatory responses. We found that altering both size and surface functionalization significantly affected the *in vivo* behavior of the particle system.

In Chapter 4, we describe the synthesis of a second-generation biocompatible, acid-sensitive particle system for siRNA delivery. The synthesis of spermine-modified acetalated-dextran (Spermine-Ac-DEX) is presented and the preparation of particles with high siRNA loading efficiency is described. The ability of these particles to silence protein expression *in vitro* is investigated. Spermine-Ac-DEX particles demonstrated efficient gene knockdown in a model cell line with minimal toxicity.

Chapter 5 investigates the synthesis and biological evaluation of functionalizable, acetal-modified dextran, a modular system with tunable functionality, degradation rate, and degree of modification. The preparation of acid-degradable, amine-functionalized dextran is described and the role of type of amine modification (primary, secondary, or tertiary amine) and degradation rate on the efficacy of siRNA delivery is studied *in vitro*. Altering both the type of amine as well as the degradation rate significantly affected the transfection efficiency. We found that two of the amine-dextrans were able to efficiently deliver siRNA and lead to gene silencing in HeLa-*luc* cells.

Table of Contents

Acknowledgements

This doctoral work would not have been possible without the help of many people. I would like to start by thanking my advisor, Professor Fréchet, for his guidance and support during my Ph.D. studies. He has helped me grow both personally and professionally. Thank you for helping me to achieve my dreams.

I would also like to acknowledge all of the members of the Fréchet group, past and present. You have all helped me in so many ways. Thank you for making my time in Berkeley so enjoyable. In particular, I would like to thank my mentor, Adah Almutairi, for all of her advice and for training me. She is not only a terrific mentor but also a great friend. In addition, I wish to thank Joel Cohen, who taught me most of what I know about particles and cell culture. I would also like to thank a number of people who have collaborated with me over the years: Lina Cui, Stephanie Schubert, Peter Wich, Tristan Beaudette, and Kyle Broaders. I have greatly enjoyed working with each of you. Finally, I would like to thank Jill Millstone for all of her career advice and for always making me smile.

It has been my pleasure to mentor an outstanding undergraduate student, Sunil Joshi. Thank you for making the past two years in lab so much fun. I would also like to thank all of my former and current labmates, Andrew Goodwin, Terence Choy, Daniel Kahakeaw, Derek van der Poll, Paul Kierstead, and Heidi Kieler-Ferguson. Thank you for making lab such a great place to work. I would also like to thank Cezar Ramiro and Chona de Mesa for all of their support during my graduate studies. I wish the best for everyone in the Fréchet lab and your families in your future endeavors.

I would like to thank our PEN collaborators for their many contributions to this research. Professors Karen Wooley and Michael Welch have been great sources of knowledge and I appreciate all of their help throughout my graduate studies. In addition, I would like to thank Dr. Dan Schuster, Dr. Steven Brody, and Dr. Carolyn Cannon for their assistance and contributions to several of the projects that I have worked on within the PEN. Matt Bernstein, Yongjian Liu, Aida Ibricevic, and Sean Gunsten have helped evaluate the microparticles that I prepared by conducting *in vitro* and *in vivo* experiments. Finally, I would like to acknowledge Eileen Cler for making the PEN run smoothly.

Most importantly, I would like to thank my family; without their love, support, and encouragement none of this would be possible. My parents taught me everything that I know. Mom and Dad, thank you for always believing in me and encouraging me to reach for the stars. Even though I may not say it very often, I truly appreciate everything that you do for me. Allison and Larissa are not only my sisters, but also my best friends. Thank you for always being there for me and for making everything in life so much fun. I am so proud of both of you and look forward to many more exciting journeys ahead. I love you all very much.

Chapter 1 – Polymeric Materials Used in Gene Delivery Applications

Abstract

Gene therapy has enormous potential for the treatment or prevention of various diseases, including cancer, viral infections, and a number of inherited and acquired diseases. RNA interference (RNAi), in particular, has emerged as a promising therapeutic strategy for the treatment of diseases that are otherwise "undruggable" with current therapeutic technology. The discovery that synthetic small interfering RNA (siRNA) could achieve sequence-specific gene knockdown in mammalian cells by exploiting the RNAi machinery has lead to a surge of research using RNAi in therapeutic applications. However, the widespread use of siRNA for disease prevention and treatment is hindered by the lack of clinically suitable, safe, and effective delivery vehicles. This chapter introduces the concept of RNA interference and gives an overview of the mechanism of RNAi and some of the obstacles to efficient delivery of siRNA therapeutics. A brief discussion of various strategies currently under investigation for the delivery of siRNA is presented, and the field of pulmonary delivery is reviewed. In particular, this chapter focuses on the design of novel polymeric particulate carriers for the encapsulation and intracellular delivery of siRNA. We describe the development of advanced particulate systems capable of releasing their cargo in response to specific stimuli present in the intracellular environment, with an emphasis on acid-degradable systems. Finally, we highlight some of the current clinical trials being performed using siRNA for the treatment of human disease.

Introduction

RNA interference (RNAi) has gained significant attention since its discovery about 20 years ago. The first study to describe the phenomenon of RNAi appeared in 1998 when Andrew Fire and Craig Mello reported the ability of double-stranded RNA to silence gene expression in the nematode worm *Caenorhabditis elegans*.[1] RNAi was rapidly developed as a tool to study gene function, and was found to occur in protozoa and almost all higher eukaryotes tested.[2,3] In 2001, Tuschl *et al*. published a landmark paper demonstrating that synthetic small interfering RNA (siRNA) could achieve gene knockdown in a mammalian cell line[4] and the first successful use of siRNA for gene silencing in mice was achieved for a hepatitis C target shortly thereafter.[5] In 2006, the Nobel Prize in Physiology and Medicine was awarded to Fire and Mello for their groundbreaking discovery of RNAi. Because of its significant potential in a wide range of disciplines, RNAi is viewed as one of the most important recent discoveries in biology.[6]

RNAi is a powerful research tool for the elucidation of gene function in both health and disease. Besides the analysis of the function of individual genes, RNAi is now widely used in high-throughput screens in both basic and applied biology.[7,8] Several RNAi screens have been conducted using long dsRNA in *C. elegans* and *Drosophila melanogaster*.[9-18] These screens have identified genes involved in fundamental processes such as cell division, apoptosis and cell morphology, and physiological processes such as fat metabolism. The sequencing of the human genome has catalogued most of the genes expressed in humans. This sequencing information has opened up the potential to silence almost any gene in the human genome. Thus, RNAi can be used to provide a direct causal link between gene sequence and functional data in the form of

targeted loss-of-function phenotypes.[19] Large scale RNAi screens conducted in mammalian tissue culture cells have identified genes involved in apoptosis, signaling, cell division, and regulation of protein stability.[20-23] In addition, because RNAi allows for the rapid and efficient suppression of the expression of any protein in almost any type of cell, its use can expedite the evaluation of candidate targets for drug development.[24-26]

In addition to its use as a tool in basic research and drug target validation, RNAi is an attractive therapeutic strategy for the treatment of a variety of diseases, including viral infections, cancer, as well as inherited and acquired diseases. Many of these diseases are characterized by the inappropriate activity of specific genes, and the selective silencing of such genes using RNAi represents a potential therapeutic strategy. The first proof-of-principle experiment demonstrating the therapeutic potential of siRNA showed that delivery of siRNA targeting Fas could protect mice from fulminant hepatitis.[27] Since this first report, a large number of publications demonstrating the successful application of RNAi in the treatment of disease have been published.[28-35] It has been reported that synthetic siRNAs are capable of knocking down targets in various diseases *in vivo*, including liver cirrhosis, hepatitis B virus (HBV), human papillomavirus, ovarian cancer, and bone cancer.[36] However, the major challenge in the clinical translation of RNAi is effective delivery.

A variety of strategies have been reported for the delivery of siRNA-based therapeutics (see below). In this chapter, we focus on polymeric particulate vehicles used for the delivery of siRNA, with a focus on strategies for effective pulmonary delivery. We first give a brief overview of the rapidly growing field of RNA interference, including a review of the basics of RNAi and some of the challenges faced. We present an overview of some other delivery strategies under investigation for the delivery of siRNA. In addition, we highlight novel polymers and materials that have been designed to overcome several of the obstacles to efficient siRNA delivery. We conclude with a summary of the current clinical trials being performed using siRNA for the treatment of a variety of diseases in humans.

Overview of RNA interference (RNAi)

RNA interference (RNAi) has drawn much attention in the field of medicine due to its potential for treating chronic diseases and genetic disorders by harnessing the endogenous RNAi pathway.[37-39] RNAi is a post-transcriptional biological mechanism wherein double-stranded RNA (dsRNA) inhibits gene expression in a sequence-dependent manner through degradation of the corresponding mRNA.[40-43] Once the dsRNA is present in the cytoplasm of the cell, it is shortened and processed by the RNAse III enzyme, Dicer, resulting in a 21-23 nucleotide (nt) dsRNA duplex with symmetric 2- to 3-nt 3' overhangs.[44-46] Subsequently, the dsRNA is incorporated into a multi-subunit protein complex called the RNA-induced silencing complex (RISC).[47] One of the two strands of the short, double-stranded RNA is cleaved, and the activated RISC (which contains the guide strand of the RNA) binds to a complementary sequence of mRNA and results in its degradation.[48] The activated RISC is capable of multiple rounds of mRNA cleavage, which propagates gene silencing.[49] Due to its potential to silence genes in a sequence-specific manner, RNAi holds promise for treating many diseases that may not otherwise be accessed with current therapeutic technology.[50]

Various approaches have been developed that allow for exploitation of the RNAi process. In mammalian cells, RNAi can be triggered by exogenous synthetic small interfering RNA (siRNA), double-stranded RNAs that are typically 19-23 base pairs in length.[4,51] They guide the degradation of the cognate mRNA sequence, thus inhibiting the production of the corresponding

protein. Synthetic siRNA can be designed to target nearly any gene in the body, and is therefore attractive for a variety of medical applications. Previous reports have demonstrated that synthetic siRNAs are capable of knocking down targets in several diseases *in vivo*, including hepatitis B virus, human papillomavirus, and ovarian cancer.[36] Despite great therapeutic potential, the clinical application of siRNA is limited by delivery problems.

Extracellular and Intracellular Barriers to the Efficient Use of siRNA

A number of extracellular and intracellular barriers limit the use of siRNA as a therapeutic agent. The extracellular barriers to siRNA delivery depend upon the route of administration (e.g. intravenous, intranasal, intratracheal, subcutaneous, etc.) which, in turn, depends upon the targeted disease. One of the major barriers to efficient siRNA delivery is the lack of stability under *in vivo* conditions due to rapid degradation by serum nucleases and enzymes.[52] Even after reaching its target tissue, siRNA faces several barriers to efficient gene silencing. siRNA does not cross cellular membranes efficiently due to its relatively large size, negative charge, and hydrophilicity. Endocytosis is the main cellular uptake pathway used in the delivery of siRNA. However, in order to perform its function, siRNA needs to escape from the endosomal compartment and reach the cytoplasm of the cell where it can associate with the RISC complex. In addition, during the process of endosomal trafficking, the siRNA is exposed to degradative enzymes, including nucleases. Therefore the therapeutic siRNA must be able to exit from the endosomes/lysosomes before it is degraded. Thus, the widespread use of RNAi therapeutics for disease prevention and treatment requires the development of clinically suitable, safe, and effective delivery vehicles.[36] Even though significant advances have been made in the field, the development of vehicles that can efficiently deliver RNAi therapeutics both *in vitro* and *in vivo* remains a major challenge.

Characteristics of an Ideal Delivery System for siRNA

There are obviously a large number of challenges and parameters to consider when designing a delivery system for siRNA delivery. Here we outline a set of guiding principles to keep in mind when developing a new vector. In order to induce effective RNAi, these vehicles must overcome a variety of extracellular and intracellular obstacles. They should provide protection against nuclease activity and facilitate internalization and intracellular trafficking of the siRNA.[53] The vector should facilitate endosomal escape of the siRNA into the cytoplasm, the site of action of the RNAi machinery. Once in the cytoplasm, the carrier should dissociate from the siRNA to allow for binding to the RISC complex. This can be accomplished by using a vector that is responsive to either external or internal stimuli. Ideally the vector will be cost effective to produce and not cause any unwanted toxicity or immunogenicity. Finally, the carrier should be composed of biocompatible/biodegradable materials that can be readily cleared from the body.

Differences from DNA Delivery

Studies in non-viral DNA gene therapy have been ongoing for years and many of the delivery systems designed for DNA delivery are being adapted to siRNA delivery. Although siRNA and plasmids can be applied to achieve similar functional outcomes, siRNA and plasmids have major intrinsic structural differences.[54] For example, while plasmids often involve several thousand base pairs, siRNA is typically much shorter, usually 19-23 base pairs in length. In

addition, the persistence length (the length scale over which the chains behave as rigid rods) of double-stranded DNA and RNA is different. While the persistence length of dsDNA is ~50 nm, that of double-stranded RNA is ~70 nm, making RNA a stiffer molecule.[55] Due to their structural differences and because the site of action of siRNA is the cytosol and not the nucleus, as in the case of DNA, carriers that are shown to effectively deliver plasmids are not necessarily optimal for siRNA transfection, and vice versa. Therefore, the successful delivery of siRNA requires unique considerations and strategies.[55,56]

Delivery Strategies for siRNA

Given the potential of siRNA in both basic research and medical applications, a variety of strategies have been developed for its delivery. Presented in the following sections are some examples of strategies used in the delivery of siRNA both *in vitro* and *in vivo*. Each of these delivery strategies has advantages and disadvantages, respectively, and the choice of an appropriate delivery vector should be based on the intended target organ and disease. Significant progress has been made in the delivery of siRNA therapeutics as evidenced by a number of clinical trials being performed using siRNA (see below). Despite these advances, several challenges to the clinical translation of siRNA remain and, thus, motivate the investigation of alternative siRNA delivery systems that may be able to overcome these obstacles. A particularly attractive delivery strategy is the use of polymeric materials and polymer-based microparticles. The design, synthesis, and biological evaluation of acid-degradable polymeric materials for siRNA delivery is the subject of the remaining chapters of this work. Therefore, we conclude this section with an overview of two acid-degradable particle systems developed in our laboratory.

Chemical Modification of siRNA

Chemically-modified siRNA can be used to overcome many of the challenges associated with the successful delivery of siRNA, including short half-life *in vivo*, biodistribution, and potency.[57] A wide variety of modifications to the backbone, base, and sugar of the siRNA have been reported so far.[37,39,58-62] Numerous reports have demonstrated that chemically-modified siRNAs can silence endogenous genes both *in vitro* and *in vivo*, and there are several reviews that cover the use of modified siRNAs.[57,63,64] The most promising siRNA conjugates for siRNA delivery *in vivo* involve the attachment of cholesterol or aptamers to one of the RNA strands. For example, conjugation of siRNA to cholesterol or other lipid-like moieties can promote distribution and cellular uptake of the siRNA and lead to efficient gene silencing *in vivo*.[65-67] Aptamers can be attached to siRNA to target delivery to specific cells *in vivo*.[68,69] Promising *in vitro* and *in vivo* results have been obtained using siRNA directly linked to a prostate-specific membrane antigen aptamer.

Viral Vectors

Viral-based vectors have been widely studied for the delivery of genetic material due to their relatively high transfection efficiency compared to non-viral vectors. Such high efficiency is due to the fact that viruses have evolved biological mechanisms that allow them to efficiently enter and deliver their genetic material to target cells. The most common viral vectors for delivery of RNAi therapeutics include adenoviral,[70,71] lentiviral,[72,73] and retroviral vectors.[74,75] Although viral vectors are very efficient, they can cause immunogenic and inflammatory responses,[76,77] which raise concerns about their safety as delivery vectors. This has led to increasing research efforts focused on the design of efficient non-viral delivery systems. Non-

viral vectors provide opportunities for improved safety, greater flexibility, and more facile manufacturing.

Dendrimer-Based Vectors

The most widely studied dendrimer-based vector for siRNA delivery is the polyamidoamine (PAMAM) dendrimer.[78-82] Early studies with PAMAM dendrimers demonstrated that increasing the dendrimer generation significantly enhanced siRNA delivery efficiency, however, also increased cytotoxicity. Since then, several groups have evaluated the influence of a variety of modifications on the cytotoxicity and transfection efficiency of PAMAM dendrimers.[80-82] Modified PAMAM dendrimers often display improved transfection efficiencies and reduced cytotoxicity compared to unmodified PAMAM dendrimers.

Several other dendrimer-based vectors have been described in the literature.[83-85] Since a large diversity of modifications exist to alter the properties of dendrimers, the development of structure-activity relationships will aid in the design of optimal dendrimers for siRNA delivery.[85-87] In contrast to the non-covalent interactions of siRNA with cationic dendrimers, Hamilton *et al*. recently described the use of a dendritic molecular transporter (MT) for the efficient delivery of siRNA.[88] This system utilizes a cleavable disulfide bond to attach the siRNA covalently to the dendrimer, allowing for controlled release once it has been delivered to the reducing environment of the cytosol in a cell. The MT delivery system resulted in significant reduction of the target protein for a range of conjugate concentrations.

Lipid-Based Vectors

Both liposomes and lipoplexes have been extensively investigated for the delivery of siRNA both *in vitro* and *in vivo*.[89-92] Liposomes consist of an aqueous compartment enclosed in a phospholipid bilayer with hydrophilic drug entrapped in the center aqueous layer.[93] In contrast, lipoplexes are spontaneously formed via interaction of cationic lipids with anionic siRNA. Several commercially available cationic lipid delivery systems, including Lipofectamine (Invitrogen), TransIT TKO (Mirus), RNAifect (Qiagen), and Lipofectin have been investigated for the delivery of siRNA *in vitro*. Liposomes have been used for the delivery of nucleic acids for over 20 years,[94] and the use of lipid complexes for localized siRNA administration (ie. delivery to the eye, tumors, or mucosal surfaces) has also been successful.[36,37]

Recently, two groups reported promising results of delivery of siRNA to the liver using cationic lipids.[95,96] Semple *et al*. used a rational design approach based on structure-activity relationships.[95] They started with the ionizable cationic lipid 1,2-dilinoleyloxy-3-dimethylaminopropane (DLinDMA), which was a key lipid component of "stable nucleic acid lipid particles" (SNALP).[97,98] The lipid was separated into three functional moieties (the alkyl chain, a linker, and an amine-based head group), and each of these was individually optimized for superior siRNA delivery performance. The best performing lipid, DLin-KC2-DMA, demonstrated *in vivo* activity at siRNA doses as low as 0.01 mg/kg in rodents and 0.1 mg/kg in non-human primates. This represents a substantial improvement over the unoptimized SNALP. By contrast, Love *et al*. used a combinatorial library approach to identify novel lipids.[96] They synthesized a library of lipid-like materials, termed "lipidoids", using epoxide chemistry. The best performing lipidoid, C12-200, enabled siRNA-directed liver gene silencing at doses as low as 0.01 mg/kg in mice and 0.03 mg/kg in non-human primates. The unprecedented low-dose delivery achieved by these groups demonstrates the potential utility of lipid-based vectors for siRNA delivery.

Polymeric Vectors

Polymer-based materials are attractive as they allow for advanced synthetic and conjugation chemistry. Polymer chemistry offers the capacity to generate a wide variety of particles with diverse modifications providing unique possibilities for siRNA delivery. The most common polymer-based vectors involve complexes (polyplexes) formed between cationic polymers and siRNA through electrostatic interactions between the negative phosphates along the nucleic acid backbone and the positive charges displayed on the vector.[52,99-101] One of the most-widely studied synthetic cationic polymers for siRNA delivery is polyethylenimine (PEI).[102-104] Although PEI is an efficient delivery vector both *in vitro* and *in vivo*, it is limited by high toxicity and limited biodegradability. In addition, PEI has been shown to trigger necrosis and apoptosis in a variety of cell lines.[105] A variety of modifications to PEI have been introduced to reduce the toxicity, including conjugation to more biocompatible polymers, such as PEG, and amine modification.[106,107]

Besides complexation, siRNA can also be conjugated directly to polymers for delivery.[108-111] One example of this approach is called Dynamic PolyConjugates.[108] Key features of the Dynamic PolyConjugate technology include a membrane-active polymer, the ability to reversibly mask the activity of this polymer until it reaches the acidic environment of the endosome, and the ability to target the polymer specifically to hepatocytes after intravenous injection. The siRNA cargo is attached to the polymer through a reversible disulfide linkage. This system demonstrated effective knockdown of two endogenous genes in mouse liver. The knockdown resulted in phenotypic changes consistent with the known function of the proteins. Dynamic PolyConjugates were non-toxic and well tolerated in mice.

Particle-based Systems

Various particle systems have been developed for siRNA delivery, including quantum dots,[112,113] gold nanoparticles,[114,115] magnetic nanoparticles,[116,117] and carbon nanotubes.[118-120] Many of these studies demonstrate the importance of releasing the siRNA from the carrier system for subsequent gene silencing.[113,118] For example, Dai *et al*. described the modification of single-walled carbon nanotubes (SWNTs) with siRNA via a cleavable disulfide linkage. These constructs showed higher gene knockdown levels when compared with a thioether linked analogue. The authors attribute this higher silencing efficiency to active release of the siRNA, thus maximizing the endosome/lysosome escape. In addition, the siRNA may be less perturbed when in a free form than when attached to the SWNT surface.

Polymeric Particles as Delivery Vehicles

As an alternative to the delivery strategies described above, particles made from biodegradable and non-toxic materials have been explored as *in vivo* gene delivery vectors. Polymeric particles are promising siRNA delivery vehicles due to their synthetic addressability, tunability, and their ability to integrate multiple functions into a single carrier system. For example, particles can be prepared that protect the encapsulated cargo from physical and chemical damage, release the siRNA at specific rates and under certain physiological conditions, and localize to specific parts of the body through modification of the surface with certain targeting groups. The following sections describe the development of polymer-based particles for siRNA delivery with an emphasis on stimuli-responsive materials.

PLGA Particles

By far, the most studied material for use in polymeric nano- and microparticulate siRNA delivery vehicles is poly(lactic-co-glycolic acid) (PLGA).[121-126] PLGA is an FDA approved material with an impressive safety record associated with its use in resorbable sutures and implantable devices. PLGA is commercially available from a number of suppliers, and this accessibility has led to an enormous amount of research by investigators in the fields of engineering, materials science, and pharmaceutical science. However, several significant challenges exist with the use of PLGA in siRNA delivery vehicles. One major problem involves the low encapsulation efficiency of siRNA in PLGA particles. Due to the negative charge of PLGA and the relatively small size of siRNA, siRNA is not easily incorporated into particles prepared from PLGA by standard emulsion techniques. Additionally, it is well known that PLGA particles suffer from an initial "burst release" phase followed by a slow release of the remainder of the encapsulated cargo, typically over the course of several weeks. To overcome these limitations, several research groups have studied the addition of cationic polymers[122,125] or small molecules[121] to improve siRNA loading in particles as well as better control the siRNA release profile. Various PLGA-based siRNA delivery systems have been reported in the literature and the *in vivo* application of these materials is an area of ongoing research.

Stimuli-Responsive Particle Systems

In contrast to PLGA, which was originally designed to degrade slowly in the body, there exist a number of polymeric delivery systems which have been engineered to rapidly release their cargo under specific biological conditions.[127,128] For the purpose of delivering siRNA therapeutics, the most relevant stimuli for release include acidic and oxidizing environments, both of which are found in phagolysosomal compartments. These systems facilitate the release of siRNA from the endolysosomal compartment and delivery to the cytosol of the cell, where the siRNA can enter the RNAi pathway and lead to reduction in protein expression. The rate of payload release under the conditions of interest is an important parameter to consider and could be useful in optimizing the transfection efficiency as well as the duration of gene silencing. The slow and sustained release of siRNA from PLGA has been proposed as a method to prolong gene silencing after siRNA delivery.[121] This might be especially important for the delivery of siRNA to tumor cells, which exhibit rapid growth with doubling times in the order of only a few days.[129] However, slow degradation and release of siRNA over the course of weeks to months may not be ideally suited for biological application. For example, Nguyen *et al*. described a fast-degrading polyester material that can efficiently deliver siRNA for pulmonary gene therapy.[130] The rapid biodegradability led to improved biocompatibility and most likely contributed to a rapid release of the siRNA inside the cytosol. Thus, in some cases, the use of stimuli-responsive particle systems may provide more efficient gene silencing compared to slow-release systems.

Oxidation-Sensitive Delivery Vehicle

Reactive oxygen species (ROS) have emerged as important components of both physiological and pathological states of living organisms.[131-133] Elevated levels of ROS and down-regulation of ROS scavengers and antioxidant species are associated with various human diseases, including cancer.[134,135] Due to its high reactivity and cytotoxicity, ROS has also been implicated in diabetes,[136,137] atherosclerosis,[138] chronic inflammation,[139] viral infection,[140] and ischemia-reperfusion injury,[141] as well as various neurodegenerative diseases,[142,143] like Parkinson's and Alzheimer's. ROS is not always harmful, however, as the controlled release and

compartmentalization of ROS is crucial to maintaining normal physiology. For example, macrophages engulf invading pathogens into phagocytic vesicles and then produce a variety of ROS inside the vesicles to help neutralize the threat.[131] Given the implication of ROS in health, aging, and disease, novel materials that respond to oxidative conditions may be useful in the delivery of diagnostic and/or therapeutic agents.

One such oxidation-sensitive polymeric particle system has been developed by Wilson *et al*., and is based on thioketal-containing polymers.[144] The thioketal nanoparticles (TKNs) are formulated from poly-(1,4-phenyleneacetone dimethylene thioketal) (PPADT), a polymer composed of ROS-sensitive thioketal linkages that are stable to acid-, base- and protease-catalyzed degradation. Orally delivered TKNs are expected to be stable in the gastrointestinal tract. However, at sites of intestinal inflammation, where infiltrating phagocytes produce unusually high levels of ROS, the TKNs degrade allowing the selective release of siRNA to the inflamed tissues. Indeed, PPADT was shown to degrade when incubated in a superoxide solution and nanoparticles formulated from the polymer released their payloads in response to ROS produced by activated macrophages. Orally administered TKNs loaded with TNF-α siRNA were able to reduce TNF-α mRNA levels in the colon and protect mice from ulcerative colitis. The importance of the oxidation-sensitive degradation mechanism was demonstrated by comparison of the efficacy of TKNs to that of PLGA nanoparticles and β-glucan particles. These experiments showed that the greater stability of the TKNs over that of PLGA nanoparticles to a simulated gastrointestinal environment as well as their ability to localize the siRNA release to inflamed tissues are important factors in their improved efficacy.

Acid-Sensitive Delivery Vehicles

Another approach that has been recently investigated is to use some form of acid-sensitive modification that enables the particles to remain stable at extracellular pH, but rapidly degrade in response to a decrease in environmental pH. A mildly acidic environment is associated with several disease states, including cancer,[145-147] inflammation,[148,149] and acute lung injury. In addition, when taken up by cells, particles encounter mildly acidic conditions present in endosomal vesicles, which can trigger cargo release.[150-153] Thus, pH-sensitive materials are attractive for many drug delivery applications.

Polymeric particles that respond to the near 250-fold difference in proton concentration between physiological (pH 7.4) and phagolysosomal (pH ~5.0) conditions have been investigated as materials for the controlled delivery of genetic material. In general, these vehicles are prepared from (1) polymers that contain amine groups that become protonated at pH values near 5.0 or (2) neutral polymers that contain hydrolyzable linkages which degrade significantly faster under acidic conditions compared to physiological conditions. Examples of the two types of pH-sensitive siRNA delivery vehicles and their biological evaluation are discussed below in more detail.

Acid-sensitive carriers based on amine-containing polymers

Acid-sensitive carriers based on the first type of material rely on the protonation of the amine moieties incorporated in the polymer structure. To obtain a pH-sensitive material that specifically targets phagolysosomal conditions, the pK_a of the protonated amine moieties should be approximately 5-7 such that the polymer is not significantly protonated under physiological conditions (pH 7.4), but becomes readily ionized in the phagosomal compartment (~ pH 5). Beyond an increase in charge, protonation may also cause the polymeric vehicle to swell or

become water-soluble due to an increase in hydrophilicity compared to the uncharged material. Delivery vehicles of this type have been extensively studied for gene delivery due to their ability to disrupt endosomes/phagosomes and deliver their associated cargo to the cytoplasm of a cell.[101,154] The proposed mechanism for cytoplasmic delivery is often referred to as the "proton sponge effect," in which the buffering capacity of amine-containing materials is thought to increase chloride counter ion concentrations, and thus the osmotic pressure in vesicles undergoing acidification, which ultimately leads to membrane destabilization and leakage of its contents into the cytoplasm.[155-157]

Poly(β-amino esters) (PBAE) are one class of acid-sensitive cationic polymer that may be used for pH-dependent siRNA release. PBAEs are synthesized through Michael addition of amine- and acrylate-terminated monomers.[158-160] Due to the ease of synthesis, large libraries of PBAEs have been synthesized and evaluated for their ability to deliver genetic material. PBAEs become protonated at lower pH and thus become soluble. However, PBAEs are polycationic under acidic conditions and must be blended with biocompatible polymers to reduce their toxicity. Yadav *et al*. reported the preparation of poly(ethylene oxide)-modified PBAE (PEO-PBAE) particles encapsulating MDR-1 siRNA by solvent displacement.[161] PEO-PBAE particles were able to efficiently encapsulate siRNA and mediate efficient gene silencing at a 100 nM siRNA dose. Administration of these particles along with PEO-modified poly(epsilon-caprolactone) particles encapsulating paclitaxel resulted in significant cytotoxicity in multi-drug resistant tumor cells.

Another example involves the use of pH-sensitive core-shell particles.[162] The core-shell particles containing a cross-linked poly(diethylaminoethyl methacrylate) (PDEAEMA) pH-sensitive core and an aminoethyl methacrylate (AEMA)-rich shell are synthesized by emulsion polymerization. As control particles, pH-insensitive poly(methyl methacrylate) (PMMA) core/AEMA-rich shell particles were prepared. The ability of the core-shell particles to deliver siRNA to the cytosol of the cell was demonstrated using confocal microscopy. When epithelial cells were incubated with siRNA-coated PDEAEMA particles, fluorescence was observed throughout the cytosol of 40% of cells, indicating intracellular delivery of siRNA. In contrast, fluorescence from the siRNA strands remained colocalized and displayed a punctuate distribution in cells receiving siRNA adsorbed to PMMA particles. These results confirm that the activity of the particles is dependent on the presence of a pH-sensitive core. Functional gene knockdown following delivery of siRNA using the pH-sensitive particles was demonstrated in epithelial cells.

In a different approach, Kissel and coworkers designed branched biodegradable polyesters by attaching hydrophilic, positively charged amine groups onto a hydrophilic backbone consisting of poly(vinyl alcohol) which was subsequently grafted with multiple PLGA side chains.[163-166] These polymers are expected to be stable at acidic pH (5.0-5.5) but degrade rapidly at physiological pH (7.4). The degradation of this class of polymers could be influenced by the degree of amine substitution, the type of amine functionality, and the PLGA side chain length.[166] As compared to linear PLGA, remarkably shorter degradation times could be achieved by grafting short PLGA side chains onto amine-modified PVA backbones. In addition, the erosion rates could be varied from less than 5 days to more than 4 weeks. The mechanism of transfection for these materials does not rely on the proton-sponge effect of the backbone,[167] but rather on the rapid degradation rates. Recently, Nguyen *et al*. demonstrated the potential of DEAPA(68)-PVA-PLGA (1:10) (P(68)-10) for pulmonary siRNA delivery.[130] Nanoparticles containing siRNA were prepared using a solvent displacement method and the degradation of the

P(68)-10 particles was shown to be pH-dependent. At slightly acidic pH (pH 5.0-5.5) little to no degradation of the particles was observed. In contrast, degradation of the nanoparticles was seen within 4 h in PBS (pH 7.4) with sustained release of siRNA. The particles achieved significant knockdown of a luciferase reporter gene *in vitro*. Even though these particles were able to successfully transfect H1299 cells, the exact mechanism for endosomal escape is unclear and needs to be investigated in more detail. The authors speculate that a combination of osmotic effects and interactions with the endosomal membrane could play a role. This interaction would disrupt the membrane potential generated by membrane bound ATPases, and keep the pH near the extracellular and cytosolic pH, where the degradation of the polymer is rapid. Despite the promising results obtained in this study, *in vivo* use of these polyester particles for gene delivery applications may be limited by biocompatibility issues surrounding the non-degradable vinyl polymer backbone.

Acid-sensitive carriers based on degradation of the polymer

An alternative to the acid-sensitive systems described above are polymers that contain hydrolyzable linkages that degrade faster under acidic conditions (pH 5) compared to physiological conditions (pH 7.4). Polyacetal/ketal- and poly(ortho ester)-based particles are examples of systems developed to make use of this type of degradation mechanism. Both of these systems incorporate acetal or ketal linkages in the backbone of the polymer used to formulate the carrier so that when the particle is exposed to acidic conditions, the polymer backbone rapidly hydrolyzes into small molecules, and in the process, releases the encapsulated cargo. Similar to the carriers based on amine-containing polymers discussed above, use of acetal-based, acid-sensitive delivery vehicles leads to efficient endosomal escape and delivery of the cargo to the cytosol of the cell. A possible explanation for this observed activity, known as the "colloid osmotic mechanism," is predicated on the hypothesis that the generation of a large concentration of small molecule or polymeric byproducts from the degradation of a particulate vehicle can lead to an increase in osmotic pressure and the subsequent destabilization of endosomal vesicles.[168,169]

An example of siRNA delivery using polyketal particles was recently reported by Lee *et al*.[170] PK3, an acid-sensitive polymer, was synthesized by copolymerizing 1,4-cyclohexanedimethanol with 1,5-pentanediol.[171] This polyketal hydrolyzes rapidly at acidic pH, with a hydrolysis half-life of 1.8 days at pH 4.5, but is relatively stable at pH 7.4 (hydrolysis half-life of 39 days). The particles (PKCNs) are composed of PK3 and chloroquine and are prepared via a single emulsion solvent evaporation procedure. PKCNs were able to efficiently deliver tumor necrosis factor-α (TNF-α) siRNA and inhibit TNF-α production *in vitro* in macrophages and *in vivo* in Kuppfer cells. In addition, delivery of siRNA using the PKCNs greatly improved the therapeutic outcome of acute liver failure in mice.

Our laboratory has had significant experience in the study of poly(acetals) and other acetal-containing materials. In our first generation system, polyacrylamide hydrogel microparticles that incorporate acid-degradable acetal crosslinks are used to encapsulate proteins and plasmid DNA.[169,172-182] This system served largely as a proof-of-concept platform to test a number of hypotheses concerning optimal particle design parameters for pulmonary delivery, including particle surface functionalization, size, and degradation. These particles are prepared using an inverse emulsion free radical polymerization technique that allows the incorporation of a number of functional monomers, including amines and antibodies (Figures 1.1 and 1.2). The hydrogel particles are relatively stable at physiological conditions (pH 7.4), but hydrolyze

rapidly upon exposure to acidic conditions (pH 5), resulting in the release of the encapsulated cargo. By varying the acetal substituents of the crosslinker, the half-life of the crosslinker at pH 5 can be tuned to occur on the order of minutes to hours.[177] We have demonstrated the ability of these particles to successfully deliver protein antigens both *in vitro* and *in vivo* for vaccine applications.[169,181] Despite these promising results, the microparticles discussed above were only intended for use as a proof-of-concept platform due to concerns over the potential for toxicity caused by residual acrylamide monomers and the lack of biodegradability of the high molecular weight polyacrylamide degradation byproducts.

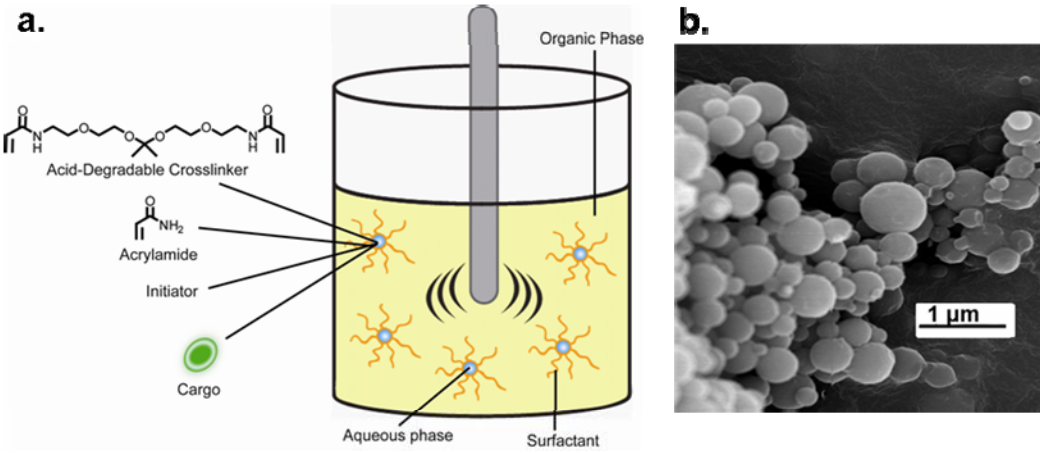

Figure 1.1. (a) Scheme for the synthesis of an acid-sensitive, polyacrylamide-based particle system. (b) Representative scanning electron microscope image of particles synthesized by inverse emulsion polymerization method.

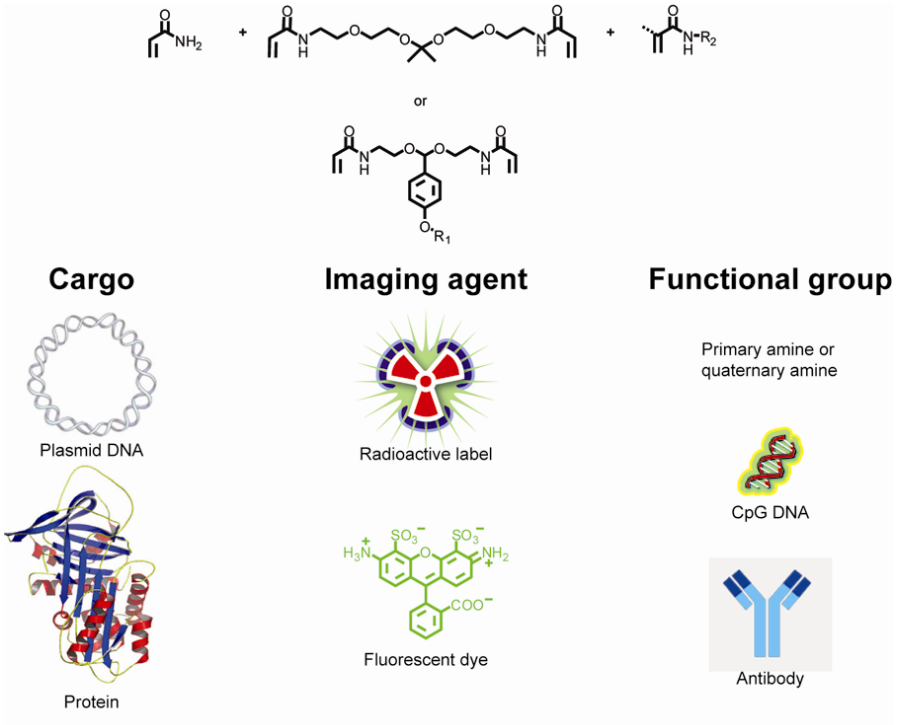

Figure 1.2. Overview of polyacrylamide acid-degradable hydrogel particles. Monomers used to synthesize particles (top) and some of the cargoes and modifications explored (bottom).

In an effort to overcome some of the limitations associated with the polyacrylamide particle system and generate a more biocompatible particle platform, we developed a second generation acid-degradable delivery vehicle. This new material, acetalated-dextran (Ac-DEX), is based on the non-toxic, naturally-occurring, FDA-approved polysaccharide, dextran.[183-187] Unlike the first generation particles described above that contained pH-sensitive acetal crosslinkers, the acetals of Ac-DEX provide a solubility switch, which under acidic conditions allows the release of encapsulated cargo in a controlled manner. Ac-DEX is synthesized in a one-step reaction by protecting the hydroxyl groups of dextran with pendant acetals (Figure 1.3). Conversion of the alcohols to acetals interrupts the hydrogen bonding of dextran and changes the solubility of the polymer. While native dextran is water-soluble, Ac-DEX is insoluble in aqueous solution but soluble in many common organic solvents, such as dichloromethane, THF, and DMF. The hydrophobic Ac-DEX can be easily processed into particles using a variety of emulsion techniques.

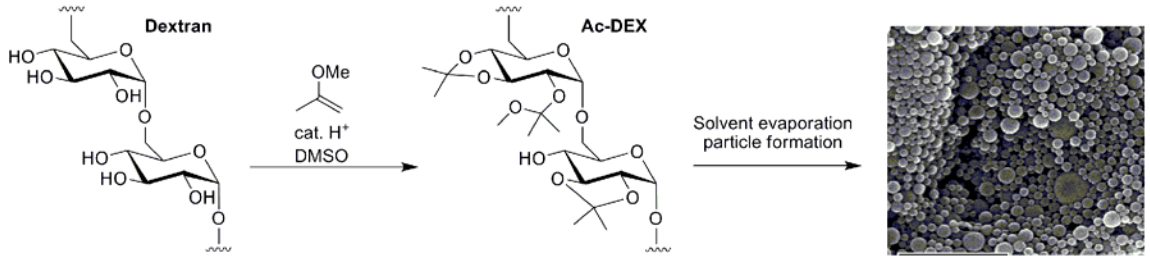

Figure 1.3. Particle system based on acetalated-dextran (Ac-DEX). Synthesis of Ac-DEX and formulation into microparticles.

Upon exposure to acidic conditions, Ac-DEX particles degrade via hydrolyis of the acetals, regenerating native dextran and minimal amounts of small molecule byproducts. The degradation rate of Ac-DEX is easily tuned by modulating a single reaction parameter, time, which dictates the degree and type of acetal modification of the dextran backbone.[184] By varying the ratio of faster-degrading acyclic acetals to slower-degrading cyclic acetals, a range of materials were prepared with particle degradation rates spanning two orders of magnitude (from 16 minutes to 27 hours at pH 5.0). Particles encapsulating either hydrophobic payloads[186] or hydrophilic macromolecules[184,187] have been prepared by single or double emulsion techniques, respectively. Additionally, we have developed a facile and chemoselective method for modifying the surface of Ac-DEX particles with targeting groups or imaging agents using the masked aldehydes present at the reducing ends of dextran.[185] A schematic overview of this system is depicted in Figure 1.4.

Specifically, we are interested in designing siRNA delivery vehicles for pulmonary administration. The lung presents unique opportunities and challenges for siRNA delivery (see discussion below). In Chapters 2 and 3, we explore the effects of varying a number of physicochemical properties on the *in vitro* and *in vivo* efficacy of our polyacrylamide hydrogel particles. These studies were performed with the goal of identifying the optimal features of particle-based delivery systems for pulmonary siRNA delivery (see below for discussion of parameters influencing pulmonary delivery). With the limitations of the polyacrylamide system in mind, we investigate the application of our biocompatible Ac-DEX particle system for siRNA delivery. In Chapter 4, we describe the modification of this particle system with amines for optimal activity as a gene delivery vector.

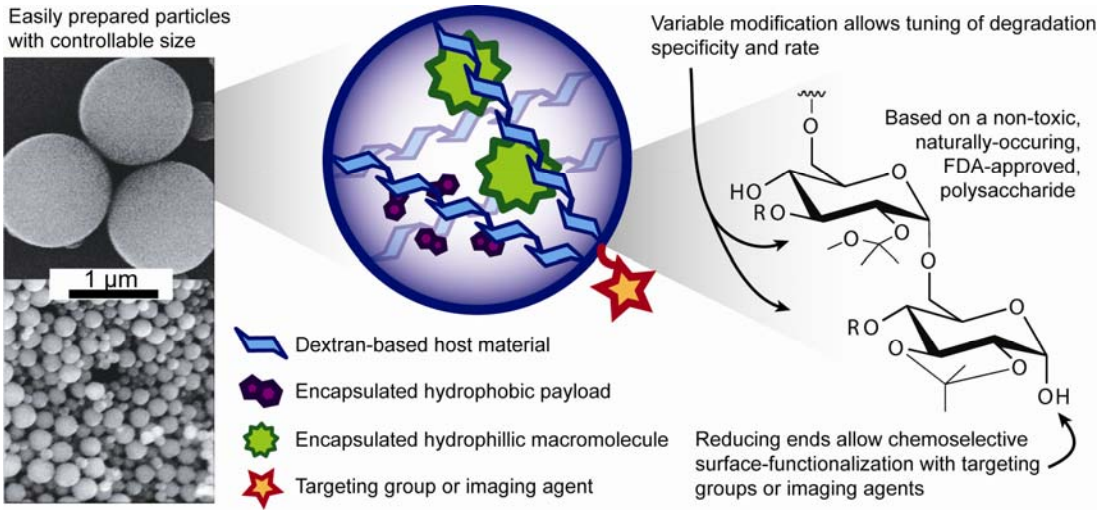

Figure 1.4. Overview of Ac-DEX as a material for the formation of acid-sensitive particles.

siRNA Delivery to the Lung

The lung represents a particularly attractive target for siRNA-based therapeutics due to the lethality and prevalence of lung diseases. The lung is susceptible to many diseases due to its location and physiological function.[188] Pulmonary delivery has been explored for the delivery of various therapeutic agents because the lung is accessible via multiple routes (including through the nose and mouth). For example, inhalation of drugs for the treatment of local diseases such as asthma, cystic fibrosis, and chronic obstructive pulmonary disease (COPD) has been common for many years. Local delivery has several advantages over other methods of administration. It allows the non-invasive delivery of siRNA directly to the diseased tissue, allowing similar therapeutic efficacy at lower doses and eliminating the need for targeting. This also limits the potential side effects associated with delivering therapeutic agents systemically. Finally, local pulmonary delivery avoids several of the barriers associated with therapeutic efficacy, including first-pass metabolism by the liver and degradation by serum nucleases. RNAi-based therapeutics are currently being explored for the treatment of a variety of pulmonary diseases, including lung cancer, influenza, acute lung injury, and severe acute respiratory syndrome (SARS).

Methods of Administration – direct delivery vs. intravenous delivery

Introduction of siRNA to the lung can be achieved by a variety of routes, for example inhalation, intranasal, intratracheal, or systemic. The first two methods are particularly attractive since the particles are delivered directly to the disease site and thus avoid first-pass metabolism. Inhalation is the most common method for pulmonary delivery and siRNA for inhalation can be formulated into either a liquid aerosol or dry powder aerosol. Direct pulmonary delivery in humans is achieved by inhalation of aerosol generated by either an inhaler or nebulizer. The intranasal route is also common for the delivery of therapeutics to the lungs due to the ease of administration into the nasal cavity. Intratracheal injections are commonly used in animal studies, however this method of administration is relatively invasive and not applicable to humans.

Barriers to siRNA Delivery to the Lung

Pulmonary delivery poses unique challenges for the delivery of therapeutic agents due to the role of the lung in defense against pathogens and environmental pollutants. The lung has evolved both physical and immunological barriers that inhibit access to exogenous substances, thus hindering effective gene delivery. Various elimination pathways for foreign particles exist in the lungs, including coughing, mucociliary clearance, translocation from the airway to other sites, and phagocytosis by macrophages. The first barrier faced in pulmonary delivery is the high degree of branching of the respiratory tract. Since many lung diseases affect the lower region of the lungs, the therapeutic agents must be able to follow the airstream around the bend along the branched airway to the deep lung area. The size of the particles is an important factor for determining the airway deposition and this feature will be discussed in more detail below. Other major barriers to effective pulmonary delivery include mucociliary clearance, mucus, and alveolar fluid.[189-191] Ciliated and mucus-secreting epithelial cells line the conducting airways and function in rapidly removing inhaled material. Particles that are deposited on ciliated epithelial cells are rapidly removed by mucociliary clearance and are eventually coughed up or swallowed.[192] Mucus constitutes a physical barrier as it is highly adhesive and increases the viscosity of the surface of lung epithelial cells.[193-195] Inhaled particles typically stick to mucus rather than penetrating through it, thus preventing effective delivery to the underlying cells. Particles that stick to mucus are rapidly removed from the lungs and are swallowed and sterilized in the gut. Disease states pose an additional challenge, as there is often an increase in mucus secretion during infection and inflammation. The thickness, viscosity, and composition of the mucus layer depend on the pathological condition and vary between individuals.[190] Another barrier to pulmonary delivery is alveolar fluid found on the surface of airway epithelial cells. The major constituents of alveolar fluid include phospholipids, mucins, and surfactant proteins. The negatively charged components of alveolar fluid could bind to cationic particles, altering their size and overall charge, and thus their cellular uptake. Previous reports have shown that pulmonary surfactants severely inhibit transfection efficiency of lipid-based delivery systems.[196,197]

Influence of Physicochemical Properties on Pulmonary Delivery

The types of carrier systems described above are but a few of the myriad systems developed to date. Each type of carrier has its own set of associated physicochemical properties that, in part, determines the biological behavior of the particle system both *in vitro* and *in vivo*. Several particle characteristics, including size, shape, and surface properties, are important for biological interactions.[198] Below, we highlight some of the important physicochemical properties related to particulate delivery systems and the effects that changes in those properties have on their biological behavior in the lung. These properties include particle size and surface charge and functionalization.

Particle size

The size of particles is an important property in determining the site of deposition in the lungs.[199-201] In pulmonary delivery, the size of particles is expressed in terms of the aerodynamic diameter (related to the particle's geometric diameter and density). Aerosol particles deposit in the lungs by three principal mechanisms: inertial impaction, gravitational sedimentation, and Brownian diffusion. The deposition of large particles in the lungs is generally by the first two mechanisms, while deposition of smaller particles is mainly by diffusion. A particle with large

momentum may be unable to change direction with the inspired air. Large particles (greater than 6 μm) are thus more likely to be impacted on the airway wall at bifurcations in the lung instead of following the changing airstream. As a result, they are usually deposited higher up in the airway or in the mouth or throat. Particles between 2 and 6 μm flow in the slower airstream and are generally deposited by gravitational sedimentation. It has been found that the optimal particle size for efficient deposition at the lower respiratory tract is between 1 and 5 μm.[202] For small particles (less than 1 μm) their movements are determined by Brownian motion. As the particle size further decreases, deposition in the lung increases again due to the increasing diffusional mobility. For nanoparticles that are less than 100 nm, they appear to settle effectively to the alveolar region with a fractional deposition around 50%. In addition to using particles with small aerodynamic diameter, it has been reported that the use of large porous particles can effectively avoid phagocytosis by the alveolar macrophages and prolong retention time in the lungs.[203,204] Porous particles over 10 μm in geometric diameter usually have a smaller aerodynamic diameter so that they are within the ideal aerodynamic size range for effective lung deposition. Edwards *et al*. demonstrated that large porous particles composed of PLGA lead to efficient aerosolization and delivery of insulin.[203]

The design of a particulate system with the appropriate particle size will largely depend on the disease of interest and the target region of the lung. Different applications might necessitate delivery to different lung regions.[205] For example, recent developments of viral and liposomal vectors for DNA transfer to airway epithelial cells in cystic fibrosis may require targeted delivery to the bronchial airways where the defect in epithelial Cl_2 ion transport (CFTR) is manifested. Deposition of these vectors in the lung periphery would be ineffective and may also enhance any innate immune response to the deposited therapy. With these concepts in mind, we explore the role of particle size on the *in vivo* efficacy of acid-degradable hydrogel particles for pulmonary delivery in Chapter 3.

Particle charge and surface functionalization

Numerous studies have shown that human mucus immobilizes synthetic nanoparticles and therefore represents one of the major hurdles to efficient pulmonary delivery.[206] Many researchers have studied the use of mucoadhesive polymers to improve the retention of particles at mucosal surfaces and, hence, their uptake. In pulmonary delivery applications, increasing the cationic nature of the particle surface may lend mucoadhesive characteristics to the system that may enhance the retention of such particles in the airspaces.[207] One of the most widely studied mucoadhesive polymers is chitosan, a linear polysaccharide composed of glucosamine and N-acetyl-D-glucosamine.[208] Yamamoto *et al*. reported the preparation of PLGA microparticles modified on the surface with chitosan.[207] These particles demonstrated enhanced mucoadhesiveness (slower elimination from the lungs) when compared to unmodified particles and enabled the efficient delivery of the peptide elcatonin to the lungs. The pharmacological action of chitosan-modified particles was prolonged significantly compared to that of unmodified particles due to the ability of the particles to sustain drug release. Recently, Howard *et al*. demonstrated the use of chitosan to deliver siRNA to the lungs.[209,210] The aerosolized chitosan/siRNA particles showed significant EGFP silencing (68% reduction compared to the mismatch control) in the transgenic mice model.

An alternative to the approach described above is the use of mucus-penetrating particles, particles that can efficiently cross the mucus barrier. Hanes *et al*. have shown that coating particles with a high-density of low-molecular-weight PEG can reduce particle affinity to mucus

substituents and enhance their penetration through the thick mucus layers associated with certain diseases of the lungs.[211-213] Recently, the group reported the non-covalent coating of PLGA particles with Pluronics (a triblock copolymer of poly(ethylene glycol)-poly(propylene oxide)-poly(ethylene glycol), PEG-PPO-PEG).[214] The effectiveness of the Pluronic was dependent on the MW of the PPO segment. They found that PPO segments with MW $\geq$ 3 kDa effectively shielded the particle surface and enabled the rapid penetration of human mucus. Indeed, a Pluronic F127 coating markedly improved the transport of polymeric particles in human cervicovaginal mucus (CVM) as well as sputum expectorated by cystic fibrosis patients. This strategy represents a promising approach to the design of mucus-penetrating drug-delivery vehicles as one can envision using this method to coat any number of core particles. Thus, the degradation kinetics and drug release profile can be controlled by selecting the appropriate core material. Enhanced mucus penetration is expected to facilitate prolonged retention and more uniform distribution of drug carriers in the lung, leading to improved therapeutic efficacy.

In contrast to the approaches described above, another approach for improving pulmonary delivery is the use of targeting groups. Much work in recent years has been focused on modifying the surface of particle delivery systems with ligands, such as peptides, antibodies, and DNA and RNA sequences known to interact with receptors on specific subsets of cells in the body.[215-217] These interactions can mediate cell-specific internalization of particles provided an appropriate ligand is used. Of particular interest for pulmonary delivery are endothelial cell adhesion molecules (CAM, such as ICAM-1 and PECAM-1). CAMs are constitutively expressed on pulmonary endothelial cells and are functionally involved in oxidative stress and inflammation involved in pulmonary diseases. It has been shown that endothelial cells can internalize particles containing multiple copies of either ICAM-1 or PECAM-1 antibodies.[218-221] An example of targeting ICAM-1 in pulmonary endothelium was recently described by Calderon *et al*. In this report, anti-ICAM carriers were prepared by adsorption of anti-ICAM antibody on the surface of polystyrene particles. In order to optimize the design of the carriers, the influence of two particle design parameters (particle dose and density of targeting molecules) on specific and efficient endothelial targeting was investigated. Increasing the carrier dose was found to enhance specific accumulation in the lung vasculature and decrease non-specific hepatic and splenic uptake. In addition, increasing the antibody density enhanced lung accumulation with minimally reduced liver and spleen uptake.

Clinical Trials for siRNA Therapeutics

The potential of RNA interference for use in the treatment of human disease has been demonstrated by the successful application of several siRNA therapies in clinical trials.[36,222-224] A summary of these trials is provided in Table 1.1. Many of these trials are focused on direct local delivery of siRNA and on well-validated therapeutic targets. The most progress to date is in the treatment of eye diseases such as age-related macular degeneration (AMD). The use of siRNA for the treatment of AMD is currently the subject of several clinical trials.[225]

In addition to local ocular delivery, direct pulmonary administration has been explored for delivery of siRNA. Delivery to the lung by inhalation is non-invasive and directly targets the tissue, thus reducing necessary drug dosing and the likelihood of systemic side effects. Alnylam Pharmaceuticals has recently reported efficient treatment of respiratory syncytial virus (RSV) using aerosolized delivery of a naked siRNA targeting the viral nucleocapsid (N) gene (ALN-RSV01). Phase II trials in lung transplant recipients showed that ALN-RSV01 was safe and well-tolerated by patients. Administration of ALN-RSV01 was associated with a statistically

significant improvement in symptoms and decrease in the incidence of new or progressive bronchiolitis obliterans syndrome relative to placebo.[226]

Table 1.1. Current clinical trials for siRNA therapeutics.[a]

siRNA	*Delivery System*	*Route of Administration*	*Disease*	*Target*	*Company/ Institution*	*Status*
Cand5	Naked siRNA	Intravitreal, Intravenous	Wet AMD, DME	VEGF-A	Opko Health	Phase II
TD101	Naked siRNA	Injection into foot	Pachyonychia congenital	PC keratin K6a	TransDerm	Phase I
ALN-RSV01	Naked siRNA	Intranasal	RSV	RSV nucleocapsid	Alnylam	Phase II
PF-04523655	Modified siRNA	Intravitreal Injection	Wet AMD, DME	Hypoxia-inducible gene	Pfizer	Phase I
Sirna-027	Modified siRNA	Intravitreal Injection	Wet AMD	VEGFR-1	Allergan	Phase I
SYL040012	Modified siRNA	Ophthalmic drop	Glaucoma, Ocular Hypertension	Adrenergic receptor	Sylentis	Phase I/II
QPI-1002	Modified siRNA	Intravenous	Delayed Graft Function, AKI	P53	Quark	Phase I/II
QPI-1007	Modified siRNA	Intravitreal Injection	Chronic Optic Nerve Atrophy	Caspase 2	Quark	Phase I
siG12D LODER	Polymer matrix	EUS Biopsy Needle	Pancreatic Cancer	KRASG12D	Silenseed	Phase I
Atu027	Liposome	Intravenous	Advanced Solid Cancer	Protein Kinase N3	Silence Therapeutics	Phase I
CALAA-01	Cyclo-dextrin	Intravenous Infusion	Cancer	RRM2	Calando	Phase I
NA	Antigen encoding RNA-transfected dendritic cells	Intradermal Injection	Metastatic Melanoma	Immuno-proteasome beta subunits	Duke University	Phase I

a) Information obtained from http://clinicaltrials.gov

The first in-human phase I clinical trial involving the systemic administration of siRNA to patients with solid cancers using a targeted, nanoparticle delivery system (CALAA-01) is currently being conducted by Calando Pharmaceuticals.[227,228] The nanoparticle system consists of a cationic cyclodextrin-based polymer (CDP) modified with PEG-transferrin and siRNA designed to reduce the expression of ribonucleotide reductase subunit M2 (RRM2).[229,230] Initial results from these trials demonstrated that siRNA administered systemically to humans can produce a specific gene inhibition (reduction in mRNA and protein) by an RNAi mechanism.[227] These successful experimental results indicate that the therapeutic potential of RNAi is high and may be realized soon.

Conclusions

RNAi has tremendous potential to improve the prevention and treatment of human disease. Since the discovery of RNAi, numerous research groups worldwide have sought to develop efficient carrier systems for the delivery of siRNA both *in vitro* and *in vivo*. Despite several promising clinical trials, the effective delivery of siRNA *in vivo* remains a significant obstacle to the widespread application of RNAi therapeutics in a clinical setting. This challenge motivates future efforts focusing on the design of clinically suitable, safe and effective siRNA delivery vehicles. Acid-degradable polymeric materials represent a promising alternative for the delivery of siRNA. Acid-sensitive carrier systems have particularly desirable characteristics for a number of applications due to the fact that release of their payload can be triggered in response to endosomal acidification. These multifunctional vehicles can be designed to incorporate features that might allow them to overcome several of the limitations of previously reported siRNA delivery systems. The following chapters describe the design, synthesis, and biological evaluation of acid-sensitive delivery systems investigated in our laboratory for the efficient pulmonary delivery of siRNA.

References

(1) Fire, A.; Xu, S.; Montgomery, M. K.; Kostas, S. A.; Driver, S. E.; Mello, C. C. *Nature* **1998**, *391*, 806-811.
(2) Hannon, G. J. *Nature* **2002**, *418*, 244-251.
(3) Dorsett, Y.; Tuschl, T. *Nat. Rev. Drug Disc.* **2004**, *3*, 318-329.
(4) Elbashir, S. M.; Harborth, J.; Lendeckel, W.; Yalcin, A.; Weber, K.; Tuschl, T. *Nature* **2001**, *411*, 494-498.
(5) McCaffrey, A. P.; Meuse, L.; Pham, T.-T.; Conklin, D. S.; Hannon, G. J.; Kay, M. A. *Nature* **2002**, *418*, 38-39.
(6) Novina, C. D.; Sharp, P. A. *Nature* **2004**, *430*, 161-164.
(7) Echeverri, C. J.; Perrimon, N. *Nat. Rev. Genet.* **2006**, *7*, 373-384.
(8) Carpenter, A. E.; Sabatini, D. M. *Nat. Rev. Genet.* **2004**, *5*, 11-22.
(9) Kamath, R. S.; Fraser, A. G.; Dong, Y.; Poulin, G.; Durbin, R.; Gotta, M.; Kanapin, A.; Bot, N. L.; Moreno, S.; Sohrmann, M.; Welchman, D. P.; Zipperlen, P.; Ahringer, J. *Nature* **2003**, *421*, 231-237.
(10) Ashrafi, K.; Chang, F. Y.; Watts, J. L.; Fraser, A. G.; Kamath, R. S.; Ahringer, J.; Ruvkun, G. *Nature* **2003**, *421*, 268-272.
(11) Fraser, A. G.; Kamath, R. S.; Zipperlen, P.; Martinez-Campos, M.; Sohrmann, M.; Ahringer, J. *Nature* **2000**, *408*, 325-330.
(12) Gönczy, P.; Echeverri, C.; Oegema, K.; Coulson, A.; Jones, S. J. M.; Copley, R. R.; Duperon, J.; Oegema, J.; Brehm, M.; Cassin, E.; Hannak, E.; Kirkham, M.; Pichler, S.; Flohrs, K.; Goessen, A.; Leidel, S.; Alleaume, A.-M.; Martin, C.; Özlü, N.; Bork, P.; Hyman, A. A. *Nature* **2000**, *408*, 331-336.
(13) Pothof, J.; van Haaften, G.; Thijssen, K.; Kamath, R. S.; Fraser, A. G.; Ahringer, J.; Plasterk, R. H. A.; Tijsterman, M. *Genes Dev.* **2003**, *17*, 443-448.
(14) Maeda, I.; Kohara, Y.; Yamamoto, M.; Sugimoto, A. *Curr. Biol.* **2001**, *11*, 171-176.
(15) Kiger, A. A.; Baum, B.; Jones, S.; Jones, M. R.; Coulson, A.; Echeverri, C.; Perrimon, N. *J. Biol.* **2003**, *2*, 27.
(16) Boutros, M.; Kiger, A. A.; Armknecht, S.; Kerr, K.; Hild, M.; Koch, B.; Haas, S. A.; Consortium, H. F. A.; Paro, R.; Perrimon, N. *Science* **2004**, *303*, 832-835.
(17) DasGupta, R.; Kaykas, A.; Moon, R. T.; Perrimon, N. *Science* **2005**, *308*, 826-833.
(18) Lum, L.; Yao, S.; Mozer, B.; Rovescalli, A.; Von Kessler, D.; Nirenberg, M.; Beachy, P. A. *Science* **2003**, *299*, 2039-2045.
(19) Silva, J. M.; Mizuno, H.; Brady, A.; Lucito, R.; Hannon, G. J. *Proc. Natl. Acad. Sci. U. S. A.* **2004**, *101*, 6548-6552.
(20) Aza-Blanc, P.; Cooper, C. L.; Wagner, K.; Batalov, S.; Deveraux, Q. L.; Cooke, M. P. *Mol. Cell* **2003**, *12*, 627-637.
(21) Berns, K.; Hijmans, E. M.; Mullenders, J.; Brummelkamp, T. R.; Velds, A.; Heimerikx, M.; Kerkhoven, R. M.; Madiredjo, M.; Nijkamp, W.; Weigelt, B.; Agami, R.; Ge, W.; Cavet, G.; Linsley, P. S.; Beijersbergen, R. L.; Bernards, R. *Nature* **2004**, *428*, 431-437.
(22) Kittler, R.; Pelletier, L.; Heninger, A.-K.; Slabicki, M.; Theis, M.; Miroslaw, L.; Poser, I.; Lawo, S.; Grabner, H.; Kozak, K.; Wagner, J.; Surendranath, V.; Richter, C.; Bowen, W.; Jackson, A. L.; Habermann, B.; Hyman, A. A.; Buchholz, F. *Nat. Cell Biol.* **2007**, *9*, 1401-1412.

(23) Paddison, P. J.; Silva, J. M.; Conklin, D. S.; Schlabach, M.; Li, M.; Aruleba, S.; Balija, V.; O'Shaughnessy, A.; Gnoj, L.; Scobie, K.; Chang, K.; Westbrook, T.; Cleary, M.; Sachidanandam, R.; McCombie, W. R.; Elledge, S. J.; Hannon, G. J. *Nature* **2004**, *428*, 427-431.
(24) Bernards, R. *N. Engl. J. Med.* **2006**, *355*, 2391-2393.
(25) Kramer, R.; Cohen, D. *Nat. Rev. Drug Disc.* **2004**, *3*, 965-972.
(26) Eggert, U. S.; Kiger, A. A.; Richter, C.; Perlman, Z. E.; Perrimon, N.; Mitchison, T. J.; Field, C. M. *PLoS Biol.* **2004**, *2*, e379.
(27) Song, E.; Lee, S.-K.; Wang, J.; Ince, N.; Ouyang, N.; Min, J.; Chen, J.; Shankar, P.; Lieberman, J. *Nat. Med.* **2003**, *9*, 347-351.
(28) Kapadia, S. B.; Brideau-Anderson, A.; Chisari, F. V. *Proc. Natl. Acad. Sci. U. S. A.* **2003**, *100*, 2014-2018.
(29) Izquierdo, M. *Cancer Gene Ther.* **2005**, *12*, 217-227.
(30) Goldberg, M. S.; Xing, D.; Ren, Y.; Orsulic, S.; Bhatia, S. N.; Sharp, P. A. *Proc. Natl. Acad. Sci. U. S. A.* **2011**, *108*, 745-750.
(31) Seth, S.; Matsui, Y.; Fosnaugh, K.; Liu, Y.; Vaish, N.; Adami, R.; Harvie, P.; Johns, R.; Severson, G.; Brown, T.; Takagi, A.; Bell, S.; Chen, Y.; Chen, F.; Zhu, T.; Fam, R.; Maciagiewicz, I.; Kwang, E.; McCutcheon, M.; Farber, K.; Charmley, P.; Houston, M. E.; So, A.; Templin, M. V.; Polisky, B. *Mol. Ther.* **2011**, doi:10.1038/mt.2011.21.
(32) Patel, N.; Chatterjee, S. K.; Vrbanac, V.; Chung, I.; Mu, C. Y.; Olsen, R. R.; Waghorne, C.; Zetter, B. R. *Proc. Natl. Acad. Sci. U. S. A.* **2010**, *107*, 2503-2508.
(33) Aouadi, M.; Tesz, G. J.; Nicoloro, S. M.; Wang, M.; Chouinard, M.; Soto, E.; Ostroff, G. R.; Czech, M. P. *Nature* **2009**, *458*, 1180-1184.
(34) Neff, C. P.; Zhou, J.; Remling, L.; Kuruvilla, J.; Zhang, J.; Li, H.; Smith, D. D.; Swiderski, P.; Rossi, J. J.; Akkina, R. *Sci. Transl. Med.* **2011**, *3*, 66ra6.
(35) Kumar, P.; Ban, H.-S.; Kim, S.-S.; Wu, H.; Pearson, T.; Greiner, D. L.; Laouar, A.; Yao, J.; Haridas, V.; Habiro, K.; Yang, Y.-G.; Jeong, J.-H.; Lee, K.-Y.; Kim, Y.-H.; Kim, S. W.; Peipp, M.; Fey, G. H.; Manjunath, N.; Shultz, L. D.; Lee, S.-K.; Shankar, P. *Cell* **2008**, *134*, 577-586.
(36) Whitehead, K. A.; Langer, R.; Anderson, D. G. *Nat. Rev. Drug Discovery* **2009**, *8*, 129-138.
(37) de Fougerolles, A.; Vornlocher, H.-P.; Maraganore, J.; Lieberman, J. *Nat. Rev. Drug Disc.* **2007**, *6*, 443-453.
(38) Bumcrot, D.; Manoharan, M.; Koteliansky, V.; Sah, D. W. Y. *Nat. Chem. Biol.* **2006**, *2*, 711-719.
(39) Kurreck, J. *Angew. Chem., Int. Ed.* **2009**, *48*, 1378-1398.
(40) Hammond, S. M.; Caudy, A. A.; Hannon, G. J. *Nat. Rev. Genet.* **2001**, *2*, 110-119.
(41) Tuschl, T. *ChemBioChem* **2001**, *2*, 239-245.
(42) Hammond, S. M.; Bernstein, E.; Beach, D.; Hannon, G. J. *Nature* **2000**, *404*, 293-296.
(43) Zamore, P. D.; Tuschl, T.; Sharp, P. A.; Bartel, D. P. *Cell* **2000**, *101*, 25-33.
(44) Bernstein, E.; Caudy, A. A.; Hammond, S. M.; Hannon, G. J. *Nature* **2001**, *409*, 363-366.
(45) Elbashir, S. M.; Martinez, J.; Patkaniowska, A.; Lendeckel, W.; Tuschl, T. *EMBO J.* **2001**, *20*, 6877-6888.
(46) Elbashir, S. M.; Lendeckel, W.; Tuschl, T. *Genes Dev.* **2001**, *15*, 188-200.
(47) Rand, T. A.; Ginalski, K.; Grishin, N. V.; Wang, X. *Proc. Natl. Acad. Sci. U. S. A.* **2004**, *101*, 14385-14389.

(48) Ameres, S. L.; Martinez, J.; Schroeder, R. *Cell* **2007**, *130*, 101-112.
(49) Hutvagner, G.; Zamore, P. D. *Science* **2002**, *297*, 2056-2060.
(50) Fougerolles, A.; Vornlocher, H.-P.; Maraganore, J.; Lieberman, J. *Nat. Rev. Drug Discovery* **2007**, *6*, 443-453.
(51) McManus, M. T.; Sharp, P. A. *Nat. Rev. Genet.* **2002**, *3*, 737-747.
(52) Fröhlich, T.; Wagner, E. *Soft Matter* **2010**, *6*, 226-234.
(53) Pack, D. W.; Hoffman, A. S.; Pun, S.; Stayton, P. S. *Nat. Rev. Drug Discovery* **2005**, *4*, 581-593.
(54) Rao, D. D.; Vorhies, J. S.; Senzer, N.; Nemunaitis, J. *Adv. Drug Delivery Rev.* **2009**, *61*, 746-759.
(55) Gary, D. J.; Puri, N.; Won, Y.-Y. *J. Controlled Release* **2007**, *121*, 64-73.
(56) Takahashi, Y.; Nishikawa, M.; Takakura, Y. *Adv. Drug Delivery Rev.* **2009**, *61*, 760-766.
(57) Gaynor, J. W.; Campbell, B. J.; Cosstick, R. *Chem. Soc. Rev.* **2010**, *39*, 4169-4184.
(58) Braasch, D. A.; Jensen, S.; Liu, Y.; Kaur, K.; Arar, K.; White, M. A.; Corey, D. R. *Biochemistry* **2003**, *42*, 7967-7975.
(59) Chiu, Y.-L.; Rana, T. M. *RNA* **2003**, *9*, 1034-1048.
(60) Layzer, J. M.; McCaffrey, A. P.; Tanner, A. K.; Huang, Z.; Kay, M. A.; Sullenger, B. A. *RNA* **2004**, *10*, 766-771.
(61) Czauderna, F.; Fechtner, M.; Dames, S.; Aygün, H.; Klippel, A.; Pronk, G. J.; Giese, K.; Kaufmann, J. *Nucleic Acids Res.* **2003**, *31*, 2705-2716.
(62) Harborth, J.; Elbashir, S. M.; Vandenburgh, K.; Manninga, H.; Scaringe, S. A.; Weber, K.; Tuschl, T. *Antisense Nucleic Acid Drug Dev.* **2003**, *13*, 83-105.
(63) Shim, M. S.; Kwon, Y. J. *FEBS J.* **2010**, *277*, 4814-4827.
(64) Jeong, J. H.; Mok, H.; Oh, Y.-K.; Park, T. G. *Bioconjugate Chem.* **2009**, *20*, 5-14.
(65) Soutschek, J.; Akinc, A.; Bramlage, B.; Charisse, K.; Constien, R.; Donoghue, M.; Elbashir, S.; Geick, A.; Hadwiger, P.; Harborth, J.; John, M.; Kesavan, V.; Lavine, G.; Pandey, R. K.; Racie, T.; Rajeev, K. G.; Röhl, I.; Toudjarska, I.; Wang, G.; Wuschko, S.; Bumcrot, D.; Koteliansky, V.; Limmer, S.; Manoharan, M.; Vornlocher, H. P. *Nature* **2004**, *432*, 173-178.
(66) Wolfrum, C.; Shi, S.; Jayaprakash, K. N.; Jayaraman, M.; Wang, G.; Pandey, R. K.; Rajeev, K. G.; Nakayama, T.; Charrise, K.; Ndungo, E. M.; Zimmermann, T.; Koteliansky, V.; Manoharan, M.; Stoffel, M. *Nat. Biotechnol.* **2007**, *25*, 1149-1157.
(67) DiFiglia, M.; Sena-Esteves, M.; Chase, K.; Sapp, E.; Pfister, E.; Sass, M.; Yoder, J.; Reeves, P.; Pandey, R. K.; Rajeev, K. G.; Manoharan, M.; Sah, D. W. Y.; Zamore, P. D.; Aronin, N. *Proc. Natl. Acad. Sci. U. S. A.* **2007**, *104*, 17204-17209.
(68) McNamara, J. O.; Andrechek, E. R.; Wang, Y.; Viles, K. D.; Rempel, R. E.; Gilboa, E.; Sullenger, B. A.; Giangrande, P. H. *Nat. Biotechnol.* **2006**, *24*, 1005-1015.
(69) Zhou, J.; Li, H.; Li, S.; Zaia, J.; Rossi, J. J. *Mol. Ther.* **2008**, *16*, 1481-1489.
(70) Li, Y.; Li, M.; Yao, G.; Geng, N.; Xie, Y.; Feng, Y.; Zhang, P.; Kong, X.; Xue, J.; Cheng, S.; Zhou, J.; Xiao, L. *Cancer Gene Ther.* **2011**.
(71) Dai, W.; He, W.; Shang, G.; Jiang, J.; Wang, Y.; Kong, W. *Am. J. Physiol.* **2010**, *299*, H1468-H1475.
(72) Yang, T.; Zhang, B.; Pat, B. K.; Wei, M. Q.; Gobe, G. C. *J. Biomed. Biotechnol.* **2010**, *2010*.
(73) Qin, X.-F.; An, D. S.; Chen, I. S. Y.; Baltimore, D. *Proc. Natl. Acad. Sci. U. S. A.* **2003**, *100*, 183-188.

(74) Nakamura, M.; Masutomi, K.; Kyo, S.; Hashimoto, M.; Maida, Y.; Kanaya, T.; Tanaka, M.; Hahn, W. C.; Inoue, M. *Hum. Gene Ther.* **2005**, *16*, 859-868.
(75) Yang, Y.; Wu, C.; Wu, J.; Nerurkar, V. R.; Yanagihara, R.; Lu, Y. *J. Med. Virol.* **2008**, *80*, 930-936.
(76) Thomas, C. E.; Ehrhardt, A.; Kay, M. A. *Nat. Rev. Genet.* **2003**, *4*, 346-358.
(77) Zaiss, A. K.; Muruve, D. A. *Gene Ther.* **2008**, *15*, 808-816.
(78) Kang, H.; DeLong, R.; Fisher, M. H.; Juliano, R. L. *Pharm. Res.* **2005**, *22*, 2099-2106.
(79) Zhou, J.; Wu, J.; Hafdi, N.; Behr, J.-P.; Erbacher, P.; Peng, L. *Chem. Commun. (Cambridge, U.K.)* **2006**, 2362-2364.
(80) Waite, C. L.; Sparks, S. M.; Uhrich, K. E.; Roth, C. M. *BMC Biotechnol.* **2009**, *9*, 38-48.
(81) Patil, M. L.; Zhang, M.; Betigeri, S.; Taratula, O.; He, H.; Minko, T. *Bioconjugate Chem.* **2008**, *19*, 1396-1403.
(82) Patil, M. L.; Zhang, M.; Taratula, O.; Garbuzenko, O. B.; He, H.; Minko, T. *Biomacromolecules* **2009**, *10*, 258-266.
(83) Posadas, I.; López-Hernández, B.; Clemente, M. I.; Jiménez, J. L.; Ortega, P.; de la Mata, J.; Gómez, R.; Muñoz-Fernández, M.; Ceña, V. *Pharm. Res.* **2009**, *26*, 1181-1191.
(84) Taratula, O.; Garbuzenko, O. B.; Kirkpatrick, P.; Pandya, I.; Savla, R.; Pozharov, V. P.; He, H.; Minko, T. *J. Controlled Release* **2009**, *140*, 284-293.
(85) Merkel, O.; Mintzer, M. A.; Librizzi, D.; Samsonova, O.; Dicke, T.; Sproat, B.; Garn, H.; Barth, P. J.; Simanek, E. E.; Kissel, T. *Mol. Pharmaceutics* **2010**, *7*, 969-983.
(86) Taratula, O.; Savla, R.; He, H.; Minko, T. *Int. J. Nanotechnol.* **2011**, *8*, 36-52.
(87) Pavan, G. M.; Posocco, P.; Tagliabue, A.; Maly, M.; Malek, A.; Danani, A.; Ragg, E.; Catapano, C.; Pricl, S. *Chem.--Eur. J.* **2010**, *16*, 7781-7795.
(88) Hamilton, S. K.; Sims, A. L.; Donavan, J.; Harth, E. *Polym. Chem.* **2011**, *2*, 441-446.
(89) Schroeder, A.; Levins, C. G.; Cortez, C.; Langer, R.; Anderson, D. G. *J. Intern. Med.* **2010**, *267*, 9-21.
(90) Wu, S. Y.; McMillan, N. A. J. *AAPS J.* **2009**, *11*, 639-652.
(91) Tseng, Y.-C.; Mozumdar, S.; Huang, L. *Adv. Drug Delivery Rev.* **2009**, *61*, 721-731.
(92) MacLachlan, I. In *Therapeutic Oligonucleotides*; Kurreck, J., Ed.; Royal Society of Chemistry: Cambridge, 2008, p 241-266.
(93) Gao, K.; Huang, L. *Mol. Pharmaceutics* **2009**, *6*, 651-658.
(94) Malone, R. W.; Felgner, P. L.; Verma, I. M. *Proc. Natl. Acad. Sci. U. S. A.* **1989**, *86*, 6077-6081.
(95) Semple, S. C.; Akinc, A.; Chen, J.; Sandhu, A. P.; Mui, B. L.; Cho, C. K.; Sah, D. W. Y.; Stebbing, D.; Crosley, E. J.; Yaworski, E.; Hafez, I. M.; Dorkin, J. R.; Qin, J.; Lam, K.; Rajeev, K. G.; Wong, K. F.; Jeffs, L. B.; Nechev, L. V.; Eisenhardt, M. L.; Jayaraman, M.; Kazem, M.; Maier, M. A.; Srinivasulu, M.; Weinstein, M. J.; Chen, Q.; Alvarez, R.; Barros, S. A.; De, S.; Klimuk, S. K.; Borland, T.; Kosovrasti, V.; Cantley, W. L.; Tam, Y. K.; Manoharan, M.; Ciufolini, M. A.; Tracy, M. A.; de Fougerolles, A.; MacLachlan, I.; Cullis, P. R.; Madden, T. D.; Hope, M. J. *Nat. Biotechnol.* **2010**, *28*, 172-176.
(96) Love, K. T.; Mahon, K. P.; Levins, C. G.; Whitehead, K. A.; Querbes, W.; Dorkin, J. R.; Qin, J.; Cantley, W. L.; Qin, L. L.; Racie, T.; Frank-Kamenetsky, M.; Yip, K. N.; Alvarez, R.; Sah, D. W. Y.; de Fougerolles, A.; Fitzgerald, K.; Koteliansky, V.; Akinc, A.; Langer, R.; Anderson, D. G. *Proc. Natl. Acad. Sci. U. S. A.* **2010**, *107*, 1864-1869.
(97) Zimmerman, T. S.; Lee, A. C. H.; Akinc, A.; Bramlage, B.; Bumcrot, D.; Fedoruk, M. N.; Harborth, J.; Heyes, J. A.; Jeffs, L. B.; John, M.; Judge, A. D.; Lam, K.; McClintock, K.;

Nechev, L. V.; Palmer, L. R.; Racie, T.; Rohl, I.; Seiffert, S.; Shanmugam, S.; Sood, V.; Soutschek, J.; Toudjarska, I.; Wheat, A. J.; Yaworski, E.; Zedalis, W.; Koteliansky, V.; Manoharan, M.; Vornlocher, H. P.; MacLachlan, I. *Nature* **2006**, *441*, 111-114.
(98) Morrissey, D. V.; Lockridge, J. A.; Shaw, L.; Blanchard, K.; Jensen, K.; Breen, W.; Hartsough, K.; Machemer, L.; Radka, S.; Jadhav, V.; Vaish, N.; Zinnen, S.; Vargeese, C.; Bowman, K.; Shaffer, C. S.; Jeffs, L. B.; Judge, A. D.; MacLachlan, I.; Polisky, B. *Nat. Biotechnol.* **2005**, *23*, 1002-1007.
(99) Zhang, S.; Zhao, B.; Jiang, H.; Wang, B.; Ma, B. *J. Controlled Release* **2007**, *123*, 1-10.
(100)Kim, W. J.; Kim, S. W. *Pharm. Res.* **2009**, *26*, 657-666.
(101)Gao, W.; Xiao, Z.; Radovic-Moreno, A.; Shi, J.; Langer, R.; Farokhzad, O. C. *Methods Mol. Biol.* **2010**, *629*, 53-67.
(102)Urban-Klein, B.; Werth, S.; Abuharbeid, S.; Czubayko, F.; Aigner, A. *Gene Ther.* **2005**, *12*, 461-466.
(103)Grzelinski, M.; Urban-Klein, B.; Martens, T.; Lamszus, K.; Bakowshy, U.; Höbel, S.; Czubayko, F.; Aigner, A. *Hum. Gene Ther.* **2006**, *17*, 751-766.
(104)Höbel, S.; Koburger, I.; John, M.; Czubayko, F.; Hadwiger, P.; Vornlocher, H.-P.; Aigner, A. *J. Gene Med.* **2010**, *12*, 287-300.
(105)Moghimi, S. M.; Symonds, P.; Murray, J. C.; Hunter, A. C.; Debska, G.; Szewczyk, A. *Mol. Ther.* **2005**, *11*, 990-995.
(106)Neu, M.; Fischer, D.; Kissel, T. *J. Gene Med.* **2005**, *7*, 992-1009.
(107)Zintchenko, A.; Philipp, A.; Dehshahri, A.; Wagner, E. *Bioconjugate Chem.* **2008**, *19*, 1448-1455.
(108)Rozema, D. B.; Lewis, D. L.; Wakefield, D. H.; Wong, S. C.; Klein, J. J.; Roesch, P. L.; Bertin, S. L.; Reppen, T. W.; Chu, Q.; Blokhin, A. V.; Hagstrom, J. E.; Wolff, J. A. *Proc. Natl. Acad. Sci. U. S. A.* **2007**, *104*, 12982-12987.
(109)Oishi, M.; Nagasaki, Y.; Itaka, K.; Nishiyama, N.; Kataoka, K. *J. Am. Chem. Soc.* **2005**, *127*, 1624-1625.
(110)Meyer, M.; Dohmen, C.; Philipp, A.; Kiener, D.; Maiwald, G.; Scheu, C.; Ogris, M.; Wagner, E. *Mol. Pharmaceutics* **2009**, *6*, 752-762.
(111)Heredia, K. L.; Nguyen, T. H.; Chang, C.-W.; Bulmus, V.; Davis, T. P.; Maynard, H. D. *Chem. Commun. (Cambridge, U.K.)* **2008**, 3245-3247.
(112)Yezhelyev, M. V.; Qi, L.; O'Regan, R. M.; Nie, S.; Gao, X. *J. Am. Chem. Soc.* **2008**, *130*, 9006-9012.
(113)Singh, N.; Agrawal, A.; Leung, A. K. L.; Sharp, P. A.; Bhatia, S. N. *J. Am. Chem. Soc.* **2010**, *132*, 8241-8243.
(114)Giljohann, D. A.; Seferos, D. S.; Prigodich, A. E.; Patel, P. C.; Mirkin, C. A. *J. Am. Chem. Soc.* **2009**, *131*, 2072-2073.
(115)Lee, J.-S.; Green, J. J.; Love, K. T.; Sunshine, J.; Langer, R.; Anderson, D. G. *Nano Lett.* **2009**, *9*, 2402-2406.
(116)Lee, J.-H.; Lee, K.; Moon, S. H.; Lee, Y.; Park, T. G.; Cheon, J. *Angew. Chem., Int. Ed.* **2009**, *48*, 4174-4179.
(117)Medarova, Z.; Pham, W.; Farrar, C.; Petkova, V.; Moore, A. *Nat. Med.* **2007**, *13*, 372-377.
(118)Kam, N. W. S.; Liu, Z.; Dai, H. *J. Am. Chem. Soc.* **2005**, *127*, 12492-12493.
(119)Liu, Z.; Winters, M.; Holodniy, M.; Dai, H. *Angew. Chem., Int. Ed.* **2007**, *46*, 2023-2027.

(120)Yang, R.; Yang, X.; Zhang, Z.; Zhang, Y.; Wang, S.; Cai, Z.; Jia, Y.; Ma, Y.; Zheng, C.; Lu, Y.; Roden, R.; Chen, Y. *Gene Ther.* **2006**, *13*, 1714-1723.
(121)Woodrow, K. A.; Cu, Y.; Booth, C. J.; Saucier-Sawyer, J. K.; Wood, M. J.; Saltzman, W. M. *Nat. Mater.* **2009**, *8*, 526-533.
(122)Patil, Y.; Panyam, J. *Int. J. Pharm.* **2009**, *367*, 195-203.
(123)Murata, N.; Takashima, Y.; Toyoshima, K.; Yamamoto, M.; Okada, H. *J. Controlled Release* **2008**, *126*, 246-254.
(124)Singh, A.; Nie, H.; Ghosn, B.; Qin, H.; Kwak, L. W.; Roy, K. *Mol. Ther.* **2008**, *16*, 2011-2021.
(125)Mountziaris, P. M.; Sing, D. C.; Chew, S. A.; Tzouanas, S. N.; Lehman, E. D.; Kasper, F. K.; Mikos, A. G. *Pharm. Res.* **2010**.
(126)Alshamsan, A.; Haddadi, A.; Hamdy, S.; Samuel, J.; El-Kadi, A. O. S.; Uludağ, H.; Lavasanifar, A. *Mol. Pharmaceutics* **2010**, *7*, 1643-1654.
(127)Alexander, C.; Shakesheff, K. M. *Adv. Mater.* **2006**, *18*, 3321-3328.
(128)Tirelli, N. *Curr. Opin. Colloid Interface Sci.* **2006**, *11*, 210-216.
(129)Vandenbroucke, R. E.; De Geest, B. G.; Bonné, S.; Vinken, M.; Haecke, T. V.; Heimberg, H.; Wagner, E.; Rogiers, V.; De Smedt, S. C.; Demeester, J.; Sanders, N. N. *J. Gene Med.* **2008**, *10*, 783-794.
(130)Nguyen, J.; Steele, T. W. J.; Merkel, O.; Reul, R.; Kissel, T. *J. Controlled Release* **2008**, *132*, 243-251.
(131)Dickinson, B. C.; Srikun, D.; Chang, C. J. *Curr. Opin. Chem. Biol.* **2010**, *14*, 50-56.
(132)Waris, G.; Ahsan, H. *J. Carcinog.* **2006**, *5*.
(133)Fang, J.; Seki, T.; Maeda, H. *Adv. Drug Delivery Rev.* **2009**, *61*, 290-302.
(134)Finkel, T.; Serrano, M.; Blasco, M. A. *Nature* **2007**, *448*, 767-774.
(135)Ishikawa, K.; Takenaga, K.; Akimoto, M.; Koshikawa, N.; Yamaguchi, A.; Imanishi, H.; Nakada, K.; Honma, Y.; Hayashi, J. *Science* **2008**, *320*, 661-664.
(136)Nishikawa, T.; Araki, E. *Antioxid. Redox Signaling* **2007**, *9*, 343-353.
(137)Newsholme, P.; Haber, E. P.; Hirabara, S. M.; Rebelato, E. L. O.; Procopio, J.; Morgan, D.; Oliveira-Emilio, H. C.; Carpinelli, A. R.; Curi, R. *J. Physiol. (Oxford, U.K.)* **2007**, *583*, 9-24.
(138)Singh, R. B.; Mengi, S. A.; Xu, Y.-J.; Arneja, A. S.; Dhalla, N. S. *Exp. Clin. Cardiol.* **2002**, *7*, 40-53.
(139)Sarkar, D.; Fisher, P. B. *Cancer Lett. (Shannon, Irel.)* **2006**, *236*, 13-23.
(140)Schwarz, K. B. *Free Radical Biol. Med.* **1996**, *21*, 641-649.
(141)Stoner, J. D.; Clanton, T. L.; Aune, S. E.; Angelos, M. G. *Am. J. Physiol.* **2007**, *292*, H109-H116.
(142)Barnham, K. J.; Masters, C. L.; Bush, A. I. *Nat. Rev. Drug Disc.* **2004**, *3*, 205-214.
(143)Lin, M. T.; Beal, M. F. *Nature* **2006**, *443*, 787-795.
(144)Wilson, D. S.; Dalmasso, G.; Wang, L.; Sitaraman, S. V.; Merlin, D.; Murthy, N. *Nat. Mater.* **2010**, *9*, 923-928.
(145)Tannock, I. F.; Rotin, D. *Cancer Res.* **1989**, *49*, 4373-4384.
(146)Stubbs, M.; McSheehy, P. M. J.; Griffiths, J. R.; Bashford, C. L. *Mol. Med. Today* **2000**, *6*, 15-19.
(147)Helmlinger, G.; Sckell, A.; Dellian, M.; Forbes, N. S.; Jain, R. S. *Clin. Cancer Res.* **2002**, *8*, 1284-1291.
(148)Kellum, J. A.; Song, M.; Li, J. *Crit. Care* **2004**, *8*, 331-336.

(149)Andreev, O. A.; Dupuy, A. D.; Segala, M.; Sandugu, S.; Serra, D. A.; Chichester, C. O.; Engelman, D. M.; Reshetnyak, Y. K. *Proc. Natl. Acad. Sci. U. S. A.* **2007**, *104*, 7893-7898.
(150)Lynn, D. M.; Amiji, M. M.; Langer, R. *Angew. Chem. Int. Ed.* **2001**, *40*, 1707-1710.
(151)Heffernan, M. J.; Murthy, N. *Bioconjugate Chem.* **2005**, *16*, 1340-1342.
(152)Sawant, R. M.; Hurley, J. P.; Salmaso, S.; Kale, A.; Tolcheva, E.; Levchenko, T. S.; Torchilin, V. P. *Bioconjugate Chem.* **2006**, *17*, 943-949.
(153)Paramonov, S. E.; Bachelder, E. M.; Beaudette, T. T.; Standley, S. M.; Lee, C. C.; Dashe, J.; Fréchet, J. M. J. *Bioconjugate Chem.* **2008**, *19*, 911-919.
(154)Park, T. G.; Jeong, J. H.; Kim, S. W. *Adv. Drug Delivery Rev.* **2006**, *58*, 467-486.
(155)Behr, J.-P. *Chimia* **1997**, *51*, 34-36.
(156)Sonawane, N. D.; Szoka, F. C.; Verkman, A. S. *J. Biol. Chem.* **2003**, *278*, 44826-44831.
(157)Akinc, A.; Thomas, M.; Klibanov, A. M.; Langer, R. *J. Gene Med.* **2005**, *7*, 657-663.
(158)Anderson, D. G.; Akinc, A.; Hossain, N.; Langer, R. *Mol. Ther.* **2005**, *11*, 426-434.
(159)Zugates, G. T.; Tedford, N. C.; Zumbuehl, A.; Jhunjhunwala, S.; Kang, C. S.; Griffith, L. G.; Lauffenburger, D. A.; Langer, R.; Anderson, D. G. *Bioconjugate Chem.* **2007**, *18*, 1887-1896.
(160)Green, J. J.; Zugates, G. T.; Langer, R.; Anderson, D. G. *Methods Mol. Biol.* **2009**, *480*, 1-11.
(161)Yadav, S.; van Vlerken, L. E.; Little, S. R.; Amiji, M. M. *Cancer Chemother. Pharmacol.* **2009**, *63*, 711-722.
(162)Hu, Y.; Atukorale, P. U.; Lu, J. J.; Moon, J. J.; Um, S. H.; Cho, E. C.; Wang, Y.; Chen, J.; Irvine, D. J. *Biomacromolecules* **2009**, *10*, 756-765.
(163)Wittmar, M.; Unger, F.; Kissel, T. *Macromolecules* **2006**, *39*, 1417-1424.
(164)Unger, F.; Wittmar, M.; Kissel, T. *Biomaterials* **2007**, *28*, 1610-1619.
(165)Oster, C. G.; Wittmar, M.; Unger, F.; Barbu-Tudoran, L.; Schaper, A. K.; Kissel, T. *Pharm. Res.* **2004**, *21*, 927-931.
(166)Unger, F.; Wittmar, M.; Morell, F.; Kissel, T. *Biomaterials* **2008**, *29*, 2007-2014.
(167)Wittmar, M.; Ellis, J. S.; Morell, F.; Unger, F.; Schumacher, J. C.; Roberts, C. J.; Tendler, S. J. B.; Davies, M. C.; Kissel, T. *Bioconjugate Chem.* **2005**, *16*, 1390-1398.
(168)Okada, C. Y.; Rechsteiner, M. *Cell* **1982**, *29*, 33-41.
(169)Standley, S. M.; Kwon, Y. J.; Murthy, N.; Kunisawa, J.; Shastri, N.; Guillaudeu, S. J.; Lau, L.; Fréchet, J. M. J. *Bioconjugate Chem.* **2004**, *15*, 1281-1288.
(170)Lee, S.; Yang, S. C.; Kao, C.-Y.; Pierce, R. H.; Murthy, N. *Nucleic Acids Res.* **2009**, *37*, e145.
(171)Yang, S. C.; Bhide, M.; Crispe, I. N.; Pierce, R. H.; Murthy, N. *Bioconjugate Chem.* **2008**, *19*, 1164-1169.
(172)Murthy, N.; Thng, Y. X.; Schuck, S.; Xu, M. C.; Fréchet, J. M. J. *J. Am. Chem. Soc.* **2002**, *124*, 12398-12399.
(173)Murthy, N.; Xu, M. C.; Schuck, S.; Kunisawa, J.; Shastri, N.; Fréchet, J. M. J. *Proc. Natl. Acad. Sci. U. S. A.* **2003**, *100*, 4995-5000.
(174)Kwon, Y. J.; James, E.; Shastri, N.; Fréchet, J. M. J. *Proc. Natl. Acad. Sci. U. S. A.* **2005**, *102*, 18264-18268.
(175)Goh, S. L.; Murthy, N.; Xu, M. C.; Fréchet, J. M. J. *Bioconjugate Chem.* **2004**, *15*, 467-474.
(176)Kwon, Y. J.; Standley, S. M.; Goh, S. L.; Fréchet, J. M. J. *J. Controlled Release* **2005**, *105*, 199-212.

(177)Kwon, Y. J.; Standley, S. M.; Goodwin, A. P.; Gillies, E. R.; Fréchet, J. M. J. *Mol. Pharmaceutics* **2005**, *2*, 83-91.
(178)Standley, S. M.; Mende, I.; Goh, S. L.; Kwon, Y. J.; Beaudette, T. T.; Engleman, E. G.; Fréchet, J. M. J. *Bioconjugate Chem.* **2007**, *18*, 77-83.
(179)Cohen, J. L.; Almutairi, A.; Cohen, J. A.; Bernstein, M.; Brody, S. L.; Schuster, D. P.; Fréchet, J. M. J. *Bioconjugate Chem.* **2008**, *19*, 876-881.
(180)Cohen, J. A.; Beaudette, T. T.; Tseng, W. W.; Bachelder, E. M.; Mende, I.; Engleman, E. G.; Fréchet, J. M. J. *Bioconjugate Chem.* **2009**, *20*, 111-119.
(181)Beaudette, T. T.; Bachelder, E. M.; Cohen, J. A.; Obermeyer, A. C.; Broaders, K. E.; Fréchet, J. M. J. *Mol. Pharmaceutics* **2009**, *6*, 1160-1169.
(182)Liu, Y.; Ibricevic, A.; Cohen, J. A.; Cohen, J. L.; Gunsten, S. P.; Fréchet, J. M. J.; Walter, M. J.; Welch, M. J.; Brody, S. L. *Mol. Pharmaceutics* **2009**, *6*, 1891-1902.
(183)Bachelder, E. M.; Beaudette, T. T.; Broaders, K. E.; Dashe, J.; Fréchet, J. M. J. *J. Am. Chem. Soc.* **2008**, *130*, 10494-10495.
(184)Broaders, K. E.; Cohen, J. A.; Beaudette, T. T.; Bachelder, E. M.; Fréchet, J. M. J. *Proc. Natl. Acad. Sci. U. S. A.* **2009**, *106*, 5497-5502.
(185)Beaudette, T. T.; Cohen, J. A.; Bachelder, E. M.; Broaders, K. E.; Cohen, J. L.; Engleman, E. G.; Fréchet, J. M. J. *J. Am. Chem. Soc.* **2009**, *131*, 10360-10361.
(186)Bachelder, E. M.; Beaudette, T. T.; Broaders, K. E.; Fréchet, J. M. J.; Albrecht, M. T.; Mateczun, A. J.; Ainslie, K. M.; Pesce, J. T.; Keane-Myers, A. M. *Mol. Pharmaceutics* **2010**, *7*, 826-835.
(187)Cohen, J. A.; Beaudette, T. T.; Cohen, J. L.; Broaders, K. E.; Bachelder, E. M.; Fréchet, J. M. J. *Adv. Mater.* **2010**, *22*, 3593-3597.
(188)Thomas, M.; Lu, J. J.; Chen, J.; Klibanov, A. M. *Adv. Drug Delivery Rev.* **2007**, *59*, 124-133.
(189)Labiris, N. R.; Dolovich, M. B. *Br. J. Clin. Pharmacol.* **2003**, *56*, 588-599.
(190)Sanders, N.; Rudolph, C.; Braeckmans, K.; De Smedt, S. C.; Demeester, J. *Adv. Drug Delivery Rev.* **2009**, *61*, 115-127.
(191)Lam, J. K.-W.; Liang, W.; Chan, H.-K. *Adv. Drug Delivery Rev.* **2011**, doi:10.1016/j.addr.2011.02.006.
(192)Wanner, A.; Salathé, M.; O'Riordan, T. G. *Am. J. Respir. Crit. Care Med.* **1996**, *154*, 1868-1902.
(193)Lippmann, M.; Yeates, D. B.; Albert, R. E. *Br. J. Ind. Med.* **1980**, *37*, 337-362.
(194)Knowles, M. R.; Boucher, R. C. *J. Clin. Invest.* **2002**, *109*, 571-577.
(195)Lai, S. K.; Wang, Y.-Y.; Hanes, J. *Adv. Drug Delivery Rev.* **2009**, *61*, 158-171.
(196)Rosenecker, J.; Naundorf, S.; Gersting, S. W.; Hauck, R. W.; Gessner, A.; Nicklaus, P.; Müller, R. H.; Rudolph, C. *J. Gene Med.* **2003**, *5*, 49-60.
(197)Duncan, J. E.; Whitsett, J. A.; Horowitz, A. D. *Hum. Gene Ther.* **1997**, *8*, 431-438.
(198)Petros, R. A.; DeSimone, J. M. *Nat. Rev. Drug Disc.* **2010**, *9*, 615-627.
(199)Heyder, J.; Gebhart, J.; Rudolf, G.; Schiller, C. F.; Stahlhofen, W. *J. Aerosol. Sci.* **1986**, *17*, 811-825.
(200)Heyder, J.; Svartengren, M. U. In *Drug delivery to the lung*; Bisgaard, H., O'Callaghan, C., Smaldone, G. C., Eds.; Marcel Dekker: New York, 2002, p 38.
(201)Newman, S. P.; Agnew, J. E.; Pavia, D.; Clarke, S. W. *Clin. Phys. Physiol. Meas.* **1982**, *3*, 1-20.

(202)Scheuch, G.; Kohlhaeufl, M. J.; Brand, P.; Siekmeier, R. *Adv. Drug Delivery Rev.* **2006**, *58*, 996-1008.
(203)Edwards, D. A.; Hanes, J.; Caponetti, G.; Hrkach, J.; Ben-Jebria, A.; Eskew, M. L.; Mintzes, J.; Deaver, D.; Lotan, N.; Langer, R. *Science* **1997**, *276*, 1868-1871.
(204)Edwards, D. A.; Ben-Jebria, A.; Langer, R. *J. Appl. Physiol.* **1998**, *85*, 379-385.
(205)Bennett, W. D.; Brown, J. S.; Zeman, K. L.; Hu, S.-C.; Scheuch, G.; Sommerer, K. *J. Aerosol Med.* **2002**, *15*, 179-188.
(206)Lai, S. K.; Wang, Y.-Y.; Hanes, J. *Adv. Drug Delivery Rev.* **2009**, *61*, 158-171.
(207)Yamamoto, H.; Kuno, Y.; Sugimoto, S.; Takeuchi, H.; Kawashima, Y. *J. Controlled Release* **2005**, *102*, 373-381.
(208)Mao, S.; Sun, W.; Kissel, T. *Adv. Drug Delivery Rev.* **2010**, *62*, 12-27.
(209)Howard, K. A.; Fahbek, U. L.; Liu, X.; Damgaard, C. K.; Glud, S. Z.; Anderson, M. Ø.; Hovgaard, M. B.; Schmitz, A.; Nyengaard, J. R.; Besenbacher, F.; Kjems, J. *Mol. Ther.* **2006**, *14*, 476-484.
(210)Nielsen, E. J. B.; Nielsen, J. M.; Becker, D.; Karlas, A.; Prakash, H.; Glud, S. Z.; Merrison, J.; Besenbacher, F.; Meyer, T. F.; Kjems, J.; Howard, K. A. *Pharm. Res.* **2010**, *27*, 2520-2527.
(211)Lai, S. K.; O'Hanlon, D. E.; Harrold, S.; Man, S. T.; Wang, Y.-Y.; Cone, R.; Hanes, J. *Proc. Natl. Acad. Sci. U. S. A.* **2007**, *104*, 1482-1487.
(212)Wang, Y.-Y.; Lai, S. K.; Suk, J. S.; Pace, A.; Cone, R.; Hanes, J. *Angew. Chem. Int. Ed.* **2008**, *47*, 9726-9729.
(213)Tang, B. C.; Dawson, M.; Lai, S. K.; Wang, Y.-Y.; Suk, J. S.; Yang, M.; Zeitlin, P.; Boyle, M. P.; Fu, J.; Hanes, J. *Proc. Natl. Acad. Sci. U. S. A.* **2009**, *106*, 19268-19273.
(214)Yang, M.; Lai, S. K.; Wang, Y.-Y.; Zhong, W.; Happe, C.; Zhang, M.; Fu, J.; Hanes, J. *Angew. Chem. Int. Ed.* **2011**, *50*, 2597-2600.
(215)Oba, M.; Aoyagi, K.; Miyata, K.; Matsumoto, Y.; Itaka, K.; Nishiyama, N.; Yamasaki, Y.; Koyama, H.; Kataoka, K. *Mol. Pharmaceutics* **2008**, *5*, 1080-1092.
(216)Kwon, Y. J.; James, E.; Shastri, N.; Fréchet, J. M. J. *Proc. Natl. Acad. Sci. U. S. A.* **2005**, *102*, 18264-18268.
(217)Farokhzad, O. C.; Cheng, J.; Teply, B. A.; Sherifi, I.; Jon, S.; Kantoff, P. W.; Richie, J. P.; Langer, R. *Proc. Natl. Acad. Sci. U. S. A.* **2006**, *103*, 6315-6320.
(218)Li, S.; Tan, Y.; Viroonchatapan, E.; Pitt, B. R.; Huang, L. *Am. J. Physiol.* **2000**, *278*, L504-L511.
(219)Rossin, R.; Muro, S.; Welch, M. J.; Muzykantov, V. R.; Schuster, D. P. *J. Nucl. Med.* **2008**, *49*, 103-111.
(220)Muro, S.; Garnacho, C.; Champion, J. A.; Leferovich, J.; Gajewski, C.; Schuchman, E. H.; Mitragotri, S.; Muzykantov, V. R. *Mol. Ther.* **2008**, *16*, 1450-1458.
(221)Calderon, A. J.; Bhowmick, T.; Leferovich, J.; Burman, B.; Pichette, B.; Muzykantov, V. R.; Eckmann, D. M.; Muro, S. *J. Controlled Release* **2011**, *150*, 37-44.
(222)Guo, J.; Fisher, K. A.; Darcy, R.; Cryan, J. F.; O'Driscoll, C. *Mol. BioSyst.* **2010**, *6*, 1143-1161.
(223)Edelstein, M. L.; Abedi, M. R.; Wixon, J. *J. Gene Med.* **2007**, *9*, 833-842.
(224)de Fougerolles, A.; Vornlocher, H.-P.; Maraganore, J.; Lieberman, J. *Nat. Rev. Drug Discovery* **2007**, *6*, 443-453.

(225)Kaiser, P. K.; Symons, R. C.; Shah, S. M.; Quinlan, E. J.; Tabandeh, H.; Do, D. V.; Reisen, G.; Lockridge, J. A.; Short, B.; Guerciolini, R.; Nguyen, Q. D. *Am. J. Ophthalmol* **2010**, *150*, 33-39.e2.
(226)Zamora, M. R.; Budev, M.; Rolfe, M.; Gottlieb, J.; Humar, A.; DeVincenzo, J.; Vaishnaw, A.; Cehelsky, J.; Albert, G.; Nochur, S.; Gollob, J. A.; Glanville, A. R. *Am. J. Respir. Crit. Care Med.* **2011**, *183*, 531-538.
(227)Davis, M. E.; Zuckerman, J. E.; Choi, C. H. J.; Seligson, D.; Tolcher, A.; Alabi, C. A.; Yen, Y.; Heidel, J. D.; Ribas, A. *Nature* **2010**, *464*, 1067-1070.
(228)Davis, M. E. *Mol. Pharmaceutics* **2009**, *6*, 659-668.
(229)Bartlett, D.; Davis, M. E. *Biotechnol. Bioeng.* **2008**, *99*, 975-985.
(230)Heidel, J. D.; Yu, Z.; Liu, J. Y.-C.; Rele, S. M.; Liang, Y.; Zeidan, R. K.; Kornbrust, D. J.; Davis, M. E. *Proc. Natl. Acad. Sci. U. S. A.* **2007**, *104*, 5715-5721.

Chapter 2 – Synthesis and Initial Biological Evaluation of Acid-Degradable Particles Functionalized with Cell-Penetrating Peptides

Abstract

Biopharmaceuticals, such as proteins and DNA, have demonstrated their potential to prevent and cure diseases. The success of such therapeutic agents hinges upon their ability to cross complex barriers in the body and reach their target intact. In order to reap the full benefits of these therapeutic agents, a delivery vehicle capable of delivering cargo to all cell types, both phagocytic and non-phagocytic, is needed. The lung is a particularly attractive target for drug delivery due to the possibility of direct and non-invasive administration via inhalation aerosols. However, pulmonary delivery is complicated by the complexity of the anatomic structure of the human respiratory system as well as the diversity of cell types present. In this chapter, we describe the synthesis, characterization, and initial biological evaluation of acid-degradable microparticles which may be suitable delivery vehicles for use in lung imaging and therapy. This microparticle delivery vehicle is capable of cell penetration and sub-cellular triggered release of an encapsulated payload. pH-sensitive polyacrylamide particles functionalized with a polyarginine cell-penetrating peptide (CPP) were synthesized. The incorporation of a CPP into the microparticles led to efficient uptake by non-phagocytic lung epithelial cells in culture. In addition, the CPP-modified particles showed no cytotoxic effects at concentrations used in this study. The results suggest that these particles may provide a vehicle for the successful delivery of therapeutic agents to various cell types in the lung.

Introduction

In addition to small-molecule based drugs, biopharmaceuticals, such as proteins and DNA, have tremendous potential to prevent and cure diseases.[1-3] Currently there are over 400 biotechnology medicines in development for the treatment of over 100 diseases, including medications to treat or help prevent multiple sclerosis, hepatitis, breast cancer, and diabetes.[4] The widespread success of such therapeutic agents hinges upon their ability to cross complex barriers in the body and to reach their target intact. Exogenous therapeutic agents are notoriously unstable in the harsh *in vivo* environment due to proteolytic degradation, sequestration, and renal clearance. These factors limit their use as therapeutic agents. However, encapsulation strategies have successfully mitigated some of these stability and delivery issues by providing protection from physical and chemical damage.[5-11] Recent advances in polymer synthesis have allowed formulations capable of encapsulation and controlled release of macromolecular therapeutic agents, thereby increasing their stability and ultimately their bioavailability.[12-15] In addition, by incorporating certain ligands or compounds into the polymer backbone, it is possible to enhance delivery and targeting of the vehicle.[16,17] A recent delivery strategy involves the use of cell-penetrating peptides to enhance cellular uptake of cargo by non-phagocytic cells.[18] Herein, we show the integration of ligands for cell penetration and subcellular triggered release in a single delivery vehicle.

Biodegradable polymers have been extensively investigated as potential carriers for biopharmaceuticals.[19-21] Delivery of a therapeutic agent via encapsulation in particles incorporating programmed release mechanisms, such as acid-degradable crosslinks, allows for

their controlled release at select targets, such as inflammatory tissues, tumors, and cells of the immune system. This selective delivery through triggered release mechanisms enables enhanced therapeutic efficiency, allowing lower doses of the therapeutic agent to be used, with less toxicity.[22-27] Recently, we described the synthesis of polyacrylamide microparticles that incorporated acid-labile crosslinks into the polymer scaffold, as well as targeting groups on the surface.[28-31] These acid-degradable particles were capable of encapsulating and delivering a protein antigen to phagocytic cells of the immune system, specifically macrophages and dendritic cells. These cell types specialize in taking up foreign matter and trafficking it to acidic sub-cellular lysosomal compartments. After the particles are phagocytosed in this manner, they degrade rapidly in the acidic lysosome, causing the protein payload to be released into the cytoplasm.[29,30,32] This is hypothesized to occur through the destabilization of the lysosomal membrane as a result of the sudden increase in osmotic pressure, due to particle swelling and degradation.[33]

The size of these particles (ranging from 200 nm to 1 μm in diameter) makes them well-suited for uptake by phagocytic cells, such as macrophages and dendritic cells. Thus, these particles have demonstrated great success at delivering a protected payload to cells of the immune system.[31,34] However, the majority of cells in the human body are non-phagocytic, meaning that they are not efficient at ingesting foreign matter and particulates. As a result, access to the lysosomal delivery pathway in non-phagocytic cells is limited, making it difficult to reap the full benefits of therapeutic delivery systems, such as the hydrogel system described above. Thus, one of the most important challenges facing the use of these particles to deliver therapeutic agents is overcoming their lack of uptake by non-phagocytic cells. This problem has motivated work toward making new delivery vehicles capable of encapsulation, cell membrane penetration, and programmed release. Our aim is to design a delivery vehicle that possesses these three properties. In order to create a universal delivery vehicle which would allow for the delivery of cargo to non-phagocytic cells, we have modified our existing delivery system for phagocytic cells by incorporating a cell-penetrating peptide into our pH-sensitive particles.

Cell membranes act as protective barriers for the cell, only allowing compounds within a narrow range of molecular size, polarity, and charge to enter. Overcoming the barrier of the cell membrane to deliver membrane-impermeable cargoes often requires harsh methods such as electroporation or liposomal transfection. These methods are limited to *in vitro* applications and often cause unwanted cellular effects, such as high cytotoxicity.[35] A more recently developed delivery strategy involves the use of cell-penetrating peptides. Cell-penetrating peptides (CPPs) are peptides with up to 30 amino acids with the ability to translocate across cell membranes of various cell types.[36] CPPs have been used to deliver a range of cargoes including proteins, DNA, antisense peptide nucleic acids, small-molecule drugs, liposomes, and nanoparticles into the cell both *in vitro* and *in vivo*[37] without disturbing the stability of the cell membrane and with low cytotoxic effects. CPPs offer several appealing properties as delivery agents including applicability to many cell types, no apparent size constraint of the cargo, and seemingly no immunogenic or inflammatory properties.[36] CPPs consist of a diverse group of peptides derived from such sources as HIV-Tat, the third helix of the homeodomain of Antennapedia, VP22 herpes virus protein, and other synthetic peptides,[38] including various arginine-rich sequences.[39-44] One common feature among these CPPs is the high number of cationic residues, such as arginine. In one study, it was found that the HIV-Tat sequence could be replaced with a simple nonamer of arginine,[45] suggesting that the guanidinium headgroup of arginine is the essential component of this sequence's ability to transport cargoes into the cell.[41,46,47] In addition to the

guanidine headgroup, other factors such as the number of arginine residues[47,48] and the length of the side chain[41] were found to be important factors in the control of translocation.

Building on our previous work, we describe the synthesis and evaluation of a new delivery vehicle for biopharmaceuticals. A cell-penetrating peptide (CPP) consisting of nine arginine residues was incorporated into acid-degradable polyacrylamide particles to enhance cellular uptake by non-phagocytic cells. Incorporation of the CPP was achieved by copolymerizing a functional monomer **2** with an acid-degradable crosslinker **1** and acrylamide (Figure 2.1). The cell uptake of these modified particles in two epithelial cell lines was then investigated. We demonstrate that the incorporation of a CPP into the microparticles led to efficient uptake by non-phagocytic cells in culture with minimal cytotoxic effects.

Results and Discussion

Preparation and Characterization of Microparticles Containing a Cell-Penetrating Peptide.

The pH sensitivity of our microparticulate delivery system is imparted by an acetal-containing crosslinker **1** (Figure 2.1). This dimethyl acetal crosslinker is relatively stable to hydrolysis under physiological conditions (pH 7.4) but degrades rapidly under the acidic conditions typically found in lysosomes (pH 5.0–5.5).[28] Incorporation of oligo(ethylene glycol) substituents enhances the solubility of the crosslinker in aqueous solution, an essential characteristic for the inverse emulsion polymerization technique used to prepare the particles. The inverse emulsion process allows for the encapsulation of hydrophilic molecules such as protein and DNA in the particles. Hydrolysis of crosslinker **1** produces acetone, a relatively non-toxic metabolic intermediate of fatty acid oxidation.

Particles containing a CPP were prepared using a 10 amino acid sequence that was modified on the N-terminus with an acrylamide group, **2** (Figure 2.1). This acrylamide moiety enables the direct incorporation of the peptide into the particle during its preparation. The sequence selected for use in the particles was acrylamide-Y-$(R)_9$-COOH because nona-arginine has been shown to be the most effective cell-penetrating peptide known today that is composed of natural L-amino acid residues.[41,49] Nona-arginine (R_9) was shown to be 20-fold more efficient than HIV-$Tat_{49–57}$ at cellular uptake.[41] A tyrosine residue was also incorporated into the peptide sequence to allow for radiolabeling of the peptide for future *in vivo* studies.

Microparticles encapsulating bovine serum albumin-Alexa Fluor 488 (BSA-Alexa Fluor 488), a model protein conjugated with a fluorescent tracer, and including CPP were successfully prepared and characterized to investigate the possibility of enhancing cellular uptake of the particles by non-phagocytic cells. The particles were prepared using an inverse emulsion polymerization technique similar to one described previously,[30] forming protein-loaded polymer particles incorporating CPP. In this process, CPP and BSA-Alexa Fluor 488 conjugate were dissolved in an aqueous buffer along with acrylamide, acid-sensitive crosslinker **1**, and ammonium persulfate. The aqueous phase was then dispersed as droplets in an organic phase consisting of hexanes and a mixture of two surfactants. Free-radical polymerization was initiated by the addition of ammonium persulfate and TMEDA, resulting in cross-linked polymer particles decorated with cell-penetrating peptide throughout the particles but most importantly at the surface. A schematic representation of the synthesis and subsequent degradation of these particles is depicted in Figure 2.1. Exposure of the cross-linked particles to an acidic environment leads to rapid hydrolysis of the acetal linkages. Degradation of the polymer particles thus results in the release of BSA-Alexa Fluor 488, acetone, and the CPP-containing polymer backbone.

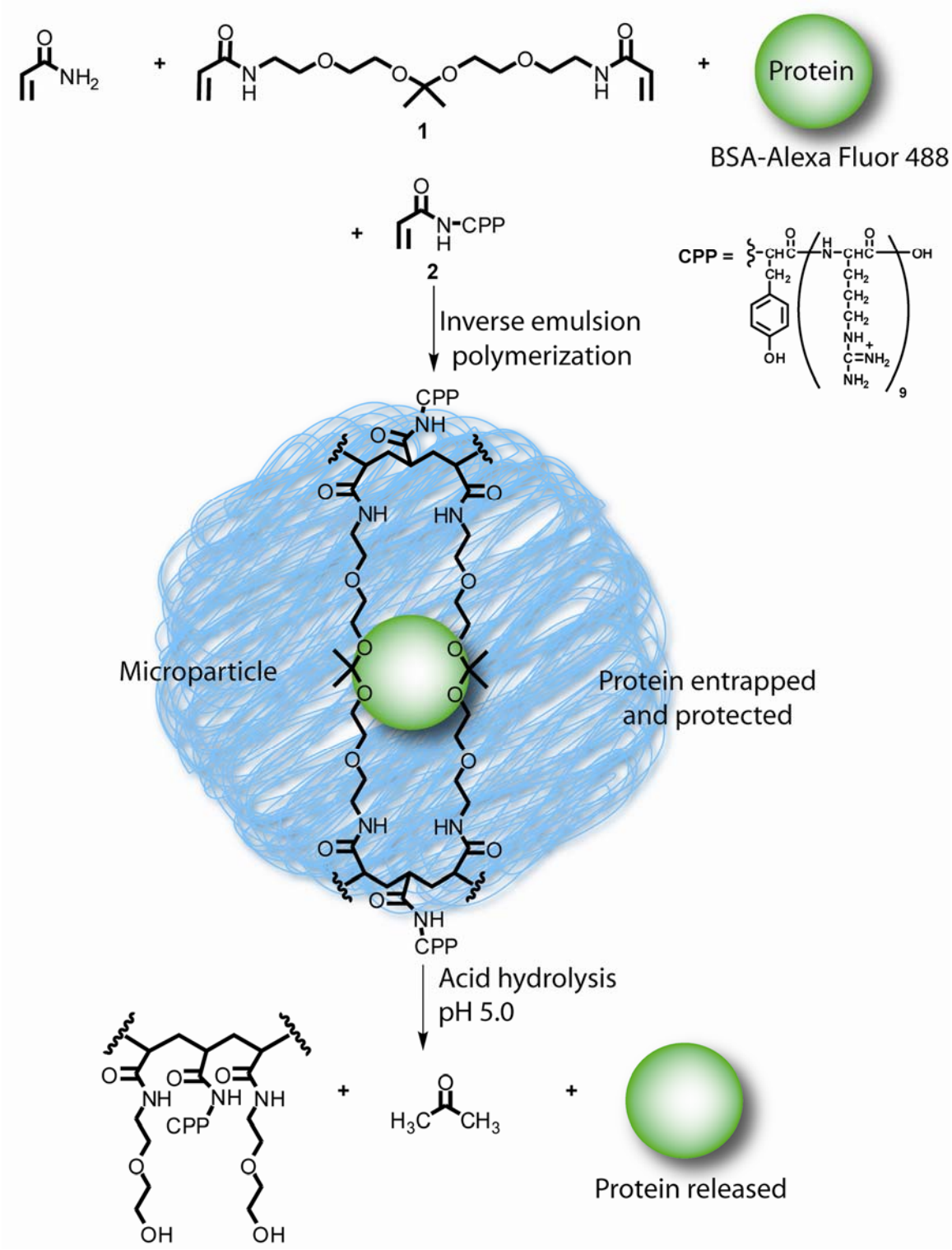

Figure 2.1. General scheme for the preparation and acid-catalyzed degradation of CPP-modified microparticles loaded with protein.

The isolated particles analyzed in the dry state using scanning electron microscopy (Figure 2.2) had sizes ranging from 0.2 to 1 μm. Peptide incorporation was measured by degrading a sample of particles under acidic conditions and analyzing the concentration of peptide using a bicinchoninic acid (BCA) assay, a colorimetric detection method used for the quantification of proteins. In this method, BCA acts as the detection reagent for Cu^{+1}, which is formed when Cu^{+2} is reduced by protein in an alkaline environment.[50] Using this method, the peptide content in the particles was found to be 1.7% by mass.

Unmodified microparticles free of CPP were also prepared using the same inverse emulsion method but omitting monomer **2**. These particles contain the same mole percent of crosslinking acetal as the functionalized particles described above. Non-degradable microparticles both with and without cell-penetrating peptide were also prepared as described above using *N,N′*-methylene-bis-acrylamide as the crosslinker instead of monomer **1**. SEM examination of these particles showed that they were similar in size and shape to the degradable CPP-modified particles (data not shown).

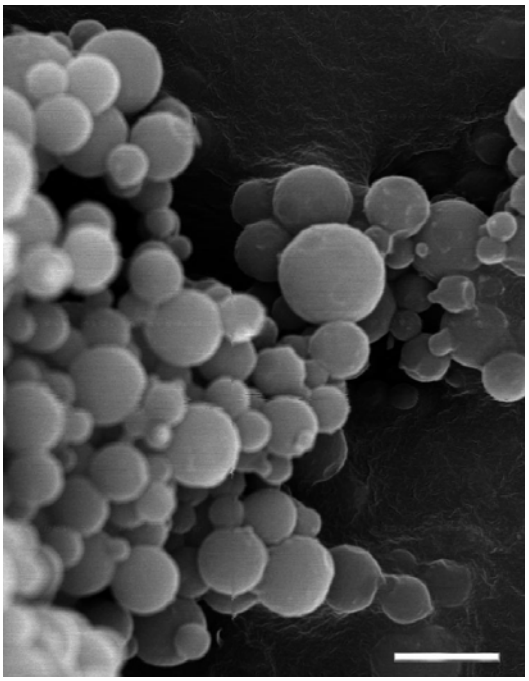

Figure 2.2. Representative SEM image of CPP-modified microparticles. The scale bar is equal to 1 μm.

Cellular Uptake of CPP-Modified Microparticles by Non-Phagocytic Cells.

The effect of the CPP modification of the microparticles on their interaction with BEAS-2B epithelial cells is shown in Figure 2.3. In the absence of microparticle incubation, cell membranes and elements of the intracellular actin skeleton are clearly evident by phalloidin staining. As expected, no fluorescence from the Alexa Fluor 488 is seen, even at high magnification. When cells were incubated with unmodified non-degradable microparticles (panel A), midcell images obtained by confocal microscopy showed little fluorescence - only visible under high magnification - despite 24 h of incubation time. In contrast, the intracellular accumulation of CPP-modified non-degradable microparticles over the 24 h incubation period was readily evident.

Much research has been done to elucidate the mechanism by which cell-penetrating peptides mediate the transport of various cargoes across the cell membrane. The punctate appearance of microparticles within the cells shown in Figure 2.3 is consistent with endosomally mediated uptake. Studies by others suggest that uptake is facilitated by positively charged arginine residues (including those present in the CPP used in this study) forming bidentate hydrogen bonds with negatively charged phosphates, sulfates, and carboxylates on the cell surface.[49,51]

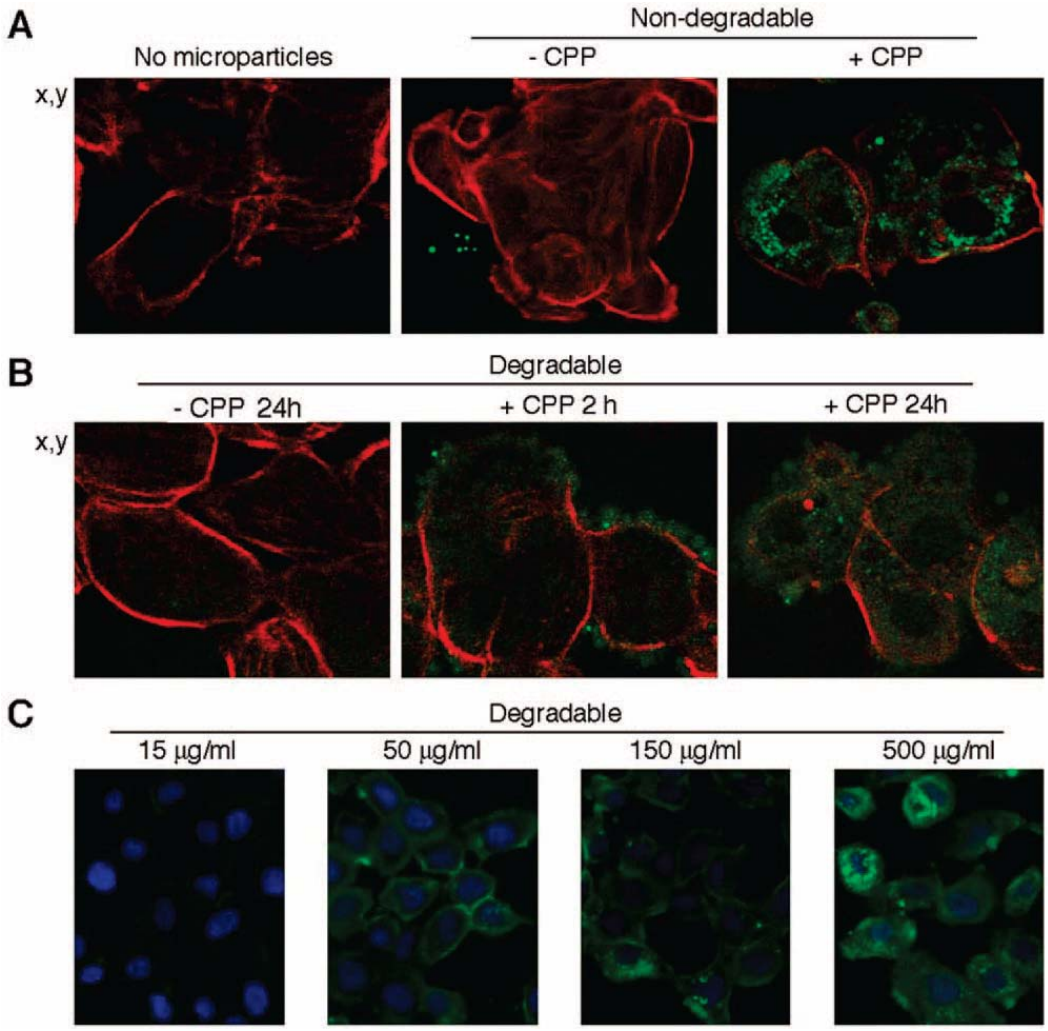

Figure 2.3. Representative confocal microscope images of BEAS-2B cells, taken at midcell level, 24 h after incubation with microparticles. Cell membranes and cytoskeleton are stained red by phalloidin. Panel A: The cellular accumulation of CPP-modified microparticles 500 µg/mL is markedly greater compared with cells incubated with particles without CPP modification. Panel B: A time dependency is seen when cells are incubated with microparticles at room temperature. At 2 h, most particles appear to be adherent on the cell surface. By 24 h, intracellular accumulation has increased markedly. Note also that the overall fluorescence appears to be more diffuse and less intense than with non-degradable particles. Panel C: Increasing fluorescence is seen intracellularly as microparticle concentration is increased in the medium.

These results can be contrasted with those observed after cells were incubated with acid-degradable microparticles (panel B, Figure 2.3). In the absence of the CPP modification, only low levels of fluorescence were seen intracellularly, even after 24 h of incubation (again, most evident at high magnification). With CPP modification, however, high levels of fluorescence are obvious. After just 2 h incubation, microparticles are present both intracellularly as well as clustered on the cell surface. A similar pattern was seen when HeLa cells were incubated with

acid-degradable CPP-modified microparticles (data not shown). This association with the cell membrane is probably due to the hydrogen bonding ability of the guanidine headgroup of arginine and the highly cationic nature of the cell-penetrating peptide. After 24 h incubation, the intracellular accumulation of the microparticles is even greater. Again, a similar phenomenon was observed when HeLa cells were incubated with these microparticles. Furthermore, in addition to a time dependency, the accumulation of the CPP-modified microparticles was also concentration-dependent (panel C, Figure 2.3).

Note, however, that the intensity of fluorescence is more diffuse and less intense than when cells were incubated with the non-degradable particles (compare panel B with panel A). We interpret this difference in appearance to be compatible with time-dependent intracellular microparticle degradation and release of the encapsulated protein. As mentioned above, acid-sensitive crosslinker **1** is chemically stable at pH 7.4, but rapidly hydrolyzes in the acidic environment (pH 5.0) of the lysosome. This hydrolysis is believed to result in an increase in osmotic pressure, leading to lysosomal disruption, thus providing delivery of the encapsulated cargo to the cytoplasm.[28-30] These results are thus suggestive of release of the encapsulated BSA-Alexa Fluor 488 conjugate into the cytoplasm of the cell.

Importantly, there was no evidence of any cytotoxicity associated with intracellular accumulation of either degradable or non-degradable microparticles. Cells appeared viable with normal cell shape and morphology when viewed microscopically, and DAPI staining showed no evidence of nuclear fragmentation indicative of apoptosis. Furthermore, LDH concentrations in the media of cells incubated with degradable particles (with or without CPP modification) were <100 IU/mL (Figure 2.4). The LDH concentration in cells incubated without microparticles was also <100 IU/mL, whereas LDH levels were 4 times higher in cells treated with 10 mM H_2O_2 as a positive control.

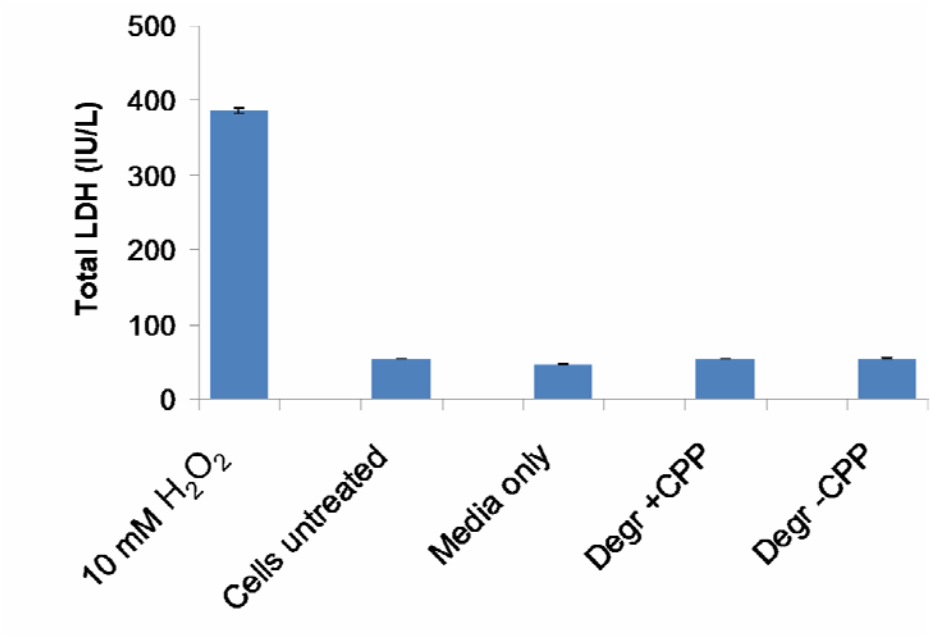

Figure 2.4. Results from LDH assay. Microparticles do not disrupt the cell membrane.

CPP modification would be expected to be effective in any tissue. Thus, widespread intracellular accumulation of microparticles would be expected after intravenous administration *in vivo*. For some applications, this may be advantageous, but it is detrimental in others due to unwanted toxicities. It is possible that the microparticles could be further modified with highly specific tissue-targeting moieties that would result in reduced uptake in non-targeted tissues. However, with the lungs, a very attractive delivery strategy is to administer the microparticles intratracheally (e.g., as an aerosol). In this case, cellular uptake would likely remain confined to the lung epithelium, and indeed, it was for this reason that we chose a lung epithelial cell line as the primary target for these studies. Future studies will determine if CPP-modified microparticles will accumulate in lung epithelium after intratracheal delivery *in vivo*.

Conclusions

A microparticle delivery vehicle encapsulating a fluorescently labeled model protein and containing a cell-penetrating peptide was successfully prepared. *In vitro* studies demonstrated that this delivery vehicle is effective at promoting particle uptake in non-phagocytic epithelial cells. Thus, incorporation of a cell-penetrating peptide expands the potential applications of this delivery vehicle for use in non-phagocytic, as well as phagocytic, cell lines. In addition, by incorporating an acid-degradable crosslinker, the particles are capable of releasing the encapsulated payload upon uptake by these cells. Future studies will explore the feasibility of using these particles to deliver plasmid DNA, peptide nucleic acids, or small molecule therapeutic cargoes to lung epithelial cells to treat acute and chronic lung disease.

Experimental Procedures

General Procedures and Materials

All reagents were purchased from commercial sources and were used without further purification unless otherwise stated. The cell-penetrating peptide (acrylamide-Y-$(R)_9$-COOH) was purchased from Applied Peptech Suzhou. Acryloyl chloride was distilled prior to use. Triethylamine and tetrahydrofuran (THF) were dried by passing through two columns of neutral alumina within a commercial solvent purification apparatus. Combined organic layers after extractions were dried over $MgSO_4$, which was removed by filtration. Solvents were removed under reduced pressure using a rotary evaporator. Reactions requiring anhydrous conditions were performed in flame-dried vessels and under a positive pressure of dry nitrogen. ^{1}H NMR spectra were recorded at 300 or 400 MHz on a Bruker spectrometer. $CDCl_3$ was passed through a plug of basic alumina prior to recording NMR spectra of acid-sensitive samples. To prevent acid-catalyzed hydrolysis of acetal-containing compounds during chromatographic separation, 1% triethylamine was added to the solvents used for elution. Absorbance was measured using a microplate reader (Molecular Dynamics).

Crosslinker synthesis. Compound **1** was prepared following a literature procedure.[28]

Particle Preparation

Degradable CPP-Modified Microparticles. Microparticles were prepared via an inverse emulsion free radical polymerization.[29,30] The organic phase consisted of 3% (w/v) of 3:1 (w/w)

Span 80/Tween 80 in hexanes. The aqueous phase was prepared by dissolving cell-penetrating peptide monomer **2** (2.13 mg, 1.3×10^{-6} mol) in 250 μL of phosphate buffered saline (pH 8.0) containing 2 mg/mL BSA-Alexa Fluor 488 conjugate. The pH of this solution was adjusted by the addition of 0.1 M NaOH until the solution had a pH of approximately 8. Acrylamide (85 mg, 1.20 mmol) and acid-labile crosslinker **1** (37 mg, 0.10 mmol, 8 mol %) were dissolved in the aqueous phase. A 50% (w/v) ammonium persulfate solution (10 μL) was added to the aqueous phase. The aqueous phase was then combined with 2.5 mL of the organic phase. The emulsion was prepared by sonicating the solution in a water bath at rt for 30 cycles (ca. 1 s each) in rapid succession using a Branson 450 Sonifier with a ½ in flat tip, an output setting of 2, and a duty cycle of 40%. Polymerization was initiated by the addition of 20 μL of *N,N,N′,N′*-tetramethylethylenediamine (TMEDA) and continued for 10 min at room temperature with constant stirring. The particles were recovered by centrifugation at 1380*g* (rt) for 10 min using 5 μm PVDF spin filters (Ultrafree-CL Durapore, Millipore). The particles were washed with hexanes (2 × 2 mL) and acetone (3 × 2 mL), centrifuging after each wash. After collecting the particles, residual acetone was removed by drying under high vacuum overnight.

Non-degradable CPP-Modified Particles. Non-degradable particles were prepared following the method described above using *N,N′*-methylene-bis-acrylamide as the crosslinker. The aqueous phase consisted of acrylamide (103 mg, 1.45 mmol), *N,N′*-methylene-bis-acrylamide (19.0 mg, 0.12 mmol, 8 mol %), and cell-penetrating peptide (2.62 mg, 0.1 mol %) dissolved in 250 μL of phosphate buffered saline (pH 8.0) containing 2 mg/mL BSA-Alexa Fluor 488 conjugate.

Unmodified Microparticles. Unmodified degradable and non-degradable microparticles encapsulating BSA-Alexa Fluor 488 conjugate were prepared in a similar fashion as described above omitting monomer **2**. For the degradable particles, the aqueous phase consisted of acrylamide (87 mg, 1.22 mmol) and crosslinker **1** (38 mg, 0.11 mmol, 8 mol %) dissolved in 250 μL of phosphate buffered saline (pH 8.0) containing 2 mg/mL BSA-Alexa Fluor 488 conjugate. For the non-degradable particles, the monomer composition contained acrylamide (105 mg, 1.48 mmol) and *N,N′*-methylene-bis-acrylamide (20 mg, 0.13 mmol, 8 mol %) dissolved in 250 μL of phosphate buffered saline (pH 8.0) containing 2 mg/mL BSA-Alexa Fluor 488 conjugate. It was unnecessary to adjust the pH of the aqueous phase in these cases.

Particle Characterization

CPP Quantification. CPP quantification was performed using a Micro BCA Protein Assay Kit (Pierce Biotechnology, Rockford, IL). The particles were dispersed in 300 mM acetic acid buffer pH 5.0 at a concentration of 5 mg/mL and incubated at 37°C overnight to degrade the particles. The solution was then analyzed for the concentration of peptide using the kit according to the manufacturer's instructions, and the fluorescence of the resulting solution was quantified on a microplate reader. A standard curve was prepared using known concentrations of peptide in acidic buffer (pH 5.0, 300 mM acetic acid).

Scanning Electron Microscopy (SEM). Microparticles were imaged as bulk dry powders. A sample of the dried particle powder was sputter-coated with a 35 Å platinum film and visualized using a Hitachi S5000 SEM at 10 kV.

Studies Performed with Particles

Cell Culture. A lung epithelial cell line derived from transformed normal human airway epithelial cells (BEAS-2B, CRL-9609, American type Tissue Culture Collection, Manassas, VA) was used for the majority of cell-based studies. Confirmatory experiments were also conducted in an alternative epithelial cell line (HeLa, obtained from ATCC, catalog no. CCL-2). With both lines, cells were grown overnight to 50% confluence on four-well LabTek plastic chamber slides using Optimem (Invitrogen) media supplemented with 5% FBS and penicillin/streptomycin (approx 50 μg/mL final). Microparticles were added to the media when the cells were 50–60% confluent.

Cell Uptake Studies. Microparticles were sonicated for two 2 s pulses just prior to incubation with cells using concentrations ranging from 15 μg/mL to 500 μg/mL in a 500 μL volume. Cells were incubated with microparticles for 2 h then washed three times in PBS and allowed to incubate an additional 24 h (HeLa cells) or simply allowed to incubate for 2 or 24 h (BEAS-2B cells). At the end of the incubation period, cells were then fixed and imaged. All studies were conducted in duplicate using 2–3 different preparations of microparticles.

Confocal Microscopy. After incubation, chamber slides were washed with PBS and fixed in 4% paraformaldehyde for 15 min at rt. Following additional PBS washes, Alexa Fluor 568 conjugated phalloidin (1:80, Molecular Probes no. A12380) was added to each well and incubated 30 min at rt to label filamentous actin. Chambers were then removed from the slides, and slides were washed again in PBS with a final rinse in water. Following shaking to remove excess water, cells were covered with mounting media (Vectashield, Vector Laboratories, Burlingame, CA) containing 4′,6-diamidino-2-phenylindole (DAPI) to stain intracellular DNA, coverslipped, and sealed with Cytoseal-60. Cells were examined by indirect fluorescent microscopy using an Olympus BX51 and/or confocal microscopy using a Zeiss 510 LSM laser scanning fluorescent confocal microscope. Cells not treated with microparticles and a well with microparticles but no cells were also prepared to measure background fluorescence.

Cytotoxicity Assay. Possible cytotoxicity associated with cell microparticle uptake was assessed by measuring the release of lactic dehydrogenase (LDH) into cell media using a commercially available kit according to the manufacturer's instructions (Roche Laboratories). BEAS-2B cells were cultured in 100 mm dishes with DMEM/10% FBS to approximately 80% confluence. Cells were washed and then incubated for 24 h in fresh media containing 500 μg/mL degradable microparticles, 10 mM H_2O_2 (ensuring cell death, thereby serving as a positive control), or no treatment. Testing was done in duplicate. After incubation, media was recovered, centrifuged, and LDH concentrations were measured in 1 mL of supernatant.

References

(1) Pack, D. W.; Hoffman, A. S.; Pun, S.; Stayton, P. S. *Nat. Rev. Drug Discovery* **2005**, *4*, 581-593.
(2) Dembowsky, K.; Stadler, P. *Novel Therapeutic Proteins*; Wiley-VCH: New York, 2001.
(3) Carter, P. J. *Nat. Rev. Immun.* **2006**, *6*, 343-357.
(4) Walsh, G. *Trends Biotechnol.* **2005**, *23*, 553-558.
(5) Reis, C. P.; Neufeld, R. J.; Ribeiro, A. J.; Veiga, F. *Nanomedicine* **2006**, *2*, 8-21.
(6) Allen, T. M.; Cullis, P. R. *Science* **2004**, *303*, 1818-1822.
(7) Goldberg, M.; Langer, R.; Jia, X. *J. Biomater. Sci., Polym. Ed.* **2007**, *18*, 241-268.
(8) Luo, D.; Saltzman, M. *Nat. Biotechnol.* **2000**, *18*, 33-37.
(9) Nishiyama, N.; Kataoka, K. *Pharmacol. Ther.* **2006**, *112*, 630-648.
(10) Park, T. G.; Jeong, J. H.; Kim, S. W. *Adv. Drug Delivery Rev.* **2006**, *58*, 467-486.
(11) Rawat, M.; Singh, D.; Saraf, S.; Saraf, S. S. *Biol. Pharm. Bull.* **2006**, *29*, 1790-1798.
(12) Vogelson, C. T. *Mod. Drug Discovery* **2001**, *4*, 49-50.
(13) Henry, C. M. *Chem. Eng. News* **2002**, *80*, 39-47.
(14) Jin, S.; Ye, K. *Biotechnol. Prog.* **2007**, *23*, 32-41.
(15) Pannier, A. K.; Shea, L. D. *Mol. Ther.* **2004**, *10*, 19-26.
(16) Montet, X.; Funovics, M.; Montet-Abou, K.; Weissleder, R.; Josephson, L. *J. Med. Chem.* **2006**, *49*, 6087-6093.
(17) Bae, Y.; Jang, W.; Nishiyama, N.; Fukushima, S.; Kataoka, K. *Mol. Biosyst.* **2005**, *1*, 242-250.
(18) Gupta, B.; Levchenko, T. S.; Torchilin, V. P. *Adv. Drug Delivery Rev.* **2005**, *57*, 637-651.
(19) Panyam, J.; Labhasetwar, V. *Adv. Drug Delivery Rev.* **2003**, *55*, 329-347.
(20) *Biodegradable Polymers as Drug Delivery Systems*; Chasin, M.; Langer, R., Eds.; CRC Press: New York, 1990.
(21) Amiji, M. *Polymeric Gene Delivery: Principles and Applications*; CRC Press: New York, 2004.
(22) Lynn, D. M.; Amiji, M. M.; Langer, R. *Angew. Chem., Int. Ed.* **2001**, *40*, 1707-1710.
(23) Haining, W. N.; Anderson, D. G.; Little, S. R.; von Berwelt-Baildon, M. S.; Cardoso, A. A.; Alves, P.; Kosmatopoulos, K.; Nadler, L. M.; Langer, R.; Kohane, D. S. *J. Immunol.* **2004**, *173*, 2578-2585.
(24) Little, S. R.; Lynn, D. M.; Ge, Q.; Anderson, D. G.; Puram, S. V.; Chen, J.; Eisen, H. N.; Langer, R. *Proc. Natl. Acad. Sci. U.S.A.* **2004**, *101*, 9534-9539.
(25) Khaja, S. D.; Lee, S.; Murthy, N. *Biomacromolecules* **2007**, *8*, 1391-1395.
(26) Lee, S.; Yang, S. C.; Heffernan, M. J.; Taylor, W. R.; Murthy, N. *Bioconjugate Chem.* **2007**, *18*, 4-7.
(27) Heffernan, M. J.; Murthy, N. *Bioconjugate Chem.* **2005**, *16*, 1340-1342.
(28) Kwon, Y. J.; Standley, S. M.; Goodwin, A. P.; Gillies, E. R.; Fréchet, J. M. J. *Mol. Pharm.* **2005**, *1*, 83-91.
(29) Murthy, N.; Xu, M.; Schuck, S.; Kunisawa, J.; Shastri, N.; Fréchet, J. M. J. *Proc. Natl. Acad. Sci. U.S.A.* **2003**, *100*, 4995-5000.
(30) Standley, S. M.; Kwon, Y. J.; Murthy, N.; Kunisawa, J.; Shastri, N.; Guillaudeu, S.; Lau, L.; Fréchet, J. M. J. *Bioconjugate Chem.* **2004**, *15*, 1281-1288.
(31) Standley, S. M.; Mende, I.; Goh, S. L.; Kwon, Y. J.; Beaudette, T. T.; Engleman, E. G.; Fréchet, J. M. J. *Bioconjugate Chem.* **2007**, *18*, 77-83.

(32) Murthy, N.; Thng, Y. X.; Schuck, S.; Xu, M.; Fréchet, J. M. J. *J. Am. Chem. Soc.* **2002**, *124*, 12398-12399.
(33) Moore, M. W.; Carbone, F. R.; Bevan, M. J. *Cell* **1988**, *54*, 777-785.
(34) Goh, S. L.; Murthy, N.; Xu, M.; Fréchet, J. M. J. *Bioconjugate Chem.* **2004**, *15*, 467-474.
(35) Webster, A.; Compton, S. J.; Aylott, J. W. *The Analyst* **2005**, *130*, 163-170.
(36) Langel, U.; Lundberg, P. *J. Mol. Recognit.* **2003**, *16*, 227-233.
(37) Deitz, G. P.; Bahr, M. *Mol. Cell. Neurosci.* **2004**, *27*, 85-131.
(38) Bhorade, R.; Weissleder, R.; Nakakoshi, T.; Moore, A.; Tung, C. H. *Bioconjugate Chem.* **2000**, *11*, 301-305.
(39) Futaki, S.; Suzuki, T.; Ohashi, W.; Yagami, T.; Tanaka, S.; Ueda, K. *J. Biol. Chem.* **2001**, *276*, 5836-5840.
(40) Futaki, S. *Adv. Drug Delivery Rev.* **2005**, *57*, 547-558.
(41) Wender, P. A.; Mitchell, D. J.; Pattabiraman, K.; Pelkey, E. T.; Steinman, L.; Rothbard, J. B. *Proc. Natl. Acad. Sci. U.S.A.* **2000**, *97*, 13003-13008.
(42) Melikov, K.; Chernomordik, L. V. *Cell. Mol. Life Sci.* **2005**, *62*, 2739-2749.
(43) Sheldon, K.; Liu, D.; Ferguson, J.; Gariepy, J. *Proc. Natl. Acad. Sci. U.S.A.* **1995**, *92*, 2056-2060.
(44) Zhang, L.; Torgerson, T. R.; Liu, X. Y.; Timmons, S.; Colosia, A. D.; Hawiger, J.; Tam, J. P. *Proc. Natl. Acad. Sci. U.S.A.* **1998**, *95*, 9184-9189.
(45) Calnan, B. J.; Tidor, B.; Biancalana, S.; Hudson, D.; Frankel, A. D. *Science* **1991**, *252*, 1167-1171.
(46) Rothbard, J. B.; Garlington, S.; Lin, Q.; Kirschberg, T.; Kreider, E.; McGrane, P. L.; Wender, P. A.; Khavari, P. A. *Nat. Med.* **2000**, *6*, 1253-1257.
(47) Mitchell, D. J.; Kim, D. T.; Steinman, L.; Fathman, C. G.; Rothbard, J. B. *J. Peptide Res.* **2000**, *56*, 318-325.
(48) Suzuki, T.; Futaki, S.; Niwa, M.; Tanaka, S.; Ueda, K.; Sugiura, Y. *J. Biol. Chem.* **2002**, *277*, 2437-2443.
(49) Fuchs, S. M.; Raines, R. T. *Biochemistry* **2004**, *43*, 2438-2444.
(50) Smith, P. K.; Krohn, R. I.; Hermanson, G. T.; Mallia, A. K.; Gartner, F. H.; Provenzano, M. D.; Fujimoto, E. K.; Goeke, N. M.; Olson, B. J.; Klenk, D. C. *Anal. Biochem.* **1985**, *150*, 76-85.
(51) Rothbard, J. B.; Jessop, T. C.; Wender, P. A. *Adv. Drug Delivery Rev.* **2005**, *57*, 495-504.

Chapter 3 – The Impact of Particle Size and Surface Functionalization on *In Vivo* Behavior of Hydrogel-Based Particles for Pulmonary Applications

Abstract

Polymer chemistry offers the possibility of synthesizing multifunctional nanoparticles which incorporate moieties that enhance diagnostic and therapeutic targeting of cargo delivery to the lung. However, the lung presents a challenging delivery environment since rules for predicting particle behavior following pulmonary administration are poorly understood. Significant barriers to efficient particle delivery exist in the lung due to the presence of complex mechanisms built into the pulmonary physiology designed to effectively prevent particulate material from accumulating in the deep lung airspaces. Given the promising *in vitro* results obtained with our cell-penetrating peptide functionalized hydrogel particles described in the previous chapter, we decided to evaluate the behavior of these particles *in vivo* for applications in lung imaging and therapy. In this chapter, we describe the design of polyacrylamide-based hydrogel particles of differing sizes, functionalized with a nona-arginine cell-penetrating peptide (Arg_9), and labeled with imaging components to assess lung retention and cellular uptake after intratracheal administration. We explore the effects of varying a variety of parameters related to hydrogel structure on the potential utility of this particle system to serve as a delivery vehicle in the pulmonary environment. Specifically, we investigate the role of both particle size and functionalization with cationic cell-penetrating/mucoadhesive peptides on (i) lung retention, redistribution, and elimination following intratracheal delivery, (ii) cellular localization of particles within the lung, and (iii) the induction of undesired inflammatory immune responses for this system. We demonstrate that whereas microparticles may be advantageous for short-term applications, nanosized particles constitute an efficient high-retention and non-inflammatory vehicle for the delivery of diagnostic imaging agents and therapeutics to lung airspaces and alveolar macrophages that can be enhanced by CPP. Importantly, our results elucidate the influence of several important particle design features on *in vivo* behavior in the complex pulmonary environment and may help in the design of future delivery vehicles for use in the treatment of various lung diseases.

Introduction

Polymer chemistry offers the capacity to generate a wide variety of nanoparticles with diverse classes of functional groups to provide unique possibilities for diagnostic imaging and therapy.[1-3] Tailoring particles with specialized functions can therefore enhance behavior in specific organs or cell microenvironments.[4,5] In this regard, each disease target presents challenges related to the route of administration, the properties of the particle system, and the biologic responses. Acute and chronic respiratory diseases caused by infectious, inflammatory and genetic etiologies have a high morbidity and mortality and are thus excellent candidates for novel nanotechnology-based diagnostic and treatment strategies.[6-8] The respiratory tract provides an easily accessed route for organ-specific delivery, with an established record of success in the clinic for inhaled drug therapies and nuclear imaging. To date, the primary focus of evaluation of nanoparticles in the respiratory tract has been on the toxicity of environmental particulate

pollutants and metal particles.[9,10] Thus, the development of synthetic nanoparticles for delivery to the respiratory tract for clinical application is still in its early stages, and the effects of structural features, and addition of components for imaging, cell targeting, and permeation on *in vivo* particle behavior are not yet well defined, and therefore require comprehensive assessment.[6-8]

Existing polymeric particle systems for lung delivery are primarily composed of hydrophobic materials such as poly(lactic-*co*-glycolic acid) (PLGA) chains condensed into particles and dispersion-polymerized poly(butyl cyanoacrylate) particles.[8,11] Few systems for lung delivery have been explored that employ hydrophilic polymer networks based on crosslinked hydrogels. Our group has recently described the synthesis of hydrogel-based polyacrylamide microparticles (PMPs, 1-5 μm diameter) and nanoparticles (PNPs, <100 nm diameter) that can be tuned for size and degradation rate through the incorporation of pH-sensitive crosslinks, and functionalized to carry cargoes such as imaging probes, proteins, or nucleic acids.[12-16] In addition, small molecules and peptides for targeting and improved cell uptake can be built into the particle backbone through copolymerization. These modifications are especially important in the case of non-malignant lung diseases where the phenomenon of enhanced permeation and retention (EPR) and tumor-specific cell membrane targets are not applicable.[17] Thus, we have been particularly interested in functionalizing PMPs and PNPs with cell-penetrating peptides (CPPs) that may increase cellular uptake of particles *in vivo* and display mucoadhesive characteristics in the lung.[18]

CPPs are short cationic peptides derived from biological sources, including the HIV TAT (trans-activator of transcription) protein.[19] Over the past 20 years, numerous studies have demonstrated that naturally occurring or synthetic CPPs such as oligomers of arginine (e.g., the nonamer Arg_9) enhance the cellular uptake of proteins, nucleic acids, drugs, and nanoparticles.[20-23] Similarly, we have demonstrated that modifying PMPs with CPP enhances cellular particle uptake *in vitro*.[12] However, only a few reports have described CPP-mediated transport of molecules in the lung. In pioneering studies, intraperitoneal or intravenous injection of a TAT-bound protein was shown to result in uptake in multiple organs including low quantities in the lungs, although the cell type targeted was not identified.[24,25] More recently, TAT bound to plasmid DNA encoding a luciferase reporter and administered intratracheally to mice was found to be superior to plasmid alone for enhancing transfection efficiency, albeit with low levels of luciferase expression, and accompanied by lung inflammation.[26] In contrast, gene silencing with siRNA conjugated to TAT delivered intratracheally was not superior to siRNA alone.[27] Thus, while potentially powerful, the value of CPP-modified structures is not well understood for lung delivery. Moreover, there is little information available to guide the design and assessment of particulate carrier systems complexed with CPPs for respiratory tract delivery.

In the work described in this chapter, we hypothesized that both particle size and functionalization with CPP would significantly impact particle behavior in the lung as characterized by retention, cell uptake and immune response. We thus focused on interactions of particles of varying sizes and surface modification with the airspace environment, epithelial and immune cells, and extra-pulmonary organs. Additionally, since it has been shown that particles can rapidly move out of the lung to other organs, we used imaging and biodistribution studies as critical assays for understanding particle fate *in vivo*.[28] We took advantage of our ability to incorporate multiple imaging probes to enable (i) non-invasive tracking of particles *in vivo* using positron emission tomography, (ii) quantification of specific organ distribution, and (iii) analysis of cellular uptake following intratracheal delivery. Finally, with concern for minimizing particle-

associated inflammatory responses, we assessed the presence of markers of lung inflammation following instillation of PMPs and PNPs in the lungs.

Results and Discussion

Synthesis and Characterization of Hydrogel Particles.

To explore the effects of carrier size and functionalization with a cell-penetrating peptide (CPP) on the behavior of hydrogel-based particles following intratracheal administration, we synthesized polyacrylamide microparticles (PMPs) and nanoparticles (PNPs) that were (CPP+) or were not (CPP-) co-polymerized with a monomer containing a pendant nona-arginine peptide (Figure 3.1A). While these particles can be synthesized to hydrolyze and release their cargo,[12] non-degradable particles were used in this study to enable the tracking of particle fate. All particles encapsulated a conjugate of bovine serum albumin and Alexa Fluor 488 dye (BSA-488) for fluorescence-based assays and for tyrosine radiolabeling. PNP radiolabel stability was improved by co-polymerizing a tyramine-functionalized monomer into the particle structure, in addition to thoroughly washing the particles using ultrafiltration. In the dry state, particles had a spherical shape when imaged by SEM (Figure 3.1B and C).

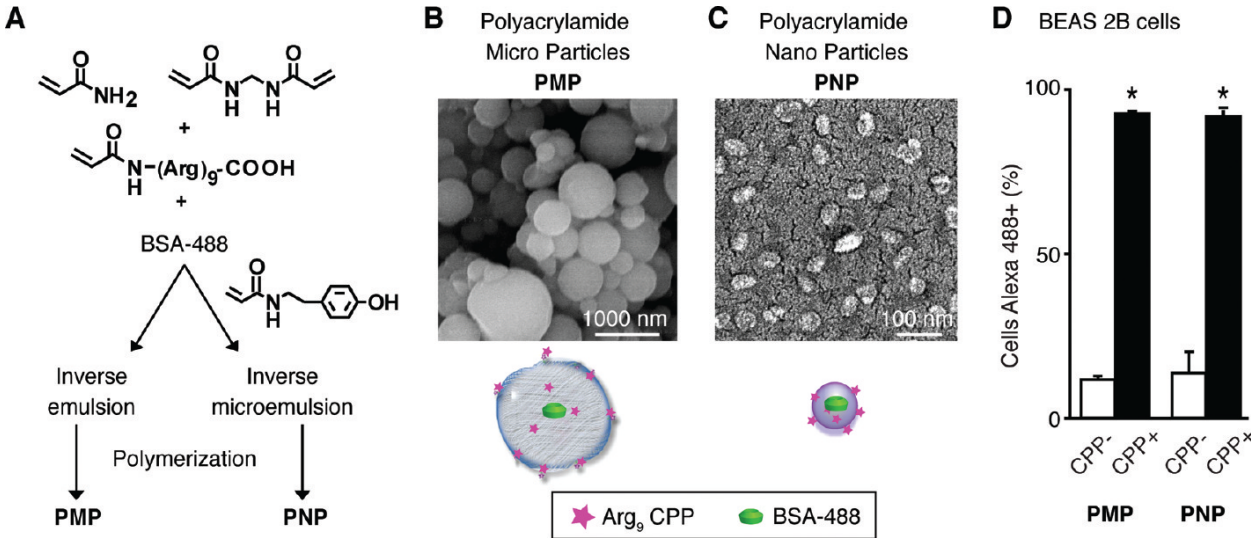

Figure 3.1. Synthesis, functionalization, and *in vitro* behavior of polyacrylamide hydrogels. (A) Particles were generated and co-polymerized in the absence or presence of a nona-arginine cell penetrating peptide (CPP). All particles encapsulated bovine serum albumin conjugated with Alexa Fluor 488 dye (BSA-488) for fluorescence detection. Emulsion conditions were varied to yield polyacrylamide microparticles (PMPs) or nanoparticles (PNPs) as shown in the SEM images (B, C) of the particles in the dry state. (D) The human bronchial epithelial cell line BEAS 2B was incubated with the indicated particles for 24 h and then assayed by flow cytometry to determine the proportion of cells containing BSA-488-labeled particles. Shown is the mean ± SD of replicate samples from at least 2 independent experiments (*$p < 0.05$).

When hydrated, the PMPs were 1 to 5 μm in diameter and PNPs were 20 to 40 nm in diameter, as measured by light scattering (Table 3.1). The surface charge of the particles, as indicated by zeta-potential measurements, was positive with the exception of the CPP- PMPs, which were near neutral. We previously demonstrated preferential uptake of the CPP+ PMPs

compared to CPP- PMPs in cell lines,[12] and thus extended these studies to evaluate the PNPs in parallel with PMPs (Figure 3.1D). The addition of the CPP into the structure of both PMPs and PNPs significantly enhanced their cellular uptake *in vitro* ($p < 0.05$).

Table 3.1. Properties of nanoparticles tested for respiratory tract delivery[a]

Particle type	Hydrated Diameter[b]	Peptide	Zeta-potential[b]	Cargo	Radiolabels
CPP- PMPs	1.8 ± 1.2 μm	None	-0.1 ± 4.5 mV	BSA-488	^{125}I, ^{76}Br
CPP+ PMPs	2.7 ± 1.4 μm	CPP	+12.3 ± 4.0 mV	BSA-488	^{125}I, ^{76}Br
CPP- PNPs	31.0 ± 9.3 nm	None	+7.6 ± 4.8 mV	BSA-488	^{125}I, ^{76}Br
CPP+ PNPs	31.7 ± 14.5 nm	CPP	+11.9 ± 4.0 mV	BSA-488	^{125}I, ^{76}Br

[a]Abbreviations: PMPs, polyacrylamide microparticles; PNPs, polyacrylamide nanoparticles; CPP, cell-penetrating peptide; BSA-488, bovine serum albumin/Alexa Fluor 488 conjugate.
[b]Mean ± S.D.

***In Vivo* PET/CT Imaging of Radiolabeled Particles Following Intratracheal Delivery.**

As an initial evaluation of the *in vivo* behavior of PMPs and PNPs in the lung, particles were hydrated, radiolabeled with ^{76}Br for PET imaging, and administered to mice *via* the direct intratracheal (IT) injection route to ensure accurate respiratory tract delivery. Radiolabeled IT particles were well tolerated without animal distress or mortality. Mice were imaged serially by whole body microPET/CT scanning over an 18 h period (Figure 3.2A). For all particles at all time points, the microPET/CT co-registered images clearly showed a general restriction of the particles to the lung. Particles present in the gastrointestinal (GI) tract post-delivery were best revealed in three-dimensional reconstructions of the images obtained after 3 h (Figure 3.2B). Based on these studies, the PNPs had a more prolonged retention in the lung relative to the PMPs.

Image analysis using the standardized uptake values (SUV) of the two types of PMPs showed that the lung activity of each particle decreased at a similar rate over time, but mice administered the CPP+ PMPs had 34-50% lower lung activity than those receiving CPP- PMPs (Figure 3.2C). Both PNP types displayed higher lung activity compared to each of the PMP forms. In addition, the PNPs had a similar and constant lung signal over 18 h that appeared to be independent of the CPP. Collectively, this initial analysis demonstrated a consistent behavior related to size; the larger PMPs were rapidly cleared, likely through mucociliary clearance to the gastrointestinal tract (GI), while the smaller PNPs had sustained lung retention.

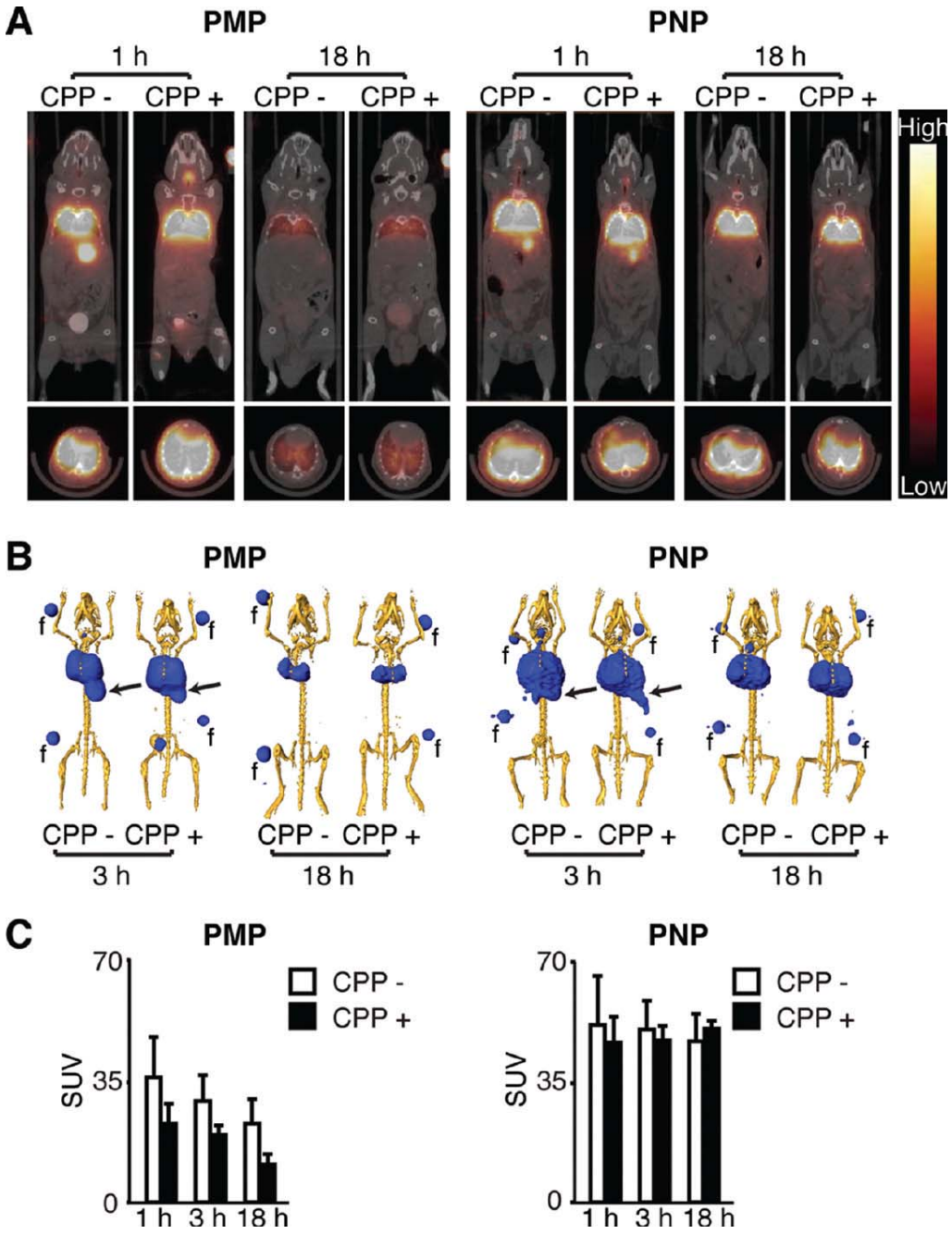

Figure 3.2. MicroPET/CT imaging of ^{76}Br-labeled particles following intratracheal delivery. (A) Representative mid-thoracic coronal (top) and transverse (bottom) slices of serial microPET and CT co-registered images obtained from mice at the indicated time following intratracheal administration of ^{76}Br-labeled particles described in Figure 3.1. (B) Three-dimensional reconstructions of PET scan activity (blue) merged with X-ray CT images that were signal-adjusted to reveal the skeleton (yellow). Arrows indicate gastrointestinal tract activity. Fiduciaries (f) used for co-registration are included. (C) The standardized uptake values (SUV) of the PET activity within the lung region from images as in (A), shown as the mean ± SD of 3-4 mice per particle type.

***In Vivo* Lung Retention and Biodistribution of Particles Following Intratracheal Delivery.**

To more precisely quantify the lung retention and fate of particles, biodistribution studies were performed in mice after IT delivery of ^{125}I-labeled particles. Retention of particles in the lung was determined by measuring activity in total lung tissue. Evaluation of all four types of particles again demonstrated that the majority of the initial activity was localized in the lung (Figure 3.3). Consistent with the PET images, the activity of the smaller particles (PNPs) in the lung was both higher and more persistent than that of the larger ones (PMPs). However, in this more sensitive assay, an effect of the CPP was observed, but differed for the two sizes of particles. For PMPs, the presence of the CPP resulted in a lower lung retention profile at all times ($p < 0.05$). The pattern was reversed in the case of the PNPs, where the presence of the CPP resulted in significantly higher lung retention at all time points ($p < 0.05$).

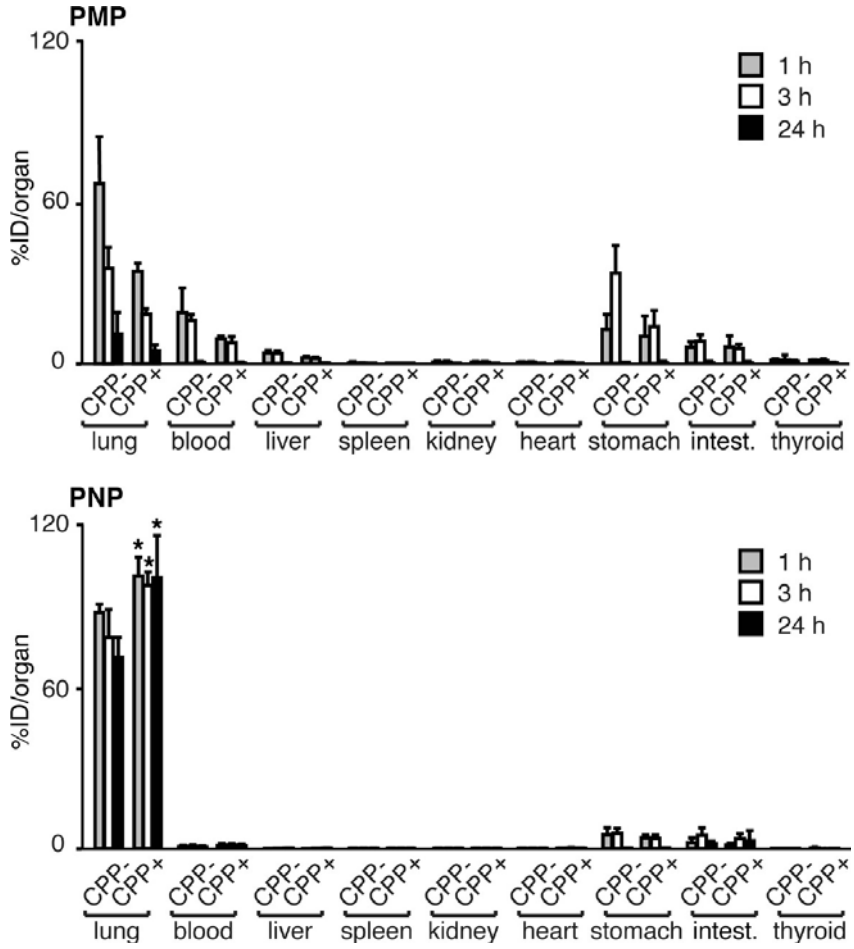

Figure 3.3. Lung retention and biodistribution of particles following intratracheal delivery. Biodistribution of ^{125}I-labeled particle activity in the indicated organs performed 1, 3, and 24 h post-delivery. Activity was determined as the mean ± SD of the percent of the injected dose per organ (% ID/organ) from 3-5 mice per group. Particles were functionalized without (CPP-) or with (CPP+) cell-penetrating peptide. The lung activity of CPP+ PNPs was significantly greater than CPP- PNPs at all times (*$p < 0.05$).

Studies by other groups have demonstrated that, following respiratory tract administration, particles could be cleared from the lung to either the GI tract by mucociliary activity (after particles are swallowed in the posterior pharynx) or to the systemic circulation by transit from the air space through the alveolar epithelium-capillary endothelial barrier.[28] To analyze extra-pulmonary particle fate, organs of interest were collected and activity was quantified using a gamma counter. These biodistribution studies showed higher activity of PMPs than PNPs in the GI tract (stomach and intestines; 1 and 3 h; $p < 0.05$), suggesting rapid mucociliary clearance of the larger particles from the lung. Also, the blood clearance of the PMPs was higher than that of the PNPs at all time points, suggesting movement from the alveolar air space to the systemic circulation ($p < 0.05$).

For all particles, activity was extremely low or undetectable in all other organs assayed. The possibility of central nervous system uptake was also determined, which we anticipated would be minimal as IT delivery avoids passage from the olfactory epithelium to the brain.[29] For all particle types, activity was not detected in the brains isolated from mice after PET imaging (data not shown). Together, these biodistribution studies were consistent with the PET imaging studies, confirming rapid GI tract clearance of the PMPs and a high specificity of lung retention of PNPs that was significantly enhanced by the addition of CPP ($p < 0.05$).

Localization of Intracellular Targeting of Polyacrylamide Particles *In Vivo*.

Prior studies of particle modification have indicated that changes in surface characteristics such as that imparted by the addition of a polyarginine peptide may significantly alter predicted patterns of particle distribution and cellular localization in the body.[30,31] To define features of lung retention and particle fate, an additional cohort of animals was intratracheally administered ^{125}I-labeled particles and then subjected to bronchoalveolar lavage (BAL) at 1, 3, or 24 h post delivery (Figure 3.4A). Radioactivity in the BAL fluid and the post-BAL lung was determined to quantify particles in different lung compartments with the knowledge that the BAL fluid would contain both free and immune cell-associated particles, while the post-BAL lung would additionally include parenchymal cell-associated particles. Consistent with the studies above, analysis of BAL fluid and remaining activity in the lung revealed that a greater fraction of PNPs than PMPs was retained in the lung. There was no significant difference in post-BAL lung activity imparted by addition of CPP to the PMPs ($p > 0.05$). In contrast, at all time points, CPP+ PNPs were retained at higher levels in the post-BAL lung than CPP- PNPs ($p < 0.05$) suggesting that the addition of the CPP enhanced the association of the smaller nanoparticle within the lung parenchymal compartment.

To identify the specific cell types in the lung taking up the particles, tissue sections of lung were examined for co-localization of the BSA-488-labeled particles with cell-specific markers. Low power examination of lung sections showed that delivery of all particle types resulted in regional dispersal, variable clumping of particles and delivery within alveolar airspaces, which in some cases associated with cell surfaces (Figure 3.4B and data not shown). No significant particle fluorescence activity was identified in the airway epithelial cells of bronchi or bronchioles of any of the animals. All particle types were found in alveolar epithelial cells (Figure 3.4B, arrowheads). These were identified by morphology as alveolar epithelial type I cells or by immunostaining as type II cells using the marker prosurfactant protein C. Particles were more commonly observed within cells of macrophage morphology (Figure 3.4B, arrows). Consistent with this observation, BAL cells obtained 24 h post-instillation revealed particles in

cells that expressed the macrophage marker CD68 (Figure 3.4C). These studies suggested that there was enhanced alveolar macrophage uptake of PNPs compared to PMPs.

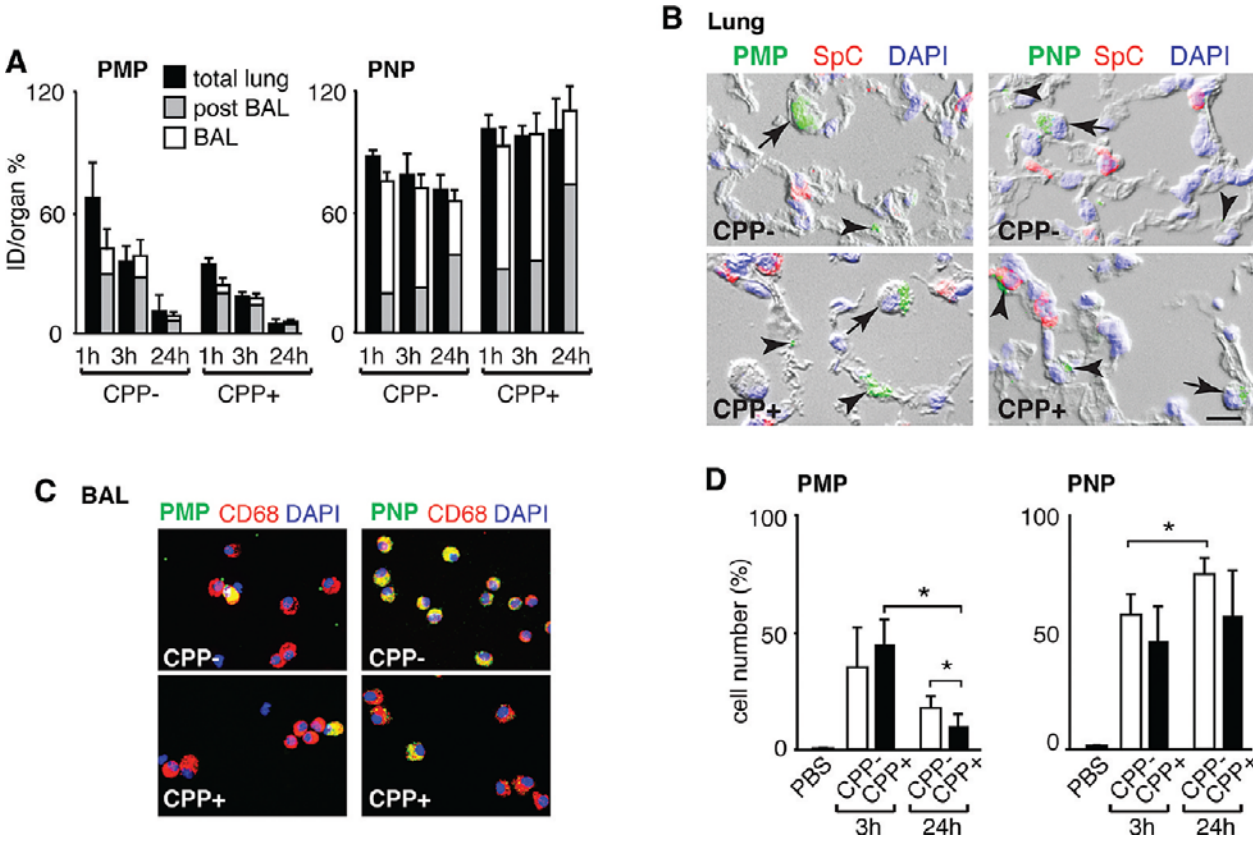

Figure 3.4. Localization of particles in the lung following intratracheal delivery. (A) Activity of the indicated ^{125}I-labeled particle 1, 3, and 24 h post-delivery in the total lung, post-BAL lung and BAL fluid determined as the mean ± SD of the percent of the intratracheal dose per organ (% ID/organ) from 3-5 mice per group. (B) Photomicrographs of lung sections obtained 24 h after particle delivery show BSA-488-labeled particles (green) in alveolar epithelial cells (arrowheads) and cells with alveolar macrophage morphology (arrows). Tissue sections were stained to identify alveolar type II epithelial cells (prosurfactant protein C, SPC; red) and nuclei (DAPI; blue). Bar = 10 µm. (C) Photomicrographs of cells obtained by BAL 24 h after delivery of BSA-488-labeled particles that were immunostained with alveolar macrophage marker antibody CD68 (red) and DAPI (blue). (D) Quantification of BAL alveolar macrophages that contain BSA-488-labeled particles. At 3 and 24 h post-delivery of PBS or particles, cells recovered in BAL fluid were immunostained for macrophage marker F4/80 and analyzed by flow cytometry. Shown is the mean ± SD of the percentage of macrophages containing BSA-488-labeled particles in 3-5 mice per group (*$p < 0.05$).

Quantification of Particle Uptake by BAL Alveolar Macrophages *In Vivo*.

Optimal particle diameters for phagocytosis by alveolar macrophages are reported to be 1-3 μm, and phagocytosis is considered to decrease with particle size and time after delivery to the lung.[32,33] To more specifically quantify alveolar macrophage uptake, we examined BAL cells

from different time points after IT delivery using flow cytometry. Rapid uptake was observed for all particle types in 30-60% of the macrophages in samples obtained 3 h post-delivery (Figure 3.4D). By 24 h, there was a decrease in the percentage of macrophages containing PMPs, while macrophage uptake of the PNPs remained high (>50%). There was no apparent effect of CPP to augment macrophage uptake of either particle.

Determination of the Acute Inflammatory Cell Response in the Lung after Delivery of Particles.

The respiratory system response to particulate invasion is typically accompanied by a rapid inflammatory response that can be monitored by assay of immune cells and accompanying inflammatory mediators in BAL fluid.[34,35] Few studies have explored responses to synthetic particles specifically developed for nanomedicine.[10,36,37] It was therefore important to next determine if there was a toxic inflammatory response in the lung following IT delivery of particles (Figure 3.5A and B). Cells in BAL fluid recovered from naive mice include at least 95% alveolar macrophages, reflecting the normal innate cell population. After 24 h, CPP- PMPs, CPP- PNPs, or CPP+ PNPs did not induce a significant change in the number or type of immune cells recovered compared to PBS alone (Figure 3.5B). Only the CPP+ PMPs induced an inflammatory response characterized by an increase in BAL fluid neutrophils and a decrease in macrophages. In agreement with the inflammatory cell profiles in the BAL fluid, further analysis that quantified multiple cytokines, chemokines and growth factors in cell-free BAL fluid showed increased levels only in samples from mice administered CPP+ PMPs (Figure 3.5D). The inflammatory mediators with increased concentrations were CXCL1/KC, CCL2/JE, CCL3/MIP-1α and G-CSF, consistent with the function of these molecules as neutrophil chemotaxis factors.[35]

The inflammatory response observed with the CPP+ PMPs could not be directly attributed to the CPP since there was no inflammatory response observed in BAL fluid of mice delivered free CPP (Figure 3.5C). This suggests that the multivalent presentation of the cationic CPP on the surface of the PMP structure may have enhanced toxicity. This would be analogous to the lung inflammation observed when cationic TAT-derived peptides were linked to different types of siRNA or DNA, resulting in the induction of inflammation in the lung. However, as noted, the surface charge of the CPP+ PMPs was similar to the relatively non-inflammatory CPP+ PNPs (Table 3.1), again indicating that combinations of size, charge and other particle design features may influence the development of inflammation.

The source of this inflammation may be the result of an interaction of peptide-bearing particles with alveolar macrophages, or airway or alveolar epithelial cells as reported.[38,39] However, when we exposed primary alveolar macrophages to particles and measured cytokines in supernatants, we did not observe an increase in cytokine or chemokine production (data not shown), in contrast to macrophage responses observed by others.[39] We further recognized that the present experiments were designed to study only an acute effect where prolonged retention of particles may induce a chronic response as observed in the case of intratracheally administered carbon nanotubes.[40]

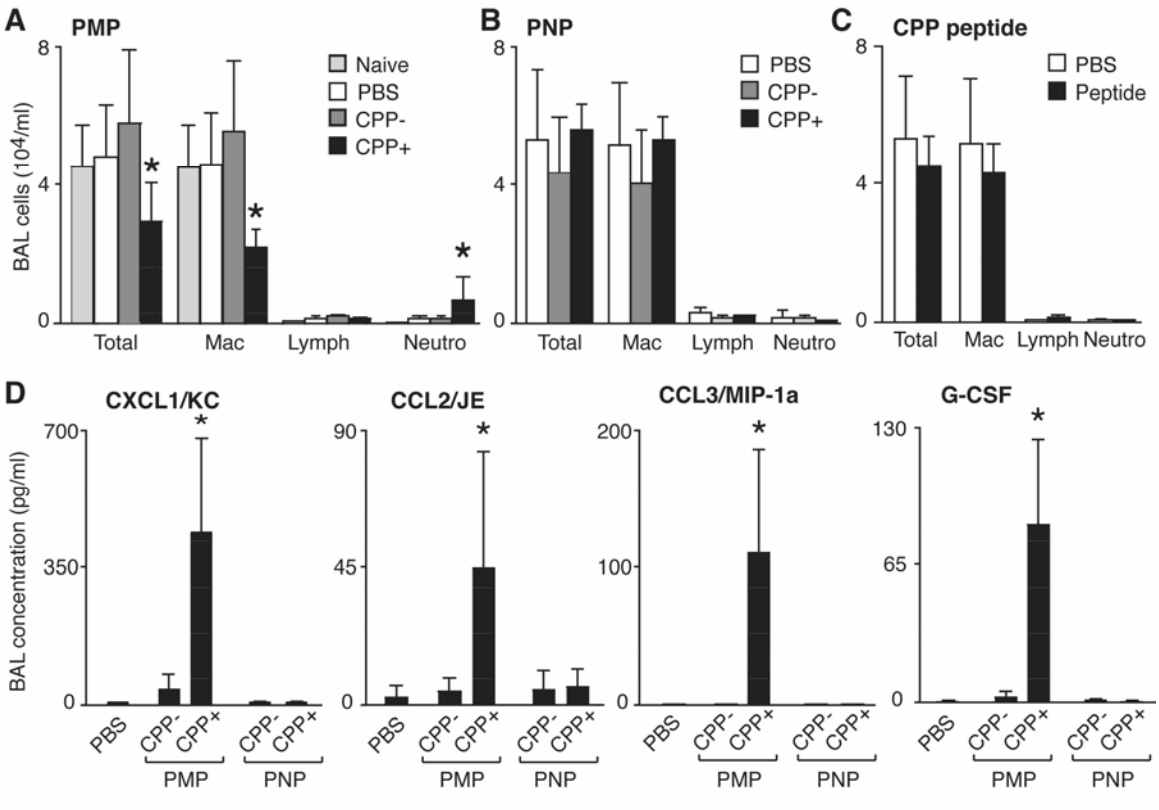

Figure 3.5. Inflammatory response in the lung following intratracheal delivery of particles. (A-C) Quantification of cell types recovered by BAL 24 h post-delivery of the indicated particle or CPP alone. Shown is the mean ± SD of total and individual cell types (Mac, alveolar macrophage; Lymph, lymphocyte; Neutro, neutrophil) from at least 3 mice. (D) BAL fluid cytokines measured in cell-free supernatant by BioPlex assay from 3 mice. A significant difference compared to other treatments is indicated (*$p < 0.05$).

***In Vivo* Lung Retention and Biodistribution of Degradable Particles Following Intratracheal Delivery.**

The primary focus of this study was to investigate the utility of hydrogel-based particulate systems delivered *via* the respiratory tract for potential pulmonary imaging and therapy applications. Therefore, we chose to evaluate non-degradable particles to enable straightforward tracking of particle fate over time. These studies provided us with important information regarding particle size and surface functionalization that will help guide our future particle design. For clinical applications, however, a particulate delivery vehicle that degrades under physiologically relevant conditions is highly desirable.

We have described, in the previous chapter, the preparation of acid-degradable polyacrylamide hydrogels incorporating the same cell-penetrating peptide (CPP) utilized in the above studies. These particles contain a pH-sensitive acetal crosslinker that is relatively stable at pH 7.4, but degrades rapidly under the slightly acidic conditions typically found in the lysosome (pH 5.0-5.5). Such acid-sensitive systems are particularly attractive as cargo release can be triggered in response to endosomal acidification upon cellular uptake. Acid-degradable particles

of this type encapsulating protein antigens and immunostimulatory molecules have shown success in eliciting an immune response for vaccine applications.

As a first step towards understanding whether our degradable hydrogels might be an appropriate system to use in pulmonary delivery applications, we wanted to investigate the behavior of these particles following intratracheal administration. Biodistribution studies were performed in mice after IT delivery of ^{125}I-labeled particles. Retention of particles in the lung was determined by measuring activity in total lung tissue. Evaluation of degradable CPP+ PMPs showed that the majority of the initial activity was localized in the lungs, followed by a rapid decrease in activity over time (Figure 3.6). As with the biodistribution of the non-degradable particles, we also observed high activity in the stomach, suggesting rapid mucociliary clearance of these larger particles from the lung.

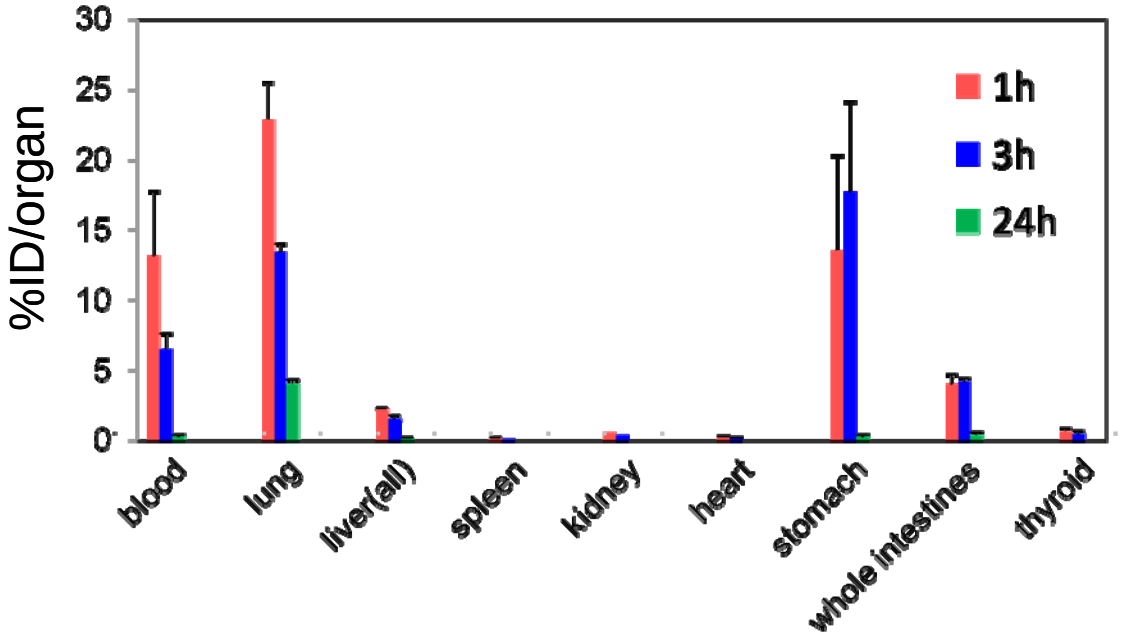

Figure 3.6. Lung retention and biodistribution of degradable CPP+ PMPs following intratracheal delivery. Biodistribution of ^{125}I-labeled particle activity in the indicated organs performed 1, 3, and 24 h post-delivery. Activity was determined as the mean ± SD of the percent of the injected dose per organ (% ID/organ) from 3-5 mice per group.

Discussion of the Overall Behavior of Polyacrylamide Microparticles and Nanoparticles Delivered *via* the Respiratory Tract.

Taken together, our *in vivo* analysis reveals that both size and functionalization impart each type of particle with its own unique behavior (Table 3.2). In this study, tracking of particle fate is made possible by the ability to multi-functionalize our particle system, reflecting one advantage of these synthetic polymer constructs. Here, we show that the direct and commonly used clinical route of respiratory tract delivery for administration of our polymer based micro- and nanoparticles results in reproducible behaviors for adaptation to imaging and therapeutic applications in the lung. We also specifically tested the functionalization of particles with CPP since it is remarkably effective for cargo delivery *in vitro* and in some cases when delivered intravenously.[20,22,23] To our knowledge, nanoparticles bearing CPPs have not been previously

studied for delivery to the respiratory tract, where cell targets and host defense mechanisms present an environment that is very different from that of the vascular system and other organs. We identified that the addition of the CPP to the carrier structure induced significant changes in particle behavior *in vivo*, particularly enhancing lung airspace retention of the PNPs without induction of inflammation when delivered to the respiratory tract of mice.

Table 3.2. Fate of nanoparticles following respiratory tract delivery[a,b]

Particle Type	Lung Retention	GI Clearance	Blood Transit	AM Uptake	Epithelial Uptake	Inflammation
CPP- PMPs	++	++++	++	++	+	-
CPP+ PMPs	++	+++	++	++	+	+
CPP- PNPs	++++	+	+	++++	+	-
CPP+ PNPs	++++	+	+	+++	+	-

[a]Abbreviations: GI, gastrointestinal; AM, alveolar macrophage.
[b]Scoring: -, not detected +, <10%; ++, 10-25%; +++, 26-50%; ++++, >50%

Our multi-modality analysis of the acute behavior of CPP functionalized micro- and nanosized particles delivered intratracheally also revealed important findings with direct implications for particle design for clinical applications. First, PET imaging showed that both large and small particle types were distributed widely throughout lung airspaces, independent of the presence of CPP and any differences in surface charge. By labeling the particles with multiple markers, we could use whole animal, tissue and cell-based analysis to determine that the PET imaging correlated well with airspace filling and mucociliary clearance. Second, using these assays, we confirmed that the routes of particle clearance were size-dependent as reported by others: the larger particles (PMPs) were more rapidly cleared by mucociliary mechanisms, likely due to a tendency for more proximal impaction in the airway of respiratory tract.[30,33] Consistent with this conclusion, the biodistribution assay (Figure 3.3) revealed significantly higher PMP than PNP GI tract activity at one and three hours postdelivery ($p < 0.05$). This is the result of movement of particles (or particles within cells), up the mucociliary escalator and subsequent swallowing. Thus lower mucociliary clearance contributed to the prolonged lung retention of PNPs. Size-dependent behavior related to transit to the blood was opposite of that predicted, based on prior reports.[28,41] These reports indicated that a significant proportion of nanoparticles transit the alveolar space to the blood. In contrast, we found a greater fraction of PMPs in the blood pool, possibly owing to some unrecognized alteration or injury to the alveolar epithelial cell basement membrane.[28] Third, both large and small particles were rapidly taken up by alveolar macrophages, without enhancement of phagocytosis by CPP. For PNPs in particular, macrophage uptake is thus likely the major route for clearance, whereas it is possible that a high proportion of PMP clearance is by mucociliary routes without phagocytosis. The relatively greater macrophage uptake of nanoparticles than microparticles may also be the result of a higher amount of PNPs than PMPs delivered since dosing was based on mass. Fourth, epithelial cell

uptake was independent of the addition of the CPP for both sizes of particles, as opposed to the enhanced uptake that we observed *in vitro*.[12] Last, in contrast to reports of inflammation induced by other particles,[10,30] acute airway inflammation, assessed at 24 h after delivery, was not induced, with the single exception of the CPP+ PMPs.

We found that the presence of CPP significantly alters the behavior of the particles in the lung. Interestingly, CPP improves the lung retention of the PNPs, while it speeds up clearance of the larger PMPs. The prolonged retention of the PNP with CPP could not be attributed to the difference in charge alone since both CPP+ PMPs and CPP+ PNPs were of similar surface charge (Table 3.1). These differences in behavior caused by a small perturbation to the carrier structure highlight the need to take into account multi-level (cell, organ, and whole organism) effects in the design of particle-based carrier systems. Prior studies of respiratory tract delivery of CPP-bearing molecules are limited and have mixed results, indicating that multiple design features must be considered. For example, IT delivery of luciferase plasmid with a TAT-derived CPP linked via a polyethylene glycol (PEG) bridge to polyethylenimine did result in a low level of total lung luciferase expression.[26] However, in that report, Kleeman *et al*. argued that TAT-derived peptide alone was insufficient to mediate *in vivo* transfection of lung cells and that the PEG conjugate was a critical component for delivery. Other investigators have suggested that the addition of hydrophilic PEG may be a critical factor for enhancing penetration of particles through the dense, thin mucous layer that normally lines the respiratory tract.[42,43] It is possible that the use of a PEG linker incorporated into our hydrogel particles could permit the CPP to function more effectively *in vivo*. On the other hand, the nanoparticles that contact the alveolar epithelial cells face a high surfactant barrier, where additional particle surface properties may need to be engineered to enable cell entry. Additional factors, such as particle shape and charge, are likely also important to maximize CPP-mediated nanoparticle uptake and represent areas for future investigation to optimize lung delivery.[44]

Although we used several assays to determine the fate and effects of intratracheal delivery of our particles, elucidating additional aspects of particle behavior will require future investigation. For example, we need to gain further insight into the mechanisms for prolonged retention of the PNPs and facilitation by CPP. While retention could be strongly influenced by particle biodegradability, it may also be associated with particle size, shape and surface charge. We have also considered that retention may be related to the movement of particles to the alveolar interstitial space, a phenomenon observed in the study of ultrafine particles.[32] However, using immunofluorescence microscopy, we did not observe BSA-488-labeled particles within the interstitial space of the alveoli. The use of immunogold-labeled anti- Alexa Fluor 488 antibodies and electron microscopy of lung tissues analyzed over a longer period of time might reveal this behavior. Also, while the mechanism of uptake of a variety of structures with CPP has been extensively investigated,[20,22,23] it is possible that unique pathways independent of CPP might exist for the polyacrylamide complexes tested here, possibly related to their inherently hydrophilic nature. Future assessment of particles functionalized with CPP will be directed toward testing designs that incorporate fully biodegradable components[45] and the addition of PEG to enhance mucous penetration,[42] as well as investigating lung retention beyond 24 h. The encapsulation of a biologically active cargo within the particle that results in the expression of a biologic or molecular marker (e.g., green fluorescent protein) or a therapeutic molecule will further enhance our ability to assess the value of nanoparticle systems for diagnostic and therapeutic applications.

Conclusions

The use of custom engineered and functionalized nanoparticles provides significant possibilities for improving diagnostic imaging and unique therapies for lung disease. However, development of these tools for human applications demands comprehensive *in vivo* assessment. Synthetic polymer-based hydrogel particles provide the flexibility required to incorporate targeting peptides and imaging probes, plus package diagnostic and therapeutic cargoes for delivery to the lung. Examination of the fate of model particles labeled to enable tracking shows that changes in size, charge and functionalization result in unique behaviors, each with clinical implications. The larger PMP are briefly retained throughout the airspaces, then cleared rapidly by the GI tract (likely via mucociliary routes), and have a short lung half-life. In the absence of the CPP, these particles did not induce acute inflammation and thus could be used for diagnostic imaging or delivery that requires a relatively brief lung dwell time such as for acute lung injury (e.g., acute lung infection and acute respiratory distress syndrome). In contrast, the smaller PNPs have a higher and more prolonged lung airspace retention, which is further augmented by CPP without acute lung inflammation. These nanoparticles may be more advantageous for serial imaging or therapy of a more persistent lung injury. The high and prolonged uptake of particles in macrophages could be capitalized on for treatment of slow growing and difficult to treat intracellular microorganisms such as *Mycobacterium tuberculosis*, as suggested by others.[8,11,46] Enhanced release of antituberculosis agents using microparticles and nanoparticle constructs has been considered based on the potential to reduce systemic toxicity, provide higher local concentrations of drug, and thereby reduce dose frequency compared to current oral drugs.[8,11,46] Clinical delivery of nanoparticles to the lung may be facilitated by existing aerosolizing devices that can be used to generate mist for impaction in airways or alveolar spaces.[11,32] As we demonstrate, functionalization of our particle systems with these or other diagnostic and therapeutic agents may further alter the material characteristics of the carrier (e.g., surface charge, size, etc.), which will continue to drive the need for comprehensive *in vivo* characterization of particle behavior.

Experimental Procedures

General Procedures and Materials for Particle Synthesis

Unless otherwise noted, all chemicals were purchased from Sigma-Aldrich and used without additional purification. Acrylamide, *N,N'*-methylene-bis-acrylamide, ammonium persulfate, and *N,N,N',N'*-tetramethylethylene-diamine (TMEDA) were purchased from Bio-Rad. The cell-penetrating peptide (CPP) consisting of nine arginine residues (acrylamide-Arg_9-COOH) was purchased from Applied Peptech Suzhou. Hexane (OmniSolv grade) was purchased from EMD. UltraPure 0.1-μm filtered water, and phosphate buffered saline (PBS, pH 7.4) were purchased from Invitrogen.

Synthesis of N-Acryloyltyramine. Tyramine (0.5 g, 3.64 mmol, 1 eq.) dissolved in N,N-dimethylformamide (15 mL) was added to a dried flask purged with dry nitrogen. Triethylamine (0.41 g, 4.01 mmol, 1.1 eq.) was added, and the flask was placed in an ice-water bath. Acryloyl chloride (0.31 g, 3.46 mmol, 0.95 eq.) was mixed with N,N-dimethylformamide (10 mL), and added dropwise to the tyramine solution. After 5 min, the flask was removed from the bath and was allowed to stir for an additional 1 h at rt. The reaction mixture was passed through a 0.2 μm

PTFE syringe filter to remove the precipitate, and the solvent was removed by rotary evaporation. The resulting clear, brown residue was dissolved in ethyl acetate (90 mL) and washed with PBS (3 x 30 mL). The organic layer was dried over $MgSO_4$, filtered, and the solvent was evaporated. The crude product was further purified by silica gel chromatography using a gradient from 3:1 to 1:3 hexane:ethyl acetate as the eluent. The product (0.42 g, 2.20 mmol, 63% yield) obtained was a white solid. Spectroscopic data was consistent with that previously reported by Bentolila, *et al.*[47]

Particle Preparation

CPP-Modified Polyacrylamide Nanoparticles (PNPs). PNPs encapsulating bovine serum albumin conjugated with Alexa Fluor 488 (BSA-488, Invitrogen) and modified with CPP (Figure 3.1) were prepared using modifications to a previously reported method.[13] Briefly, AOT (237 mg, 0.53 mmol) and Brij 30 (459 mg, 1.27 mmol) were added to a 20 mL glass vial. The vial was sealed with a Teflon-lined septum cap and purged with dry nitrogen for 10 min. All further solutions were added to the vial *via* syringe. Deoxygenated hexane (10 mL) was added to the vial and vortexed to completely dissolve the surfactants. Separately, BSA-488 (0.57 mg) was dissolved in PBS (pH 9, 285 µL), to which acrylamide (61.3 mg, 862 µmol), *N,N'*-methylene-bis-acrylamide (7.10 mg, 46.0 µmol), N-acryloyltyramine (1.80 mg, 9.41 µmol), and CPP (1.30 mg, 0.88 µmol) were added and dissolved. Dry nitrogen was bubbled through the monomer solution for 2 min, and then 255 µL of this solution was added to the surfactant solution. The vial was vortexed to form a stable microemulsion. A 50% (w/v) solution of ammonium persulfate in PBS (pH 9, 16 µL) was then added to the emulsion while vortexing. After 5 min, polymerization was initiated by the addition of TMEDA (25 µL), and the mixture was vortexed at 600 rpm at rt for 30 min. The solvent was evaporated, and absolute ethanol (10 mL) was added, resulting in a milky-white suspension. The particles were isolated by centrifugation (2000*g*, rt, 5 min), and washed with absolute ethanol (5 x 10 mL), centrifuging as before. The particles were finally suspended in UltraPure water (10 mL). Particle solution (2 mL) and UltraPure water (13 mL) were added to a pre-rinsed Centriprep Ultracel YM-50 spin filter (50,000 MWCO, Millipore) and centrifuged (1500*g*, rt, 30 min), and the particle-containing retentate was resuspended in 12 mL of UltraPure water. This wash step was repeated until the UV absorbance of the filtrate in the 200-350 nm range reached baseline values. The final retentate was serially passed through 0.2 µm PVDF (Pall) and 0.1 µm Anotop (Whatman) syringe filters and lyophilized overnight to yield a fluffy, orange powder.

Unmodified PNPs. Nanoparticles without CPP incorporated into the polymer structure were prepared as described above, with the exception that the monomer solution consisted of acrylamide (62.5 mg, 879 µmol), *N,N'*-methylene-bis-acrylamide (7.20 mg, 46.7 µmol), and N-acryloyltyramine (1.80 mg, 9.41 µmol), and omitted the CPP.

Polyacrylamide Microparticles (PMPs). PMPs encapsulating BSA-488 and either not modified or modified with CPP (Figure 3.1) were synthesized as described previously.[12]

Particle Characterization

Scanning Electron Microscopy (SEM). Particle samples were prepared as described previously[12,13] and imaged using a Hitachi S-5000 SEM at 10 kV.

Particle Size and Zeta-potential Measurements. The size distributions of particles suspended at 0.1 mg/mL in PBS were determined by light scattering using a Zetasizer Nano-ZS (Malvern Instruments) for PNPs, or a Horiba Partica LA-950 particle size distribution analyzer for PMPs, as described previously.[13] The zeta-potential of particles suspended in UltraPure water (PNPs, 4 mg/mL and PMPs, 0.5 mg/mL) were measured using a Zetasizer Nano-ZS at 25°C.

Preparation of and Studies Performed with Radiolabeled Particles

Cell Culture and *In Vitro* Particle Uptake Assay. The transformed human bronchial epithelial cell line BEAS 2B (CRL-9609, ATCC, Manassas, VA) was cultured in DMEM supplemented with 10% fetal calf serum and antibiotics. For studies with particles, 2 x 10^5 cells were incubated with 5 μg/mL of PMPs (CPP- or CPP+) or 10 μg/mL of PNPs (CPP- or CPP+) that were freshly sonicated. After 24 h, cell layers were washed 3 times with PBS and the percentage of cells containing BSA-488 was quantified by flow cytometry as described below.

Radionuclide Preparation. Carrier-free ^{125}I radionuclide was purchased from Perkin Elmer. ^{76}Br was produced at the Washington University cyclotron facility by the ^{76}Se (p,n) ^{76}Br nuclear reaction on a ^{76}Se-enriched Cu_2Se target. ^{76}Br was recovered by a modified dry distillation method,[48] filtered through a C-18 Sep-Pak light cartridge (Waters Corp.), dried under nitrogen gas, then reconstituted in water (Milli-Q, Millipore) immediately before use. Labeling efficiency and radiochemical purity of labeled particles was determined by radio-thin layer chromatography (radio-TLC, Bioscan System 2000).

Particle Radiolabeling. For biodistribution studies, particles were labeled with ^{125}I using an iodination protocol modified from Markwell.[49] All particles were labeled using the tyrosine residues of the encapsulated BSA-488 while the PNPs were additionally labeled on the tyramine residues of the polymer backbone. To achieve this, 500 μg of lyophilized particles were reconstituted in 250 μL PBS, sonicated for 5 min (Branson 1510) and mixed with 300 μCi of ^{125}I in 10 μL of diluted NaOH solution as described.[49] The reaction was then incubated at room temperature for 30 min and monitored by radio-TLC. The radio-iodinated PMPs were purified by centrifugation (5000*g*) to remove free ^{125}I. ^{125}I-labeled PNPs were precipitated with absolute ethanol then collected by repeated centrifugation. For positron emission tomography (PET) imaging, particles were labeled with ^{76}Br using a previously described approach.[4] The final radiochemical purity of all particles was greater than 95%. The *in vitro* stability of radiolabeled particles was evaluated by incubating the purified particles with mouse serum (Sigma-Aldrich) at 37°C and monitoring with radio-TLC (data not shown). Particles were diluted with PBS to a final concentration of 100 μg/50 μL for administration to mice.

Mice and Particle Delivery. Male C57BL/6J mice were obtained from Jackson Laboratory (Bar Harbor, ME) and housed under pathogen-free conditions. The Animal Studies Committee of the Washington University School of Medicine approved all protocols. Mice were anesthetized with

intraperitoneal Avertin, 200 mg/kg, prior to neck dissection for cannulation of the trachea with a 22-gauge angiocatheter. For intratracheal delivery, PBS alone or particles (100 μg/50 μL) in PBS followed by 50 μL of air as dead space was administered through the catheter as a single bolus.

Small Animal MicroPET Imaging. Anesthetized mice (n=3-5 per group) were administered 10-20 μCi of 100 μg ^{76}Br-labeled particles in 50 μL PBS by intratracheal injection. Imaging was performed 1, 3 and 18 h post-injection using a static 30 min frame with a microPET Focus 120 or 220 scanner, which have the same resolution (Siemens Medical Solutions).[50] X-ray computed tomography (CT) imaging (15 min frame) was performed immediately following acquisition of PET images using a MicroCAT II instrument (CTI-Imtek).[51] The microPET and CT images were co-registered using fiduciary markers attached to the animal positioning bed and quantitatively analyzed using AMIRA software (Mercury Computer Systems). Data were calculated as standardized uptake values (SUVs) within lung fields identified by the CT images and calculated using a tissue density of 0.3 g/mL. The SUV numbers were calculated in multiple 3-dimensional regions of interest within the lung fields as described.[52]

Biodistribution Studies. For lung biodistribution studies, anesthetized mice were injected intratracheally with 1 μCi of 100 μg ^{125}I-labeled particles in 50 μL PBS. At 1, 3, and 24 h post-injection, the mice were euthanized by CO_2 asphyxiation and organs of interest were collected for determination of activity using a Beckman Gamma Counter 8000. For analysis of lung bronchoalveolar lavage, the trachea was cannulated and lavaged three times with 1 mL aliquots of PBS. A dilution of the administered dose of ^{125}I-labeled particles (1:100 dilution) was counted in parallel with the organ samples to calculate the percentage of activity relative to the instilled dose per organ (%ID/organ) as previously described.[53] All data were corrected for radioactive decay of ^{125}I.

Bronchoalveolar Lavage (BAL) and Lung Tissue Samples. Lungs were subjected to BAL with 1 mL of PBS. BAL fluid was centrifuged and the cell-free supernatant was collected and stored for cytokine analysis, while the cell pellet was resuspended in 1 mL of PBS for total cell count, cytospin preparation, flow cytometry, or alveolar macrophage culture. The immune cell differential was determined using standard light microscopy criteria as described previously.[34] Following BAL, lungs were inflated with 1 mL of cryopreservation media (Tissue-tek), frozen on dry ice, and stored at -80°C prior to sectioning.

Flow Cytometry. Cell lines or cells collected by BAL were washed twice with flow cytometry buffer (PBS with 2% FBS). BAL cells were blocked using purified rat anti-mouse CD16/CD32 (Mouse BD Fc Block, BD Biosciences) and then immunostained with macrophage marker rat anti-mouse F4/80 (Serotec) or with IgG2b isotype control antibody, both conjugated with APC. Cells were again washed twice with FACS buffer and analyzed on a FACSCalibur flow cytometer (10,000 events per sample) using CELLquest software (BD Biosciences).

Immunostaining and Microscopy. Frozen tissue sections and BAL cytospin preparations were fixed with 4% paraformaldehyde in PBS for 10 min at rt. Primary antibodies (and dilutions) used were rabbit anti-prosurfactant protein C (1:1000, Abcam) and biotinylated anti-CD68 (dilution 1:75, Serotec). Antibody binding was detected using secondary antibodies conjugated with Alexa Fluor dyes (Invitrogen) or streptavidin, and nuclei were stained with 4',6-diamidino-2-

phenylindole (DAPI; Vector Laboratories). Images were captured using a Leica DM5000 microscope (Wetzlar, Germany) with a Retiga 200R charge-coupled device camera interfaced with QCapture Pro software (Q Imaging). Fluorescence and differential interference contrast images were overlaid in QCapture Pro. Images were composed using Photoshop and Illustrator software (Adobe Systems).

Cytokine Assays. To quantify inflammatory mediators in cell-free BAL fluid from mice following administration of particles, supernatants were analyzed in a multiplex, flow cytometry-based assay according to the manufacturer's protocol (BioPlex, Bio-Rad Laboratories). Unique beads conjugated with a distinct capture antibody were incubated with 50 μL of BAL and 0.5% BSA or a serially diluted standard mix with a known concentration of all measured inflammatory mediators and compared to the standard curves as previously described.[34]

Statistical Analysis. In experiments where replicate samples were analyzed, the results are presented as the mean ± standard deviation of triplicate samples unless otherwise noted. Groups were compared with Student's *t*-test or one-way ANOVA and Scheffé post-testing performed using SPSS statistical software. The level of significance was set at $p < 0.05$.

References

(1) Sajja, H. K.; East, M. P.; Mao, H.; Wang, Y. A.; Nie, S.; Yang, L. *Curr. Drug Discovery Technol.* **2009**, *6*, 43-51.
(2) Balazs, A. C.; Emrick, T.; Russell, T. P. *Science* **2006**, *314*, 1107-1110.
(3) Wooley, K. L.; Moore, J. S.; Wu, C.; Yang, Y. *Proc. Natl. Acad. Sci. U.S.A.* **2000**, *97*, 11147-11148.
(4) Almutairi, A.; Rossin, R.; Shokeen, M.; Hagooly, A.; Ananth, A.; Capoccia, B.; Guillaudeu, S.; Abendschein, D.; Anderson, C. J.; Welch, M. J.; Fréchet, J. M. *Proc. Natl. Acad. Sci. U.S.A.* **2009**, *106*, 685-690.
(5) Lee, C. C.; Gillies, E. R.; Fox, M. E.; Guillaudeu, S. J.; Fréchet, J. M.; Dy, E. E.; Szoka, F. C. *Proc. Natl. Acad. Sci. U.S.A.* **2006**, *103*, 16649-16654.
(6) Kumar, M.; Behera, A. K.; Lockey, R. F.; Zhang, J.; Bhullar, G.; De La Cruz, C. P.; Chen, L. C.; Leong, K. W.; Huang, S. K.; Mohapatra, S. S. *Hum. Gene Ther.* **2002**, *13*, 1415-1425.
(7) Gelperina, S.; Kisich, K.; Iseman, M. D.; Heifets, L. *Am. J. Respir. Crit. Care Med.* **2005**, *172*, 1487-1490.
(8) Azarmi, S.; Roa, W. H.; Lobenberg, R. *Adv. Drug Delivery Rev.* **2008**, *60*, 863-875.
(9) Yokohira, M.; Kuno, T.; Yamakawa, K.; Hosokawa, K.; Matsuda, Y.; Hashimoto, N.; Suzuki, S.; Saoo, K.; Imaida, K. *Toxicol. Pathol.* **2008**, *36*, 620-631.
(10) Muhlfeld, C.; Rothen-Rutishauser, B.; Blank, F.; Vanhecke, D.; Ochs, M.; Gehr, P. *Am. J. Physiol. Lung Cell Mol. Physiol.* **2008**, *294*, L817-29.
(11) Sung, J. C.; Pulliam, B. L.; Edwards, D. A. *Trends Biotechnol.* **2007**, *25*, 563-570.
(12) Cohen, J. L.; Almutairi, A.; Cohen, J. A.; Bernstein, M.; Brody, S. L.; Schuster, D. P.; Fréchet, J. M. *Bioconjugate Chem.* **2008**, *19*, 876-881.
(13) Cohen, J. A.; Beaudette, T. T.; Tseng, W. W.; Bachelder, E. M.; Mende, I.; Engleman, E. G.; Fréchet, J. M. *Bioconjugate Chem.* **2009**, *20*, 111-119.
(14) Murthy, N.; Thng, Y. X.; Schuck, S.; Xu, M. C.; Fréchet, J. M. J. *J. Am. Chem. Soc.* **2002**, *124*, 12398-12399.
(15) Murthy, N.; Xu, M.; Schuck, S.; Kunisawa, J.; Shastri, N.; Fréchet, J. M. J. *Proc. Natl. Acad. Sci. U.S.A.* **2003**, *100*, 4995-5000.
(16) Goh, S. L.; Murthy, N.; Xu, M.; Fréchet, J. M. J. *Bioconjugate Chem.* **2004**, *15*, 467-474.
(17) Bartlett, D. W.; Su, H.; Hildebrandt, I. J.; Weber, W. A.; Davis, M. E. *Proc. Natl. Acad. Sci. U.S.A.* **2007**, *104*, 15549-15554.
(18) Yamamoto, H.; Kuno, Y.; Sugimoto, S.; Takeuchi, H.; Kawashima, Y. *J. Controlled Release* **2005**, *102*, 373-381.
(19) Frankel, A. D.; Pabo, C. O. *Cell* **1988**, *55*, 1189-1193.
(20) Snyder, E. L.; Dowdy, S. F. *Pharm. Res.* **2004**, *21*, 389-393.
(21) Torchilin, V. P. *Biochem. Soc. Trans.* **2007**, *035*, 816-820.
(22) Vives, E.; Schmidt, J.; Pelegrin, A. *Biochim. Biophys. Acta, Rev. Cancer* **2008**, *1786*, 126-138.
(23) Stewart, K. M.; Horton, K. L.; Kelley, S. O. *Org. Biomol. Chem.* **2008**, *6*, 2242-2255.
(24) Fawell, S.; Seery, J.; Daikh, Y.; Moore, C.; Chen, L. L.; Pepinsky, B.; Barsoum, J. *Proc. Natl. Acad. Sci. U.S.A.* **1994**, *91*, 664-668.
(25) Schwarze, S. R.; Ho, A.; Vocero-Akbani, A.; Dowdy, S. F. *Science* **1999**, *285*, 1569-1572.

(26) Kleemann, E.; Neu, M.; Jekel, N.; Fink, L.; Schmehl, T.; Gessler, T.; Seeger, W.; Kissel, T. *J. Controlled Release* **2005**, *109*, 299-316.
(27) Moschos, S. A.; Jones, S. W.; Perry, M. M.; Williams, A. E.; Erjefalt, J. S.; Turner, J. J.; Barnes, P. J.; Sproat, B. S.; Gait, M. J.; Lindsay, M. A. *Bioconjugate Chem.* **2007**, *18*, 1450-1459.
(28) Shimada, A.; Kawamura, N.; Okajima, M.; Kaewamatawong, T.; Inoue, H.; Morita, T. *Toxicol. Pathol.* **2006**, *34*, 949-957.
(29) Oberdorster, G.; Sharp, Z.; Atudorei, V.; Elder, A.; Gelein, R.; Kreyling, W.; Cox, C. *Inhalation Toxicol.* **2004**, *16*, 437-445.
(30) Rogueda, P. G.; Traini, D. *Expert Opin. Drug Delivery* **2007**, *4*, 595-606.
(31) Yang, W.; Peters, J. I.; Williams, R. O., 3rd *Int. J. Pharm.* **2008**, *356*, 239-247.
(32) Semmler-Behnke, M.; Takenaka, S.; Fertsch, S.; Wenk, A.; Seitz, J.; Mayer, P.; Oberdorster, G.; Kreyling, W. G. *Environ. Health Perspect.* **2007**, *115*, 728-733.
(33) Geiser, M.; Casaulta, M.; Kupferschmid, B.; Schulz, H.; Semmler-Behnke, M.; Kreyling, W. *Am. J. Respir. Cell Mol. Biol.* **2008**, *38*, 371-376.
(34) Gunsten, S.; Mikols, C. L.; Grayson, M. H.; Schwendener, R. A.; Agapov, E.; Tidwell, R. M.; Cannon, C. L.; Brody, S. L.; Walter, M. J. *Immunology* **2009**, *126*, 500-513.
(35) Mizgerd, J. P. *Semin. Immunol.* **2002**, *14*, 123-132.
(36) De Jong, W. H.; Borm, P. J. *Int. J. Nanomedicine* **2008**, *3*, 133-149.
(37) Dailey, L. A.; Jekel, N.; Fink, L.; Gessler, T.; Schmehl, T.; Wittmar, M.; Kissel, T.; Seeger, W. *Toxicol. Appl. Pharmacol.* **2006**, *215*, 100-108.
(38) Barlow, P. G.; Clouter-Baker, A.; Donaldson, K.; Maccallum, J.; Stone, V. *Part. Fibre Toxicol.* **2005**, *2*, 11.
(39) Bastus, N. G.; Sanchez-Tillo, E.; Pujals, S.; Farrera, C.; Kogan, M. J.; Giralt, E.; Celada, A.; Lloberas, J.; Puntes, V. *Mol. Immunol.* **2009**, *46*, 743-748.
(40) Lam, C. W.; James, J. T.; McCluskey, R.; Hunter, R. L. *Toxicol. Sci.* **2004**, *77*, 126-134.
(41) Nemmar, A.; Hoet, P. H.; Vanquickenborne, B.; Dinsdale, D.; Thomeer, M.; Hoylaerts, M. F.; Vanbilloen, H.; Mortelmans, L.; Nemery, B. *Circulation* **2002**, *105*, 411-414.
(42) Lai, S. K.; Wang, Y. Y.; Hanes, J. *Adv. Drug Delivery Rev.* **2009**, *61*, 158-171.
(43) Wang, Y. Y.; Lai, S. K.; Suk, J. S.; Pace, A.; Cone, R.; Hanes, J. *Angew. Chem., Int. Ed.* **2008**, *47*, 9726-9729.
(44) Zhang, K.; Fang, H.; Chen, Z.; Taylor, J. S.; Wooley, K. L. *Bioconjugate Chem.* **2008**, *19*, 1880-1887.
(45) Broaders, K. E.; Cohen, J. A.; Beaudette, T. T.; Bachelder, E. M.; Fréchet, J. M. J. *Proc. Natl. Acad. Sci. U. S. A.* **2009**, *106*, 5497-5502.
(46) Verma, R. K.; Kaur, J.; Kumar, K.; Yadav, A. B.; Misra, A. *Antimicrob. Agents Chemother.* **2008**, *52*, 3195-3201.
(47) Bentolila, A.; Vlodavsky, I.; Ishai-Michaeli, R.; Kovalchuk, O.; Haloun, C.; Domb, A. J. *J. Med. Chem.* **2000**, *43*, 2591-2600.
(48) Tolmachev, V.; Lundqvist, H.; Einarsson, L. *Appl. Radiat. Isot.* **1998**, *49*, 79-81.
(49) Markwell, M. A.; Fox, C. F. *Biochemistry* **1978**, *17*, 4807-4817.
(50) Tai, Y.-C.; Ruangma, A.; Rowland, D.; Siegel, S.; Newport, D. F.; Chow, P. L.; Laforest, R. *J. Nucl. Med.* **2005**, *46*, 455-463.
(51) Paulus, M. J.; Gleason, S. S.; Kennel, S. J.; Hunsicker, P. R.; Johnson, D. K. *Neoplasia* **2000**, *2*, 62-70.

(52) Rossin, R.; Muro, S.; Welch, M. J.; Muzykantov, V. R.; Schuster, D. P. *J. Nucl. Med.* **2008**, *49*, 103-111.
(53) Edwards, W. B.; Anderson, C. J.; Fields, G. B.; Welch, M. J. *Bioconjugate Chem.* **2001**, *12*, 1057-1065.

Chapter 4 – Acid-Degradable Cationic Dextran Particles for the Delivery of siRNA Therapeutics

Abstract

Given the biocompatibility issues surrounding the polyacrylamide-based system, we sought to generate another acid-degradable material for siRNA delivery. In this chapter, we report a new acid-sensitive, biocompatible and biodegradable microparticulate delivery system, spermine modified acetalated-dextran (Spermine-Ac-DEX), which can be used to efficiently encapsulate siRNA. These particles demonstrated efficient gene knockdown in HeLa-*luc* cells with minimal toxicity. This knockdown was comparable to that obtained using Lipofectamine, a commercially available transfection reagent generally limited to *in vitro* use due to its high toxicity. Due to its ease of preparation, pH-sensitivity, and biocompatibility, spermine-Ac-DEX represents an attractive and highly efficient siRNA delivery system.

Introduction

RNA interference (RNAi) has drawn much attention in the field of medicine due to its potential for treating chronic diseases and genetic disorders by harnessing the endogenous RNAi pathway.[1-3] RNAi is a biological mechanism wherein double-stranded RNAs can be used to reduce expression of target proteins.[4,5] Once the RNA is present in the cytoplasm of the cell, it is shortened and processed by the RNAse III enzyme, Dicer,[6] and incorporated into a protein complex called the RNA-induced silencing complex (RISC).[7] One of the two strands of the short, double-stranded RNA is cleaved, and the activated RISC (which contains the guide strand of the RNA) binds to a complementary sequence of mRNA and results in its degradation.[8] The activated RISC is capable of multiple rounds of mRNA cleavage, which propagates gene silencing.[9] Due to its potential to silence genes in a sequence-specific manner, RNAi holds promise for treating many diseases that may not otherwise be accessed with current therapeutic technology.[1]

Various approaches have been developed that allow for exploitation of the RNAi process, principally through the use of exogenous synthetic small interfering RNA (siRNA), double-stranded RNAs that are typically 19-23 base pairs in length. Synthetic siRNA can be designed to target nearly any gene in the body, and is therefore attractive for a variety of medical applications. Previous reports have demonstrated that synthetic siRNAs are capable of knocking down targets in several diseases *in vivo*, including hepatitis B virus, human papillomavirus, and ovarian cancer.[10] Despite great therapeutic potential, the clinical application of siRNA is limited by delivery problems. siRNA does not cross cellular membranes efficiently due to its relatively large size, negative charge, and hydrophilicity. In addition, siRNA is unstable under *in vivo* conditions due to rapid degradation by serum nucleases.[11] Thus, the widespread use of RNAi therapeutics for disease prevention and treatment requires the development of clinically suitable, safe, and effective delivery vehicles.[10] In order to induce effective RNAi, these vehicles must overcome a variety of extracellular and intracellular obstacles; i.e. they should provide protection against nuclease activity and facilitate internalization and intracellular trafficking of the siRNA.[12] Even though significant advances have been made in the field, the development of vehicles that can efficiently deliver RNAi therapeutics both *in vitro* and *in vivo* remains a major challenge.

Both viral and non-viral carriers have been developed for the delivery of siRNA.[12-16] Although viral vectors are very efficient, they can cause immunogenic and inflammatory responses,[17,18] which raise concerns about their safety as delivery vectors. Non-viral vectors provide opportunities for improved safety, greater flexibility and more facile manufacturing, however, most of the existing carriers suffer from low delivery efficiencies. The most common non-viral vectors involve complexes formed between cationic lipids[19,20] or polymers[21,22] and siRNA through electrostatic interactions between the negative phosphates along the nucleic acid backbone and the positive charges displayed on the vector. In addition to low transfection efficiencies, these systems also suffer from high toxicity due to their polycationic nature and limited stability *in vivo* due to non-specific interactions with serum proteins. The limitations associated with current delivery vehicles motivate the development of novel systems for siRNA delivery that may be able to overcome these obstacles.

Among many alternatives to cationic polymers and lipids commonly used to form polyplexes/lipoplexes with genetic material,[10,23,24] particles made from biodegradable and non-toxic materials such as slow-hydrolyzing poly(lactic-co-glycolic acid) (PLGA),[25,26] fast-degrading polyesters (such as DEAPA-PVA-PLGA),[27] and acid-sensitive poly(orthoesters) (POEs)[28] have been explored as *in vivo* gene delivery vectors. Another system based on acid-sensitive polyketals has also recently shown promise for delivery of siRNA both *in vitro* and *in vivo*.[29] These prior examples of particulate systems for siRNA and DNA delivery typically employ small quantities of cationic polymers[25,30] (i.e. poly(β-amino ester), PBAE, or polyethylenimine, PEI), lipids such as DOTAP,[29] or small molecules such as spermine[26] blended with the carrier polymer to enhance loading of DNA/RNA and delivery efficiency. Formed by standard emulsion techniques, these particles combine physical entrapment of their payload with electrostatic complexation of genetic material while retaining biocompatible degradation mechanisms. However, some limitations of these systems relate to the synthetic flexibility, biocompatibility of the degradation products, and the paucity of chemical methods for the modification of the particle surface. For example, despite the promising transfection results obtained from PLGA microspheres, they still suffer from slow release rates[31] and the formation of DNA-damaging acidic by-products.[32,33]

Dextran, a homopolysaccharide of glucose, appears to be well poised for use as a polymeric carrier due to its biodegradability, wide availability, and ease of modification.[34] In addition, dextran already has a history of human use in clinical applications for plasma volume expansion and plasma substitution. The potential application of dextran for siRNA delivery has recently been demonstrated.[35-37] Previously, we described the development of a modular and tunable particle system based on acetal-modified dextran (Ac-DEX).[38,39] We have shown that Ac-DEX particles prepared by standard emulsion techniques - either water in oil (w/o) or water in oil in water (w/o/w) - have high encapsulation efficiencies for both hydrophobic small molecules[40] and high molecular weight hydrophilic cargoes,[38,39] such as proteins, and that the release rate of the encapsulated cargo was tunable.[39] These acid-degradable Ac-DEX particles were capable of delivering protein antigens to macrophages and dendritic cells. Besides their use as a successful vaccine carrier, microparticles prepared from Ac-DEX blended with a cationic polymer proved effective at delivering plasmid DNA to both phagocytic and non-phagocytic cells.[41] Although siRNA and plasmid can be applied to achieve similar functional outcomes, successful plasmid delivery carriers cannot necessarily achieve efficient siRNA delivery due to the major intrinsic structural differences and different location of action for siRNA and plasmid.[42,43,44] For example, reports from other groups have shown the difficulty of

encapsulating the highly charged, hydrophilic and rigid siRNA in particles by w/o/w emulsion, presumably due to leakage into the outer water phase.[45]

We now describe the preparation and preliminary evaluation of a new polymeric platform – spermine-modified Ac-DEX (spermine-Ac-DEX) – for the delivery of siRNA. The new system combines facile synthesis and biocompatibility with the additional benefit of controlled payload release sensitive to physiologically relevant acidic conditions. Acid-sensitive systems have particularly desirable characteristics, as cargo release can be triggered in response to endosomal acidification upon cellular uptake.

The ability of spermine-Ac-DEX particles to overcome a variety of cellular obstacles and function as an efficient delivery vehicle for siRNA can be rationalized by its tailor-made design (Figure 4.1). We hypothesize particulate formulation should provide protection of the encapsulated siRNA against chemical and enzymatic degradation. The cationic characteristics of spermine-Ac-DEX can facilitate the encapsulation of siRNA inside particles, and it may also favorably contribute to cellular uptake by enhancing interaction of the particles with negatively-charged cell membranes. Once inside cells, hydrolysis of the polymer in the acidic endolysosomal compartment can allow the siRNA to be released from the particles. Endosomal escape may be achieved via "proton sponge" effect of the amine moieties, as well as increased endosomal osmotic pressure by degradation of the spermine-Ac-DEX material. Overall, we speculate that it is the combination of protection and endolysosomal release that would be the most likely contributors to the successful delivery of siRNA using a spermine-Ac-DEX carrier.

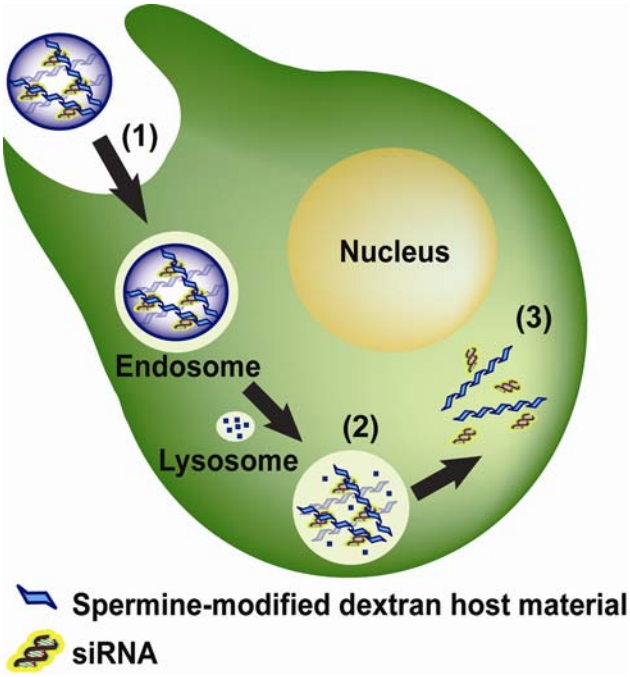

Figure 4.1. The particles are expected to efficiently transfect HeLa-*luc* cells due to their ability to overcome several obstacles to gene delivery. Ac-DEX particles should protect siRNA from degradation. (1) The particles are endocytosed by HeLa cells, and the vesicle is acidified upon fusion of the endosome with the lysosome. (2) Spermine-Ac-DEX particles degrade in the acidic environment of the endolysosome and (3) the siRNA is released into the cytoplasm.

Results and Discussion

Synthesis of Spermine-modified Ac-DEX.

Ac-DEX has several characteristics that make it well suited for the delivery of bioactive cargoes. Although this system has been used to successfully deliver protein antigens, adjuvants and small molecule agents, the neutrally charged polymer can not efficiently encapsulate siRNA. Taking advantage of the blend approach described above, we have recently reported the preparation of particles encapsulating plasmid DNA by formulating Ac-DEX with small amounts of the cationic polymer PBAE.[41] These particles were able to efficiently transfect both phagocytic and non-phagocytic cells *in vitro*. Inspired by this work, we tried to prepare Ac-DEX particles encapsulating siRNA by blending with either small polyamines or cationic polymers. While high loading and efficient delivery of plasmid DNA was achieved by blending Ac-DEX with PBAE, attempts to prepare siRNA-loaded particles by the same method only afforded particles with low loading and low encapsulation efficiency.

Domb and coworkers have reported the synthesis of various oligoamine polysaccharide conjugates for use in gene delivery.[46] They found that, of 300 different polycations prepared, only a few were active in transfecting cells. Dextran-spermine displayed especially high transfection efficiency, which they attributed to unique complexation properties between DNA and the grafted spermine moieties.[46] Dextran-spermine, and derivatives thereof, have shown high transfection of plasmid DNA both *in vitro* and *in vivo*.[47,48] Combining this pioneering work with the unique characteristics of our Ac-DEX, we have modified Ac-DEX with spermine for use in siRNA delivery.

Scheme 4.1. Schematic illustration of the synthesis of spermine-modified Ac-DEX.

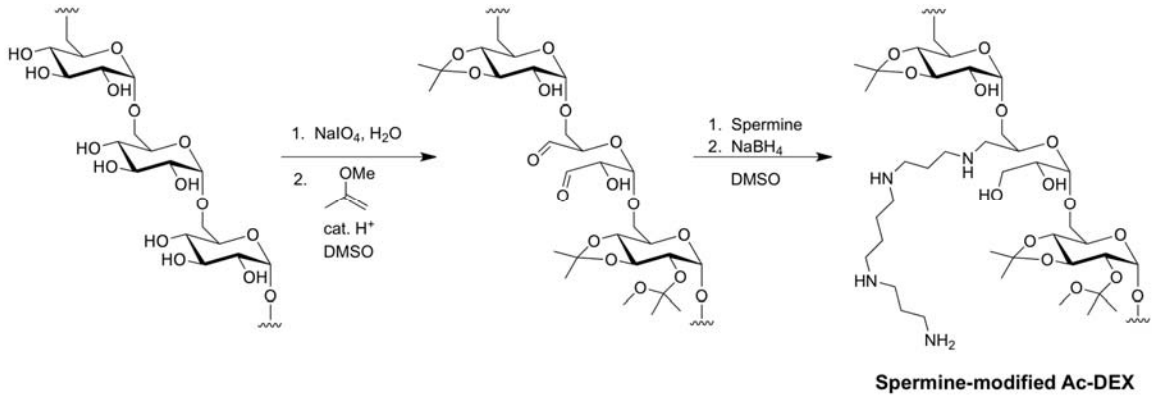

Spermine-Ac-DEX was prepared by using reductive amination chemistry for the conjugation of spermine to Ac-DEX (Scheme 4.1). To increase the number of available aldehyde functionalization sites beyond the reducing chain ends of the polysaccharide, dextran was first lightly oxidized with sodium periodate thus increasing significantly its aldehyde content[49] as evaluated by a reductometric bicinchoninic acid assay (BCA assay). Using this method, we settled on a loading of 8.4 aldehyde functions per 100 anhydroglucose units (AGU). Reaction of the remaining hydroxyl groups with 2-methoxypropene afforded partially-oxidized Ac-DEX, an acid-sensitive, hydrophobic polymer that can be easily processed into microparticles. Finally, amine modification was performed between spermine and aldehyde-containing-Ac-DEX using sodium borohydride as the reducing agent. The amount of spermine conjugated to the dextran,

calculated from the nitrogen content (%N) as determined by elemental analysis, averaged 6.6 spermine units per 100 AGU.

Preparation and Characterization of Spermine-Ac-DEX Particles.

Spermine-Ac-DEX particles encapsulating siRNA were prepared via a standard double-emulsion technique (Figure 4.2). Particles prepared from unmodified Ac-DEX and Ac-DEX blended with 10 wt% PBAE, a formulation previously used for plasmid DNA, were also made for comparison purposes. The particles were visualized by scanning electron microscopy (SEM) to determine the average particle size and morphology. All particles were found to be spherical in shape with diameters in the range of 180 to 230 nm in the dry state, irrespective of particle formulation (Table 4.1). The surface charge of the particles was determined by zeta-potential measurements. Unmodified Ac-DEX particles have a slightly negative zeta-potential due to the encapsulated siRNA. Blending the polymer with PBAE made the surface charge less negative owing to the cationic nature of the polymer, while the surface charge of spermine-Ac-DEX particles was positive. As expected, the surface charge decreased with increasing loadings of siRNA but remained positive for all particle formulations.

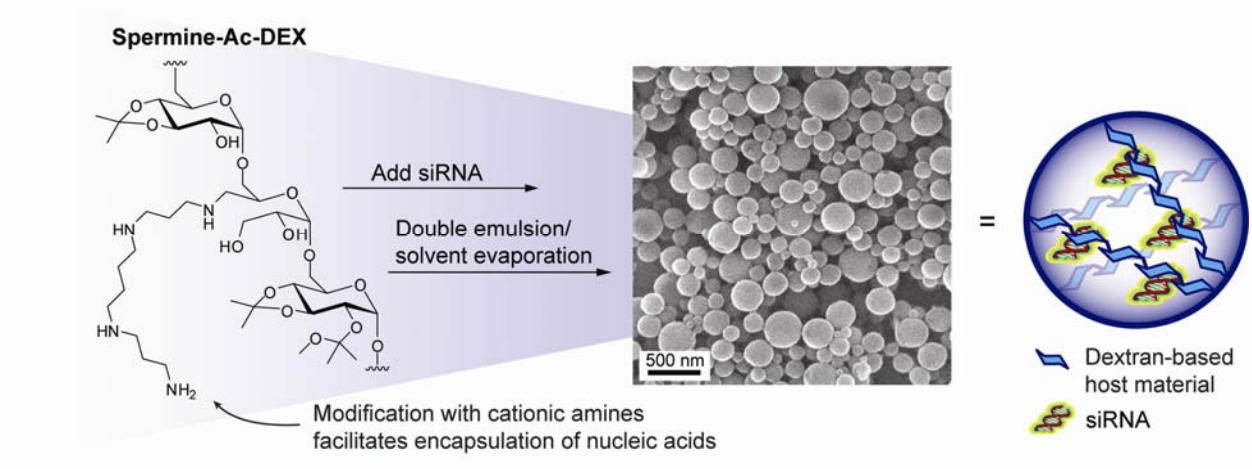

Figure 4.2. Preparation of spermine-modified Ac-DEX particles encapsulating siRNA showing a representative scanning electron micrograph of particles (scale bar = 500 nm) (center) and a cartoon illustration of siRNA-loaded particles (right).

The siRNA loading and loading efficiencies were determined by degrading a sample of particles under acidic conditions and analyzing the siRNA concentration using a Picogreen dsDNA assay (Table 4.1). The siRNA loading efficiency for unmodified Ac-DEX particles was low (5%), as expected based on previous reports with other particle systems, such as PLGA.[26] Blend particles formulated from Ac-DEX and a cationic polymer poly(β-amino ester) (PBAE) also showed low encapsulation efficiency for siRNA (7%), much lower than the plasmid encapsulation achieved with a similar particle formulation. This lower encapsulation efficiency for siRNA as compared to plasmid DNA may be due to the fact that siRNA has a lower molar mass than plasmid DNA (approximately 250x less) and, thus, may be more able to diffuse through the condensing polymer during the emulsion process, resulting in reduced loading efficiency.[50] Improved loading efficiencies (75-98%) were obtained for particles prepared from

spermine-Ac-DEX. This loading compares favorably with other particle formulations, such as PLGA blended with spermidine for which 56% of the siRNA was encapsulated.[26] In contrast to previously reported particulate delivery systems, however, particles prepared using spermine-Ac-DEX did not require blending of a cationic material with the polymer due to the ability of the polymer to electrostatically interact with siRNA.

Table 4.1. Characterization of particle formulations.

Particle Formulation (siRNA, feed)[a]	*Diameter*[b,c] *[nm]*	*Zeta-potential*[b] *[mV]*	*siRNA Loading*[b,d] *[μg mg^{-1}]*	*Loading Efficiency*[b] *[%]*
Ac-DEX (Luc, 5)	230 ± 80	-5.5 ± 0.42	0.26	5
Ac-DEX/10% PBAE (Luc, 5)	N.D.	-3.4 ± 0.44	0.34	7
Spermine-Ac-DEX (Luc, 10)	178 ± 76	9.2 ± 0.69	7.95	76[e]
Spermine-Ac-DEX (Luc, 5)	229 ± 59	16.2 ± 0.58	4.70	91
Spermine-Ac-DEX (Luc, 2.5)	185 ± 65	19.7 ± 0.63	2.28	95[f]
Spermine-Ac-DEX (Control, 5)	195 ± 45	16.1 ± 0.71	5.11	98

a) Luc – anti-luciferase siRNA, Control – Silencer Negative Control #1 siRNA, Feed – amount of siRNA used in particle preparation, μg of siRNA per mg of polymer. b) Characterized as described in the main text. c) Some particle aggregation was observed upon resuspension following lyophilization. The mean particle diameter determined by light scattering for Spermine-Ac-DEX (Luc, 5) and Spermine-Ac-DEX (Control, 5) was 2.71 ± 1.54 μm and 6.45 ± 2.47 μm, respectively (Horiba Partica LA-950, Horiba Scientific). d) siRNA loading in μg of siRNA per mg of particles (100% efficiency ≈ 5.0 μg of siRNA per mg of particles). A loading of 5 μg of siRNA per mg of particles corresponds to an N/P ratio of approximately 100. e) 100% efficiency ≈ 10 μg of siRNA per mg of particles. f) 100% efficiency ≈ 2.5 μg of siRNA per mg of particles. N.D. = not determined

A significant limitation of other commonly used particle delivery systems is their lack of ability to tune the release rate of the encapsulated cargo. Ac-DEX particles are designed to be relatively stable under physiological conditions (pH 7.4) but degrade under the mildly acidic conditions typically found in the lysosome (pH 5.0-5.5), thus allowing for the selective release of the therapeutic agent once inside the cell. We have shown that the rate of microparticle degradation can be easily varied by controlling the type of acetals (i.e. cyclic vs. acyclic) formed on the dextran.[39] To determine the degradation rate of spermine-Ac-DEX particles, empty particles were incubated at 37°C at either pH 5.0 or pH 7.4 and monitored for the release of soluble dextran (Figure 4.3a). No soluble dextran was detected after 48 h for the particles incubated at pH 7.4. In contrast, particles incubated in pH 5.0 buffer showed continuous release of dextran in the first 24 h at 37°C, with a degradation half-life of 8 h. We also monitored the release of siRNA from the particles at pH 5.0 and pH 7.4 to determine if the release occurred in a pH-controlled manner (Figure 4.3b). Little or no release was observed at pH 7.4 after 48 h, while continuous release of siRNA was observed over 24 h at pH 5.0.

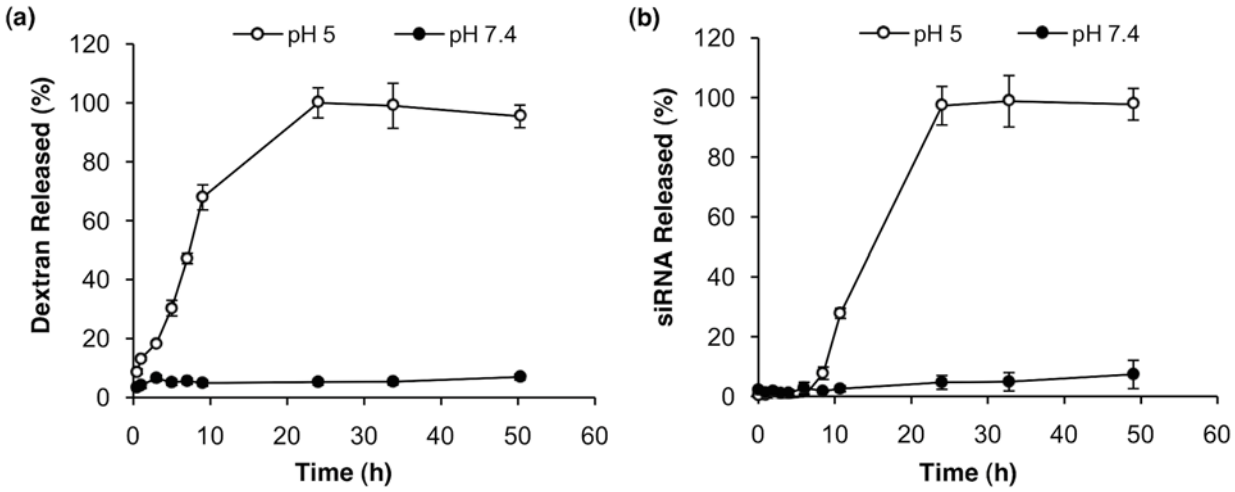

Figure 4.3. (a) Degradation of particles when incubated at pH 7.4 (black circles) and pH 5 (white circles), as determined by analysis of released soluble dextran. (b) Release of siRNA from spermine-Ac-DEX particles when incubated at pH 7.4 (black circles) or pH 5 (white circles). Data represent the mean ± standard deviation of triplicate measurements.

To study siRNA loading, three differently-loaded batches of spermine-Ac-DEX particles encapsulating luciferase siRNA were prepared. The feed values for these particles were 2.5, 5.0, and 10 μg of siRNA per mg of polymer, respectively. Following preparation, the siRNA loading of the particles was quantified as described above (Figure 4.4a). Loadings of up to 8.0 μg of siRNA per mg of particle were achieved and the loading efficiency was above 75% for all particle batches. Efficient loading of siRNA into spermine-Ac-DEX particles is important because of the high cost of siRNA.

***In Vitro* Analysis of siRNA Delivery to HeLa Cells.**

To test the transfection efficiency of spermine-Ac-DEX particles *in vitro*, we chose to knockdown a model reporter protein, firefly luciferase. Luciferase is an ideal reporter gene because it is easy to measure its enzymatic activity using a sensitive and reliable plate-based assay. HeLa cells that stably express firefly luciferase (HeLa-*luc* cells) were used as a model cell line. A more effective delivery system will lead to more cytosolic siRNA and luciferase mRNA cleavage, and thus a lower expression of luciferase protein. Firefly luciferase catalyzes the mono-oxygenation of luciferin and during this process a photon of light is produced. Thus, reduced expression of luciferase will result in the generation of fewer photons when the cells are incubated with the enzyme substrate.

We were interested in determining if particle loading or concentration influences the delivery efficiency of siRNA-loaded particles. Differentially loaded particles were prepared and HeLa-*luc* cells were incubated with particle doses equivalent to 17.2 pmol of siRNA per well. All of the particles could reduce luciferase expression of the cells (approximately 55-60% compared to untreated cells) with low toxicity (greater than 85% viability) (Figure 4.4b). The luciferase expression was comparable for all three batches of particles indicating that the particle loading and concentration within the tested range have a minimal impact on the overall performance, and the knockdown resulted from successful delivery of siRNA.

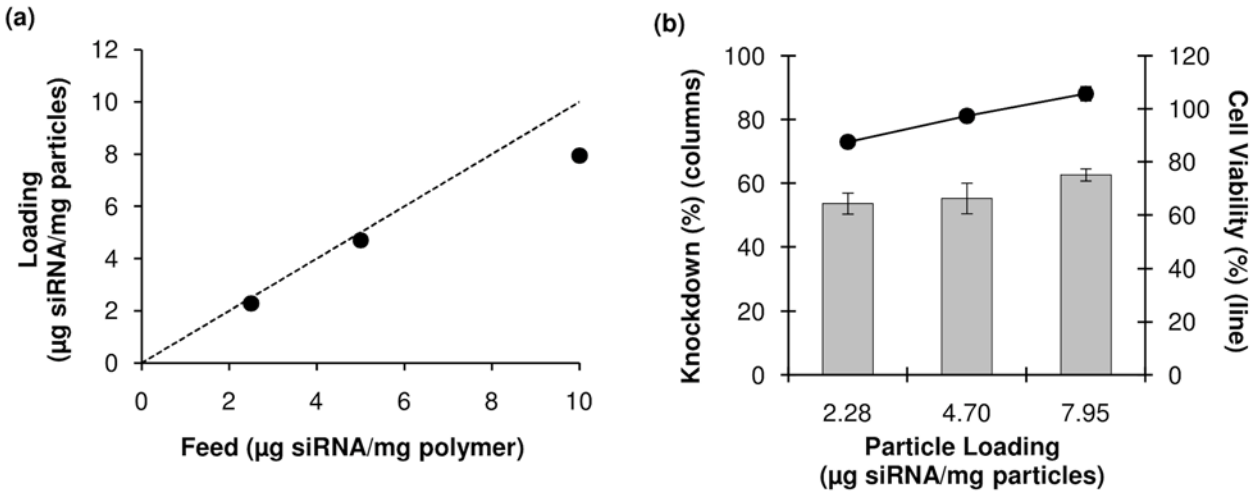

Figure 4.4. Optimized siRNA loading in particles and its effect on luciferase knockdown. (a) siRNA loading in particles compared with the feed amount of siRNA used in particle synthesis. Dashed diagonal line represents 100% loading efficiency. (b) Knockdown of luciferase activity with varying siRNA loadings. HeLa-*luc* cells were treated with particle doses equivalent to 17.2 pmol siRNA/well. Results were compared to untreated cells and the percentage knockdown of luciferase expression was calculated. Results (columns) are combined with results from a concurrently performed cytotoxicity assay (closed circles and line). Knockdown correlates with siRNA concentration, not particle loading.

To determine if the knockdown was dose-dependent, HeLa-*luc* cells were incubated with varying siRNA doses for 48 h and analyzed for the expression of luciferase. As shown in Figure 4.5, spermine-Ac-DEX particles containing luciferase-specific siRNA efficiently knockdown luciferase expression at all siRNA concentrations tested. Transfection with luciferase siRNA loaded spermine-Ac-DEX particles resulted in significant gene silencing (up to 60% knockdown compared with untreated cells). In comparison, treatment of cells with free siRNA did not affect the luciferase expression, indicating the importance of encapsulation of siRNA in particles. The extent of gene silencing depends on the amount of siRNA incubated with the cells (Figure 4.5). Treating cells with lower particle concentrations, and thus less siRNA, resulted in reduced knockdown. The optimal knockdown was obtained with the three highest siRNA dosages tested (8.75, 17.5, and 35 pmol of siRNA). This silencing effect was sequence specific as spermine-Ac-DEX particles loaded with a non-specific siRNA sequence (Silencer Negative Control #1 siRNA) did not result in obvious reduction of luciferase expression. Importantly, there was no significant cytotoxicity associated with intracellular accumulation of spermine-Ac-DEX particles. MTT assay of cells incubated with particles showed greater than 80% cell viability for all particle concentrations tested (Figure 4.6).

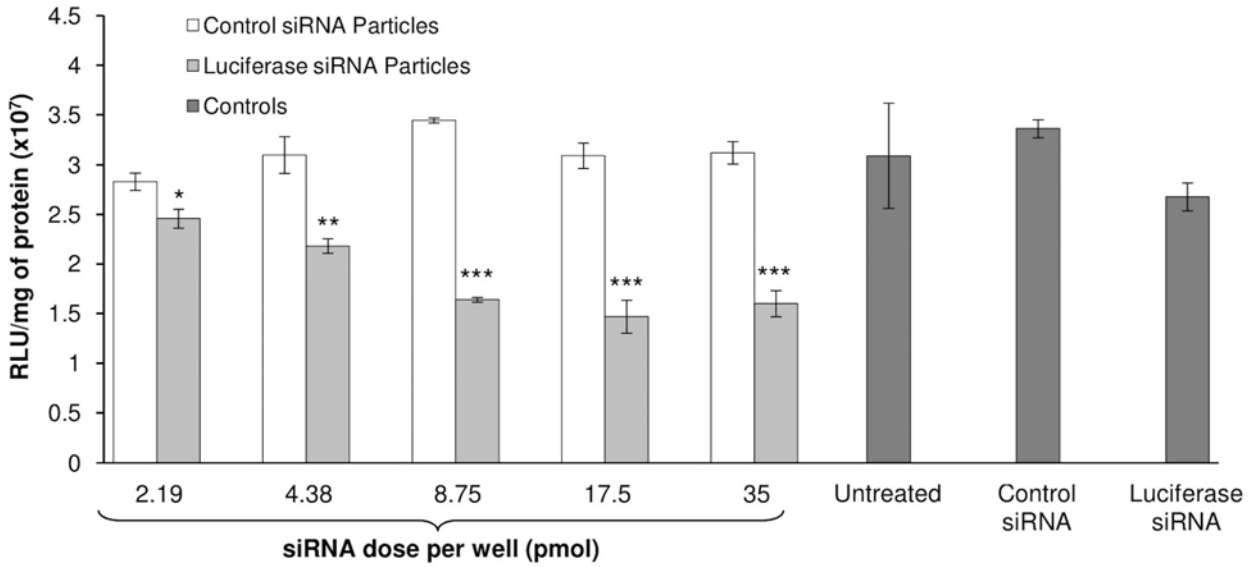

Figure 4.5. Spermine-Ac-DEX particles can efficiently deliver siRNA to HeLa-*luc* cells. *In vitro* transfection of HeLa-*luc* cells with siRNA-loaded spermine-Ac-DEX particles. HeLa-*luc* cells were treated with particles encapsulating either luciferase siRNA or control siRNA at various concentrations. Relative light units (RLU) from the luminometer were normalized to the total mass of cellular protein determined from a fluorescamine assay. Data represent the mean ± standard deviation of quadruplicate measurements. Statistical difference was performed with Student's *t*-test between untreated cells and each treatment group, $p < 0.05$ were marked with *, $p < 0.01$ with **, and $p < 0.001$ with ***.

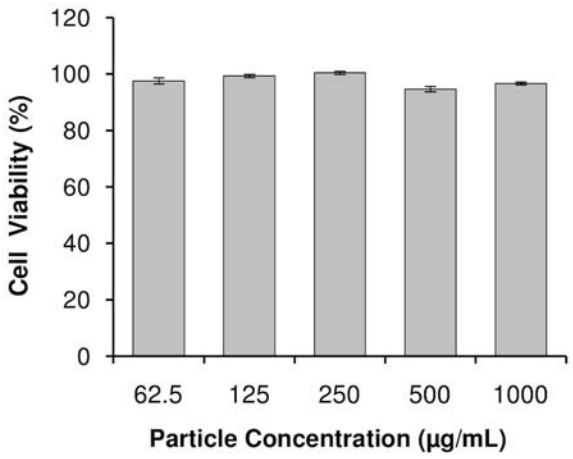

Figure 4.6. Spermine-Ac-DEX particles are non-toxic at concentrations up to 1 mg/mL. MTT assay was used to measure cell viability compared with untreated cells. Data represent the mean ± standard deviation of quadruplicate measurements.

Lipofectamine 2000, a commercially available cationic lipid-based reagent, was used as a positive control in the transfection experiment. This reagent is commonly used for *in vitro* transfection[51], but it faces several obstacles for clinical translation.[52] Lipofectamine complexes with the luciferase-targeting siRNA as well as with the control siRNA were prepared so that the dose of siRNA would match that used with two of the particle concentrations tested (35 pmol siRNA per well and 8.75 pmol siRNA per well). We observed some non-specific reduction of luciferase expression using Lipofectamine 2000, most likely due to slight toxicity of the complexes. Thus, the knockdown was normalized to the data from the cells treated with the control siRNA complexes. The knockdown obtained with the spermine-Ac-DEX particles was comparable to that obtained with Lipofectamine 2000 at both siRNA doses tested (Figure 4.7). Due to their ability to provide efficient siRNA delivery with reduced cytotoxicity (97% cell viability for spermine-Ac-DEX particles compared to 75% for Lipofectamine), spermine-Ac-DEX particles represent an attractive delivery system that may offer several advantages over previously reported materials for siRNA delivery.

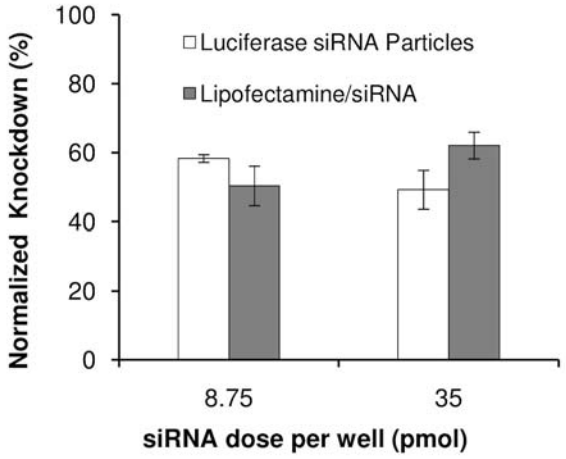

Figure 4.7. Spermine-Ac-DEX particles show comparable activity compared with Lipofectamine 2000. Knockdown was normalized to the data from the cells treated with the control siRNA particles or complexes. Data represent the mean ± standard deviation.

Conclusions

In summary, spermine-Ac-DEX particles represent a novel delivery vehicle which can efficiently deliver siRNA to cancer cells with minimal toxicity. Spermine-Ac-DEX combines the attractive properties of cationic polymers with those of polymeric particles affording a material that is safe and effective for gene delivery. Spermine modification of Ac-DEX facilitated the preparation of particles capable of encapsulating siRNA with high loading efficiency. *In vitro* evaluation demonstrated that the particles are capable of knocking down luciferase expression in HeLa-*luc* cells in a dose-dependent manner with low cytotoxicity. In comparison to previously reported gene delivery materials, spermine-Ac-DEX shows attractive new transfection and biodegradability features, and in addition can be easily modified[53] (for example with peptide targeting ligands). Due to its acid-sensitivity, spermine-Ac-DEX allows for the selective release of siRNA after cellular internalization, with potential tunability of cargo release rate. Thus, spermine-Ac-DEX expands the potential application of Ac-DEX based particles and represents a

promising vehicle for siRNA delivery. Future studies will explore the feasibility of using these particles to regulate protein expression *in vivo*.

Experimental Procedures

General Materials and Methods

All chemicals were from Sigma-Aldrich (St. Louis, MO) unless otherwise noted. The anti-luciferase siRNA (sense strand: 5'-CUU ACG CUG AGU ACU UCG A dTdT-3') was obtained from Dharmacon (Lafayette, CO) and Silencer Negative Control #1 siRNA was purchased from Ambion (Austin, TX). Phosphate buffered saline (PBS, pH 7.4) was from Invitrogen (Carlsbad, CA). Reactions requiring anhydrous conditions were performed in flame-dried vessels and under a positive pressure of dry nitrogen. Water (dd-H_2O) for buffers and particle washing steps was purified to a resistance of 18 MΩ using a NANOpure purification system (Barnstead, USA). When used in the presence of acetal containing materials, dd-H_2O was rendered basic (pH 8) by the addition of triethylamine (TEA) (approximately 0.01%). ^{1}H NMR spectra were recorded at 400 or 500 MHz on a Bruker spectrometer. Elemental analyses were performed at the UC Berkeley Mass Spectrometry Facility. Fluorescence measurements were obtained using a Spectra Max Gemini XS plate-reading fluorimeter (Molecular Devices, USA), usage courtesy of Prof. Carolyn Bertozzi. Absorbance measurements were obtained using a Spectra Max 190 microplate reader (Molecular Devices, USA), usage courtesy of Prof. Carolyn Bertozzi. Luminescence measurements were obtained using a GloMax 96 microplate luminometer (Promega, USA), usage courtesy of Prof. Eva Harris.

Polymer Synthesis

Synthesis of Spermine-Ac-DEX.

Partial Oxidation of Dextran. Dextran (5.0 g, 30.9 mmol, M_w 9-11,000 g/mol, from *Leuconostoc mesenteroides*) was dissolved in 20 mL water. After adding sodium periodate (1.1 g, 51.4 mmol), the solution was stirred for 5 h at rt. The product was purified by dialysis of the solution against distilled water using a regenerated cellulose membrane with a MWCO of 3,500 g/mol. The water was changed 5 times and the sample was lyophilized to obtain a white powder (4.2 g, 8.4 mol aldehyde functions/100 mol anhydroglucose unit, AGU). The degree of oxidation was determined colorimetrically (UV absorption at 562 nm) using a microplate reductometric bicinchoninic acid assay (Micro BCA Protein Assay Kit, Pierce, USA) according to the manufacturer's protocol and glucose monohydrate for calibration.

Synthesis of Partially-oxidized Acetalated Dextran. Acetalation of partially oxidized dextran was performed in a similar manner as described previously.[38] Briefly, 3.0 g partially oxidized dextran (18.5 mmol, 8.4 mol aldehyde functions/100 mol AGU) was modified with 2-methoxypropene (10.6 mL, 111 mmol) yielding partially-oxidized acetalated dextran (4.3 g) containing 100 mol acyclic and 72.5 mol cyclic acetals/100 mol AGU. The degree of functionalization was determined by ^{1}H NMR spectroscopy in DCl/D_2O according to the method described by Broaders *et al.*.[39] ^{1}H NMR (400 MHz, $CDCl_3$): δ 1.40 (s, br, acetal), 3.25 (br, acetal), 3.45, 3.50-4.10, 4.90, 5.10 (br, dextran).

Synthesis of Spermine-Ac-DEX. Partially oxidized Ac-DEX (2.0 g, 12.3 mmol) was stirred with spermine (4.0 g, 19.8 mmol) in 10 mL DMSO at 50°C for 22 h. The reduction was performed for 18 h at room temperature by adding $NaBH_4$ (2.0 g, 52.9 mmol) to the DMSO solution. The spermine modified dextran was precipitated in dd-H_2O (40 mL). The product was isolated by centrifugation at 4000 x g for 5 min, and the resulting pellet was washed thoroughly with dd-H_2O (5 x 40 mL, pH 8) by resuspension followed by centrifugation and removal of the supernatant. Residual water was removed by lyophilization, yielding spermine functionalized acetalated dextran, spermine-Ac-DEX, (1.6 g) as a white powder containing 6.6 mol spermine/100 mol AGU. The degree of functionalization was determined by elemental analysis using the nitrogen content. Anal. (spermine-Ac-DEX) C: found, 55.79; H: found, 8.29; N: found, 1.24. ^{1}H NMR (400 MHz, $CDCl_3$): δ 1.40 (s, br, acetal), 1.60, 1.80, 2.60, 2.65, 2.75 (br, spermine), 3.25 (br, acetal), 3.45, 3.50-4.10, 4.90, 5.10 (br, dextran).

Synthesis of Poly(β-amino ester) Polymer (PBAE). PBAE, a white solid, was synthesized by the Michael-type addition of 4,4'-trimethylenedipiperidine to 1,4-butanediol diacrylate in THF as the solvent according to the method described by Lynn *et al.* (GPC: M_n = 42.6 kDa, PDI = 2.78).[54]

Particle Preparation

Particles Encapsulating siRNA. Ac-DEX particles containing siRNA were prepared using a double emulsion water/oil/water (w/o/w) evaporation method similar to that described previously.[38,39] Stock siRNA solutions (2.66, 5.32, or 10.64 mg/mL depending on the desired initial siRNA feed) were prepared in nuclease-free distilled water. Spermine-Ac-DEX (25 mg) was dissolved in ice-cold CH_2Cl_2 (0.5 mL). The stock siRNA solution (25 µL) was added and the mixture was sonicated for 30 s on ice using a probe sonicator (Branson Sonifier 450) with a ½" flat tip, an output setting of 5, and a duty cycle of 80%. This primary emulsion was then added to an aqueous solution of poly(vinyl alcohol) (PVA, M_w = 13000 – 23000 g/mol, 87-89% hydrolyzed) (1 mL, 3% w/w in PBS) and sonicated for an additional 30 s on ice using the same settings. The resulting double emulsion was immediately poured into a second PVA solution (5 mL, 0.3% w/w in PBS) and stirred for 3 h at rt allowing the organic solvent to evaporate. The particles were isolated by centrifugation (10,250 rpm, 30 min) and washed with PBS (25 mL) and dd-H_2O (2 x 25 mL, pH 8) by vortexing and sonication followed by centrifugation and removal of the supernatant. The washed particles were resuspended in dd-H_2O (2 mL, pH 8) and lyophilized to yield a white fluffy solid. Yields were typically between 50-85% per batch based on starting polymer and siRNA mass (12.5 – 21 mg of particles).

Ac-DEX/PBAE Particles. Particles consisting of Ac-DEX and PBAE were made in the same manner as described above, except that unmodified Ac-DEX and 10 wt% PBAE were used instead of spermine-Ac-DEX.

Empty Particles. Particles that did not contain siRNA were made in the same manner as described above, except that the aqueous buffer in the primary emulsion consisted of dd-H_2O (25 µL) and no siRNA.

Particle Characterization

Quantification of Encapsulated siRNA. Particles containing siRNA were suspended at a concentration of 10 mg/mL in a 0.3 M acetate buffer (pH 5) and incubated at 37°C under gentle agitation for 3 d using a Thermomixer R heating block (Eppendorf). After the particles had been fully degraded, aliquots were taken and analyzed for siRNA content using the Quant-iT Picogreen dsDNA assay (Molecular Probes) according to the manufacturer's instructions. Empty Ac-DEX particles were degraded in a similar fashion and used to determine background fluorescence. For this experiment, all solutions included heparin at 10 mg/mL to disrupt electrostatic interactions between blend polymers and siRNA to enable quantification. The results were compared to a standard curve and the mass of siRNA encapsulated was calculated. Fluorescence was measured using a SpectraMax Gemini XS microplate reader (Molecular Devices, Sunnyvale, CA, ex. 480 nm, em. 520 nm).

Zeta-Potential Analysis. Zeta-potentials of particles were measured using a Nano ZS ZetaSizer (Malvern Instruments, UK) at 25ºC after suspending particles in HEPES buffer (5 mM, pH 7.4) at 0.1 mg/mL. Data shown represent the average zeta-potential ± standard deviation of distributions of five sequential measurements.

Characterization of Particle Size by Scanning Electron Microscopy (SEM). Particles were suspended in dd-H_2O (pH 8) at a concentration of 0.3 mg/mL and the resulting dispersions were dripped onto silicon wafers. After 15 min, the water was wicked away using tissue paper and the samples were further dried under a stream of N_2 gas. The particles were then sputter coated with a 2 nm layer of a palladium/gold alloy and imaged using a scanning electron microscope (S5000, Hitachi). The particle diameter and size distribution of the particles were determined by measuring 100 particles and analyzing the data using Excel. These micrographs were also used to assess particle morphology.

pH-Dependent Degradation of Ac-DEX Particles. Empty Ac-DEX particles were suspended in triplicate at a concentration of 1 mg/mL in either a 0.3 M acetate buffer (pH 5.0) or PBS (pH 7.4) and incubated at 37°C under gentle agitation using a Thermomixer R heating block (Eppendorf). At various time points, 50 µL aliquots were removed, centrifuged at 14,000 x g for 4 min to pellet out insoluble materials, and the supernatant was stored at -20°C. The collected supernatant samples were analyzed for the presence of reducing polysaccharides using a microplate reductometric bicinchoninic acid based assay (UV absorption at 562 nm) according to the manufacturer's protocol (Micro BCA Protein Assay Kit, Pierce, USA). The curve was made by applying a Boltzmann fit.

pH-Dependent Release of siRNA from Ac-DEX Particles. This experiment was performed essentially in the same manner as above except siRNA-loaded particles were used instead of empty particles. The quantity of siRNA in the supernatant samples was determined by using the Quant-iT Picogreen dsDNA assay (Molecular Probes) according to the manufacturer's instructions. The amount of siRNA in each sample was calculated by fitting the emission to a calibration curve using the Quant-iT Picogreen dsDNA assay (Molecular Probes). For this experiment, all solutions included heparin at 12.5 mg/mL to disrupt electrostatic interactions

between blend polymers and siRNA to enable quantification. The curve was made by applying a Boltzmann fit.

Studies Performed with Particles

Cell Lines and Culture. HeLa cell line stably expressing firefly luciferase (HeLa-*luc*) were a kind gift of Dr. Chris Contag. HeLa-*luc* cells were maintained in Dulbecco's Modified Eagle's Medium (DMEM) supplemented with 10% (v/v) fetal bovine serum (FBS), 1% GlutaMAX, and 500 μg/mL Zeocin (all from Invitrogen except the serum, which was from Hyclone (Logan, UT)). Cell incubations were performed in a water-jacketed 37°C/5% CO_2 incubator.

***In Vitro* siRNA Transfection Assay.** HeLa-*luc* cells were seeded (15,000 cells/well) into each well of a 96-well clear tissue culture plate (Costar, Corning, NY) and allowed to attach overnight in growth medium. Growth medium was composed of DMEM (with phenol red), 10% FBS, and 1% GlutaMAX. Particle samples (encapsulating either luciferase siRNA or control siRNA) were prepared in culture medium (without antibiotics) by alternately vortexing and sonicating in a Branson 2510 water bath for 20 s to generate homogeneous suspensions. The samples were then serially diluted in medium to give the indicated particle concentrations or equivalent siRNA doses. Existing medium was replaced with 100 μl of each particle dilution (2.19 – 35 pmol siRNA) in quadruple wells. The cells were allowed to grow for an additional 48 h before being analyzed for gene expression. Lipofectamine 2000 (Invitrogen, Carlsbad, CA) was used as a positive control for siRNA delivery and was prepared according to the manufacturer's instructions. Complexes containing equivalent doses of siRNA to particles were prepared by mixing Lipofectamine 2000 and siRNA (Lipofectamine (μL) to siRNA (μg) ratio of 3.5:1). As negative controls, both equivalent doses of free siRNA in medium and medium alone were used.

After 48 h, the cells were washed with PBS (containing Mg^{2+} and Ca^{2+}, 3 x 100 μL), Glo Lysis Buffer (120 μL, Promega, Madison, WI) was added to each well, and the plate was vortexed at rt for 20 min. Samples from each well (100 μL) were transferred to the wells of a white 96-well tissue culture plate (Corning, Lowell, MA). Steady-Glo luciferase assay reagent (Promega) was reconstituted according to the manufacturer's instructions and injected into each well in series (100 μL/well) using a GloMax 96 microplate luminometer (Promega). After a 10 s post-injection delay, each well was read with a 2 s integration time.

Total Protein Assay. Cells treated identically and in parallel with transfection assays were tested on a second 96-well plate. After washing, the cells were lysed with M-PER Mammalian Protein Extraction Reagent (50 μL/well, Pierce, Rockford, IL) by incubating for 10 min at rt. PBS (50 μL/well) was then added, and the plate was briefly vortexed. Samples from each well (50 μL) were transferred to a black 96-well plate (Corning) already containing PBS (100 μL/well). A solution of 3 mg/mL fluorescamine in acetone (50 μL) was added to each well and mixed well using a multi-channel pipette. After 5 min, fluorescence was measured using a SpectraMax Gemini XS reader (ex. 400 nm, em. 460 nm). Protein concentrations were determined using bovine serum albumin as a standard. Relative light units (RLU) from the luminometer were normalized to the total mass of cellular protein. The resulting data (RLU/mg of protein) are given as a mean ± standard deviation of four independent measurements. Percentage knockdown was calculated by comparison of treated cells to untreated cells. The data was compared to the

knockdown of cells treated with particles loaded with control siRNA or control siRNA/Lipofectamine complexes.

Viability Assay. Cells treated identically and in parallel with transfection assays were tested on a third 96-well plate. A 3.0 mg/mL solution of MTT (3-(4,5-dimethyl-2-thiazolyl)-2,5-diphenyl-2H-tetrazolium bromide) in medium (40 μL) was added directly to each well, and the plate was incubated for an additional 30 min. The medium was then replaced with DMSO (200 μL/well), 100 μL of which was transferred to another clear-bottom 96-well assay plate (Pro-Bind, Falcon) containing 100 μL DMSO and 25 μL of glycine buffer (0.1 M glycine, 0.1 M NaCl, pH 10.5) per well. The absorbances at 570 nm were measured using a SpectraMax 190 reader (Molecular Devices). Cell viability was normalized to the absorbance measured from untreated cells. Data are represented as a mean ± standard deviation of four measurements.

References

(1) Fougerolles, A.; Vornlocher, H.-P.; Maraganore, J.; Lieberman, J. *Nat. Rev. Drug Discovery* **2007**, *6*, 443-453.
(2) Bumcrot, D.; Manoharan, M.; Koteliansky, V.; Sah, D. W. Y. *Nat. Chem. Biol.* **2006**, *2*, 711-719.
(3) Kurreck, J. *Angew. Chem., Int. Ed.* **2009**, *48*, 1378-1398.
(4) Hammond, S. M.; Caudy, A. A.; Hannon, G. J. *Nat. Rev. Genet.* **2001**, *2*, 110-119.
(5) Tuschl, T. *ChemBioChem* **2001**, *2*, 239-245.
(6) Bernstein, E.; Caudy, A. A.; Hammond, S. M.; Hannon, G. J. *Nature* **2001**, *409*, 363-366.
(7) Rand, T. A.; Ginalski, K.; Grishin, N. V.; Wang, X. *Proc. Natl. Acad. Sci. U. S. A.* **2004**, *101*, 14385-14389.
(8) Ameres, S. L.; Martinez, J.; Schroeder, R. *Cell* **2007**, *130*, 101-112.
(9) Hutvagner, G.; Zamore, P. D. *Science* **2002**, *297*, 2056-2060.
(10) Whitehead, K. A.; Langer, R.; Anderson, D. G. *Nat. Rev. Drug Discovery* **2009**, *8*, 129-138.
(11) Fröhlich, T.; Wagner, E. *Soft Matter* **2010**, *6*, 226-234.
(12) Pack, D. W.; Hoffman, A. S.; Pun, S.; Stayton, P. S. *Nat. Rev. Drug Discovery* **2005**, *4*, 581-593.
(13) During, M. J. *Adv. Drug Delivery Rev.* **1997**, *27*, 83-94.
(14) Verma, I. M.; Somia, N. *Nature* **1997**, *389*, 239-242.
(15) Schaffer, D. V.; Koerber, J. T.; Lim, K. *Annu. Rev. Biomed. Eng.* **2008**, *10*, 169-194.
(16) Mintzer, M. A.; Simanek, E. E. *Chem. Rev.* **2009**, *109*, 259-302.
(17) Thomas, C. E.; Ehrhardt, A.; Kay, M. A. *Nat. Rev. Genet.* **2003**, *4*, 346-358.
(18) Zaiss, A. K.; Muruve, D. A. *Gene Ther.* **2008**, *15*, 808-816.
(19) Malone, R. W.; Felgner, P. L.; Verma, I. M. *Proc. Natl. Acad. Sci. U. S. A.* **1989**, *86*, 6077-6081.
(20) Zimmerman, T. S.; Lee, A. C. H.; Akinc, A.; Bramlage, B.; Bumcrot, D.; Fedoruk, M. N.; Harborth, J.; Heyes, J. A.; Jeffs, L. B.; John, M.; Judge, A. D.; Lam, K.; McClintock, K.; Nechev, L. V.; Palmer, L. R.; Racie, T.; Rohl, I.; Seiffert, S.; Shanmugam, S.; Sood, V.; Soutschek, J.; Toudjarska, I.; Wheat, A. J.; Yaworski, E.; Zedalis, W.; Koteliansky, V.; Manoharan, M.; Vornlocher, H. P.; MacLachlan, I. *Nature* **2006**, *441*, 111-114.
(21) Neu, M.; Fischer, D.; Kissel, T. *J. Gene Med.* **2005**, *7*, 992-1009.
(22) Zhang, S.; Zhao, B.; Jiang, H.; Wang, B.; Ma, B. *J. Controlled Release* **2007**, *123*, 1-10.
(23) Lares, M. R.; Rossi, J. J.; Ouellet, D. L. *Trends Biotechnol.* **2010**, *28*, 570-579.
(24) Shim, M. S.; Kwon, Y. J. *FEBS J.* **2010**, *277*, 4814-4827.
(25) Little, S. R.; Lynn, D. M.; Ge, Q.; Anderson, D. G.; Puram, S. V.; Chen, J.; Eisen, H. N.; Langer, R. *Proc. Natl. Acad. Sci. U. S. A.* **2004**, *101*, 9534-9539.
(26) Woodrow, K. A.; Cu, Y.; Booth, C. J.; Saucier-Sawyer, J. K.; Wood, M. J.; Saltzman, W. M. *Nat. Mater.* **2009**, *8*, 526-533.
(27) Nguyen, J.; Steele, T. W. J.; Merkel, O.; Reul, R.; Kissel, T. *J. Controlled Release* **2008**, *132*, 243-251.
(28) Wang, C.; Ge, Q.; Ting, D.; Nguyen, D.; Shen, H.-R.; Chen, J.; Eisen, H. N.; Heller, J.; Langer, R.; Putnam, D. *Nat. Mater.* **2004**, *3*, 190-196.
(29) Lee, S.; Yang, S. C.; Kao, C.-Y.; Pierce, R. H.; Murthy, N. *Nucleic Acids Res.* **2009**, *37*, e145.

(30) Little, S. R.; Lynn, D. M.; Puram, S. V.; Langer, R. *J. Controlled Release* **2005**, *107*, 449-462.
(31) Pack, D. W. *Nat. Mater.* **2004**, *3*, 133-134.
(32) Fu, K.; Pack, D. W.; Klibanov, A. M.; Langer, R. *Pharm. Res.* **2000**, *17*, 100-106.
(33) Walter, E.; Moelling, K.; Pavlovic, J.; Merkle, H. P. *J. Controlled Release* **1999**, *61*, 361-374.
(34) Heinze, T.; Liebert, T.; Heublein, B.; Hornig, S. *Adv. Polym. Sci.* **2006**, *205*, 199-291.
(35) Raemdonck, K.; Naeye, B.; Buyens, K.; Vandenbroucke, R. E.; Høgset, A.; Demeester, J.; De Smedt, S. C. *Adv. Funct. Mater.* **2009**, *19*, 1406-1415.
(36) Raemdonck, K.; Naeye, B.; Høgset, A.; Demeester, J.; De Smedt, S. C. *J. Controlled Release* **2010**, *145*, 281-288.
(37) Nagane, K.; Jo, J.-I.; Tabata, Y. *Tissue Eng., Part A* **2010**, *16*, 21-31.
(38) Bachelder, E. M.; Beaudette, T. T.; Broaders, K. E.; Dashe, J.; Fréchet, J. M. J. *J. Am. Chem. Soc.* **2008**, *130*, 10494-10495.
(39) Broaders, K. E.; Cohen, J. A.; Beaudette, T. T.; Bachelder, E. M.; Fréchet, J. M. J. *Proc. Natl. Acad. Sci. U. S. A.* **2009**, *106*, 5497-5502.
(40) Bachelder, E. M.; Beaudette, T. T.; Broaders, K. E.; Fréchet, J. M. J.; Albrecht, M. T.; Mateczun, A. J.; Ainslie, K. M.; Pesce, J. T.; Keane-Myers, A. M. *Mol. Pharmaceutics* **2010**, *7*, 826-835.
(41) Cohen, J. A.; Beaudette, T. T.; Cohen, J. L.; Broaders, K. E.; Bachelder, E. M.; Fréchet, J. M. J. *Adv. Mater.* **2010**, *22*, 3593-3597.
(42) Rao, D. D.; Vorhies, J. S.; Senzer, N.; Nemunaitis, J. *Adv. Drug Delivery Rev.* **2009**, *61*, 746-759.
(43) Gary, D. J.; Puri, N.; Won, Y.-Y. *J. Controlled Release* **2007**, *121*, 64-73.
(44) Takahashi, Y.; Nishikawa, M.; Takakura, Y. *Adv. Drug Delivery Rev.* **2009**, *61*, 760-766.
(45) Murata, N.; Takashima, Y.; Toyoshima, K.; Yamamoto, M.; Okada, H. *J. Controlled Release* **2008**, *126*, 246-254.
(46) Azzam, T.; Eliyahu, H.; Shapira, L.; Linial, M.; Barenholz, Y.; Domb, A. J. *J. Med. Chem.* **2002**, *45*, 1817-1824.
(47) Azzam, T.; Eliyahu, H.; Makovitzki, A.; Linial, M.; Domb, A. J. *J. Controlled Release* **2004**, *96*, 309-323.
(48) Hosseinkhani, H.; Azzam, T.; Tabata, Y.; Domb, A. J. *Gene Ther.* **2004**, *11*, 194-203.
(49) Bernstein, A.; Hurwitz, E.; Maron, R.; Arnon, R.; Sela, M.; Wilchek, M. *J. Natl. Cancer Inst.* **1978**, *60*, 379-383.
(50) Fuller, J. E., Massachusetts Institute of Technology, 2008.
(51) Dalby, B.; Cates, S.; Harris, A.; Ohki, E. C.; Tilkins, M. L.; Price, P. J.; Ciccarone, V. C. *Methods* **2004**, *33*, 95-103.
(52) Kongkaneramit, L.; Sarisuta, N.; Azad, N.; Lu, Y.; Iyer, A. K. V.; Wang, L.; Rojanasakul, Y. *J. Pharmacol. Exp. Ther.* **2008**, *325*, 969-977.
(53) Beaudette, T. T.; Cohen, J. A.; Bachelder, E. M.; Broaders, K. E.; Cohen, J. L.; Engleman, E. G.; Fréchet, J. M. J. *J. Am. Chem. Soc.* **2009**, *131*, 10360-10361.
(54) Lynn, D. M.; Langer, R. *J. Am. Chem. Soc.* **2000**, *122*, 10761-10768.

Chapter 5 – Facile and Tunable Conjugation Chemistry Toward a Biocompatible Delivery System for Controlled Release of siRNA

Abstract

In the previous chapter, we presented the synthesis of spermine-Ac-DEX, a novel polymeric platform for the delivery of siRNA therapeutics. Spermine-Ac-DEX possesses several characteristics that make it attractive for siRNA delivery, including acid-degradability and biocompatibility. For some applications, however, it might be advantageous to use a water-soluble polymer that can form small complexes with genetic material instead of the relatively larger water-insoluble particles formed with spermine-Ac-DEX. With these features in mind, we sought to create another acid-degradable material that would maintain the biocompatibility of spermine-Ac-DEX while also offering small size and water-solubility. In this chapter, we describe the synthesis and biological evaluation of functionalizable, acetal-modified dextran. Specifically, dextran was modified at its hydroxyls with acetals that bear a functionalizable moiety, which can be further conjugated to a cargo of interest. Using this facile chemistry, a library of amine-modified dextrans which vary in the type of amine modification and the degradation rate of the acetal were prepared. These polymers were found to degrade in a pH-dependent manner with degradation rates that depended on the stereoelectronic and steric properties of the linker. The polymers were able to form complexes with siRNA and to release the siRNA under slightly acidic conditions. When tested *in vitro*, two of the compounds were able to successfully transfect HeLa cells and lead to reduction in protein expression. Due to its tunability, pH-sensitivity, and biocompatibility, this type of modified dextran should find use in numerous drug delivery applications.

Introduction

RNA interference (RNAi) is an important post-transcriptional gene silencing mechanism that has prodigious impact in wide-ranging areas such as functional genomics, therapeutics, and biotechnology.[1-4] Although attractive due to its ability to knock down many diseased genes, RNAi therapy has limited applications in clinical use.[5,6] One of the major barriers is the lack of suitable clinically safe systemic carriers that can facilitate the effective delivery of RNA interfering molecules (such as small interfering RNA,[7,8] siRNA) to desired targets. To develop an ideal delivery system for RNAi, several challenges must be overcome – (1) The carrier and its degraded products should be biocompatible and/or biodegradable to minimize possible toxicity; (2) The carrier needs to provide sufficient protection of its genetic cargo from ubiquitously existing nucleases before reaching the target and from unpacking while moving through various biological fluids; (3) It has to avoid the opsonization by reticuloendothelial system (RES) which may cause unexpected toxicity and evoke innate immune responses; (4) It should be ideally able to distinguish diseased and healthy tissue to minimize adverse side effects; (5) The size of the carrier should be large enough to avoid kidney filtration, and must not exceed the passage limit to cross vascular endothelium of the target site; (6) The carrier should be able to facilitate cellular entry and endosomal release of the negatively charged genetic materials, which should also be released from the carrier upon reaching their target site in the cytoplasm (for siRNA) or in the nucleus (for DNA).

Many attempts have been made to achieve this goal, including the use of viral vectors[9] and synthetic lipids and polymers.[10] Although very effective in transfection, there have been safety concerns with the clinical use of viral vectors due to possible unwanted immune responses and inflammatory reactions.[11] In the clinic, dextran, a biocompatible non-immunogenic material from natural sources, has been approved by the FDA as a plasma expander, and it shows excellent biodistribution profile when administered systemically in a tumor model.[12] Therefore, dextran can serve as a scaffold of a drug/gene delivery carrier. Domb *et al.* have used amine-modified dextran (synthesized through reductive amination) for the delivery of plasmid DNA.[13] Although the long term side effects of the non-degradable amine modified dextran are not exactly clear, there have been reports on toxicity in liver caused by polymer-based amines.

Here we describe facile conjugation chemistry for dextran via acetals, which can degrade and release the cargo under acidic conditions and regenerate biocompatible free dextran in the end. This novel system possesses tunability in its functionalities and degradation rates (Figure 5.1), making it attractive for a variety of drug delivery applications. We applied this chemistry in developing a biodegradable siRNA delivery vehicle with controlled release rates and revealed its utility in gene knockdown studies *in vitro*.

Results and Discussion

Facile New Conjugation Chemistry for Dextran

The delivery of therapeutics using polysaccharides has been reported by many research groups, however conjugation methods have been limited to irreversible and/or non-tunable modifications.[14,15] Here we report a facile conjugation chemistry for dextran with the feature of tunability in its functionalities and degradation rates, with the additional benefit that it generates biocompatible free dextran once the cargo is released inside cells (Figure 5.1).

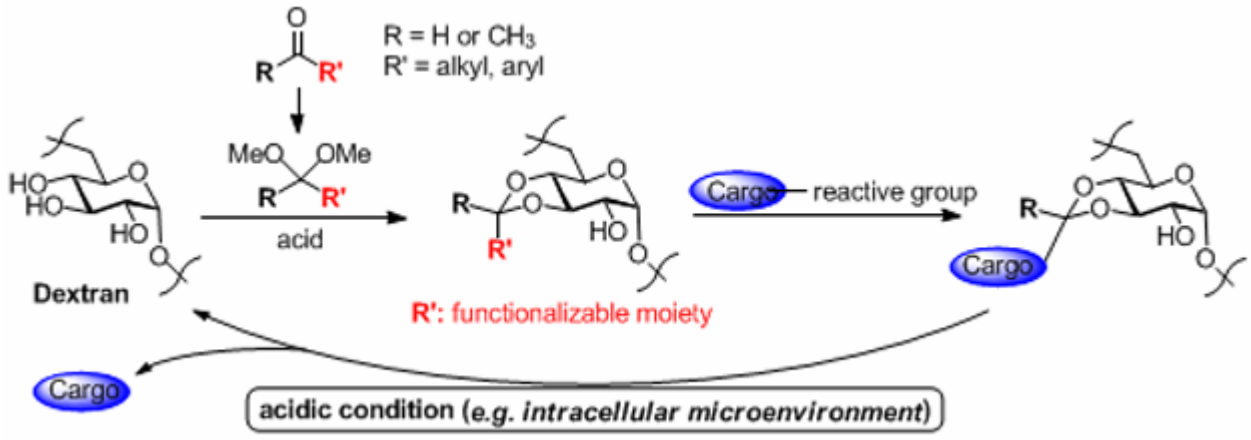

Figure 5.1. New conjugation chemistry for dextran. Dextran can be acetalated to bear a functionalizable moiety, which can be conjugated to a desired cargo. Once endocytosed by cells, the acetal linker can be cleaved to release the cargo inside cells, while generating free dextran in the end.

Acetals are commonly used as temporary protecting groups for alcohols in organic synthesis.[16] Our group has a long history of applying acetal chemistry in the preparation of smart materials for biotherapeutic delivery, owing to its possible degradability under acidic conditions,

which exist at various diseased sites and inside endocytotic compartments.[17-22] We have previously reported an acetalated dextran (Ac-DEX) material, which was able to encapsulate therapeutics such as protein antigens, vaccine adjuvants and genetic materials via physical entrapment during fabrication of nanoparticles.[23-26] Once the particles were endocytosed, acetals were degraded, and therapeutic cargo was released.

We envisioned therapeutics could be conjugated to dextran via acetal groups when desirable functional handles existed (Figure 5.1), while controllable degree of modification could provide either water-soluble or water insoluble carriers. Manipulation of peripheral groups would alter the stereoelectronic and steric properties during the acetal formation, thus giving materials with tunable degradation rates. This would provide us with opportunities to control the release of therapeutics on demand.

To test our hypothesis, we synthesized dimethyl acetals of two contrasting substrates – a small aliphatic ethyl levulinate **2** and a bulky aromatic vanillin derivative **6** (Figure 5.3a). The acetalation reaction of dextran was highly efficient, with 0.8 levulinate acetal and 0.4 vanillin ketal per glucose installed respectively, and so was the work-up of the reactions by precipitation in isopropanol. The degree of modification was determined by ^{1}H NMR (example shown in Figure 5.2). Interestingly, almost all levulinate acetals were thermodynamically stable cyclic acetals (Figure 5.3a), as opposed to the vanillin ketals, which were mainly kinetic acyclic product (as observed in ^{1}H NMR), presumably because the formation of cyclic ketal was prohibited by steric hindrance and potential strain in the fused carbohydrate and dioxolane rings.

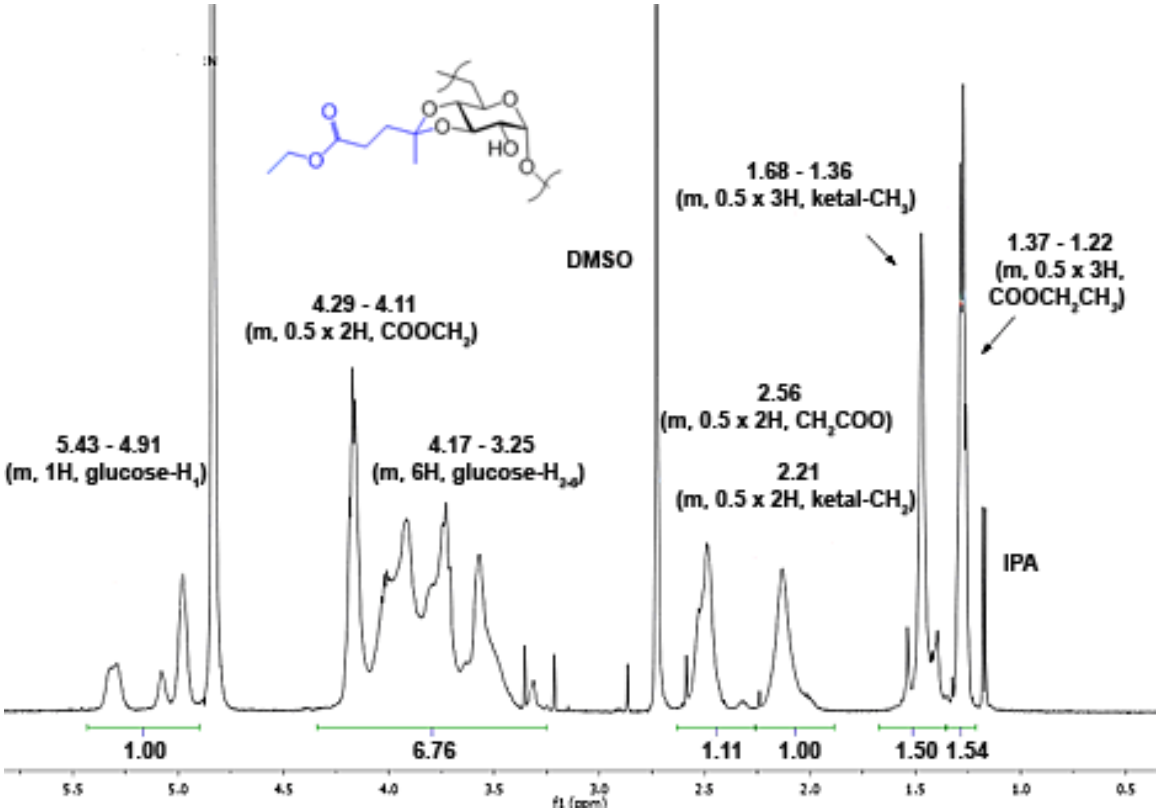

Figure 5.2. ^{1}H NMR of functionalizable acetal formation on dextran. Resonance of each proton was assigned with integration to calculate the degree of modification.

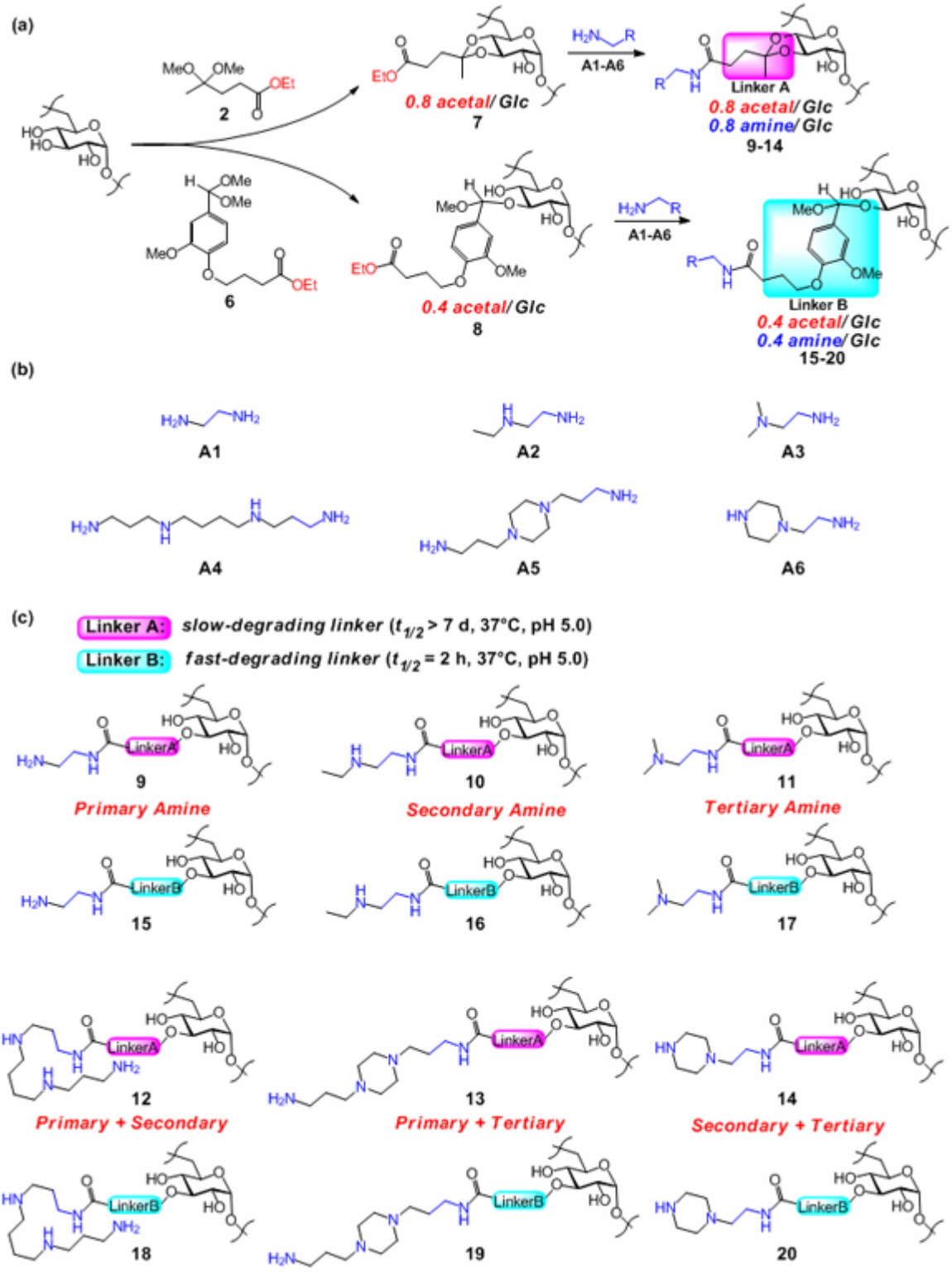

Figure 5.3. Facile synthesis of gene delivery carriers with tunable amine functionalities and degradation rates. a) Synthetic scheme. b) Amine monomers (**A1**-**A6**) used in synthesis of amine-dextrans. c) Library of amine-dextrans used as siRNA delivery carriers.

Synthesis of Gene Delivery Carriers of Tunable Amine Functionalities and Degradation Rates

In gene delivery, release of nucleic acid from its carrier is crucial to successful transfection. Once the nucleic acid is taken up by cells, it needs to escape out of endocytotic vehicles, and dissociate from its carrier before reaching the target. Most of the existing cationic gene delivery systems achieve endosomal escape via "proton sponge effect", resulting from protonation of cations on the carrier followed by osmotic swelling and rupture of endosomes. However the mechanism of how genetic material is released from the carrier and how the release affects the final transfection remains mysterious. In order to achieve an ideal gene delivery performer, and to interpret structure-property relationships, it is necessary to screen through a relatively large library of carriers, which share similar structure features with comparable variation of parameters.

Our chemistry, as expected, could generate such a library efficiently (Figure 5.3). The intentional use of ethyl ester group in the acetal linkers provided us with universal intermediates to introduce various amine functionalities to dextran (1 step from the common intermediate), which became positively charged and suitable for complexing with negatively charged genetic materials.

Commercially available amines (**A1-A6**) were heated together with ethyl ester functionalized dextrans (**7** and **8**), and desired amines (primary only, secondary only, tertiary only, primary plus secondary, primary plus tertiary, secondary plus tertiary amine) were installed to dextran through acetal linkers (Figure 5.3). Reactions were monitored by ^{1}H NMR, until the resonance of the ethyl ester disappeared (Figure 5.4). Interestingly, the replacement of ethyl groups was only observed for primary amines, and no secondary amine or tertiary amine reacted with ethyl esters on dextran. This was confirmed by a parallel experiment of ethyl ester-dextran and an amine containing only secondary and tertiary amine, which gave only starting material back over the same time span as the other reactions (observed by ^{1}H NMR). Because multiple amino groups were present in each amine structure, cross-linking of the dextran materials was thought to be a concern. However, we were delighted to observe little or no cross-linked materials by ^{1}H NMR and size exclusion chromatography (data not shown).

More interestingly, the ethyl ester precursors of the amine-dextrans were made of structures of different properties – the levulinate cyclic acetal degraded slowly at pH 5.0 (Figure 5.3, linker A) while the vanillin acyclic acetal degraded fast (Figure 5.3, linker B). The degradation of both slow- and fast-degrading amine-dextrans at 37°C at both pH 5.0 and 7.4 was studied first using NMR. For clarity, the ^{1}H NMR spectra of the simplest ethylene diamine modified acetal-dextran **9** (Figure 5.5) and **15** (Figure 5.6) were shown here. When they degrade, both **9** and **15** would form free dextran and an amide derivative of a ketone (Figure 5.5a) or aldehyde (Figure 5.6a). Therefore, the progress of degradation can be monitored by comparing the proton resonances in NMR to see the ratio of the small molecule and dextran. For the slow-degrading compound **9**, there was no obvious degradation (no resonances from the small molecule) at both pH 5.0 (Figure 5.5b) and pH 7.4 (Figure 5.5c). On the other hand, the fast-degrading compound **15** degraded and released the small aldehyde molecule (Figure 5.6b, newly formed sharp peaks) at pH 5.0 starting from 30 min, and the quantity of this aldehyde increased remarkably as the incubation time proceeded. The compound was almost completely degraded after 48 h of study. However, at pH 7.4, compound **15** did not show appreciable degradation until 4 h later, and even after 48 h, there was only very minor amount degraded (Figure 5.6c). This phenomenon is as expected for this acid-sensitive acetal linker. The degradation curves of the

above two compounds against time at both pHs were plotted (Figure 5.7). The slow-degrading compound **9** did not show observable degradation at either pH, while compound **15** showed a half life of about 2 h at pH 5.0, and an estimated half life of 120 h at pH 7.4 at 37°C. The degradation of all other amine-dextrans shared the same trend as either compound **9** or compound **15** (data not shown).

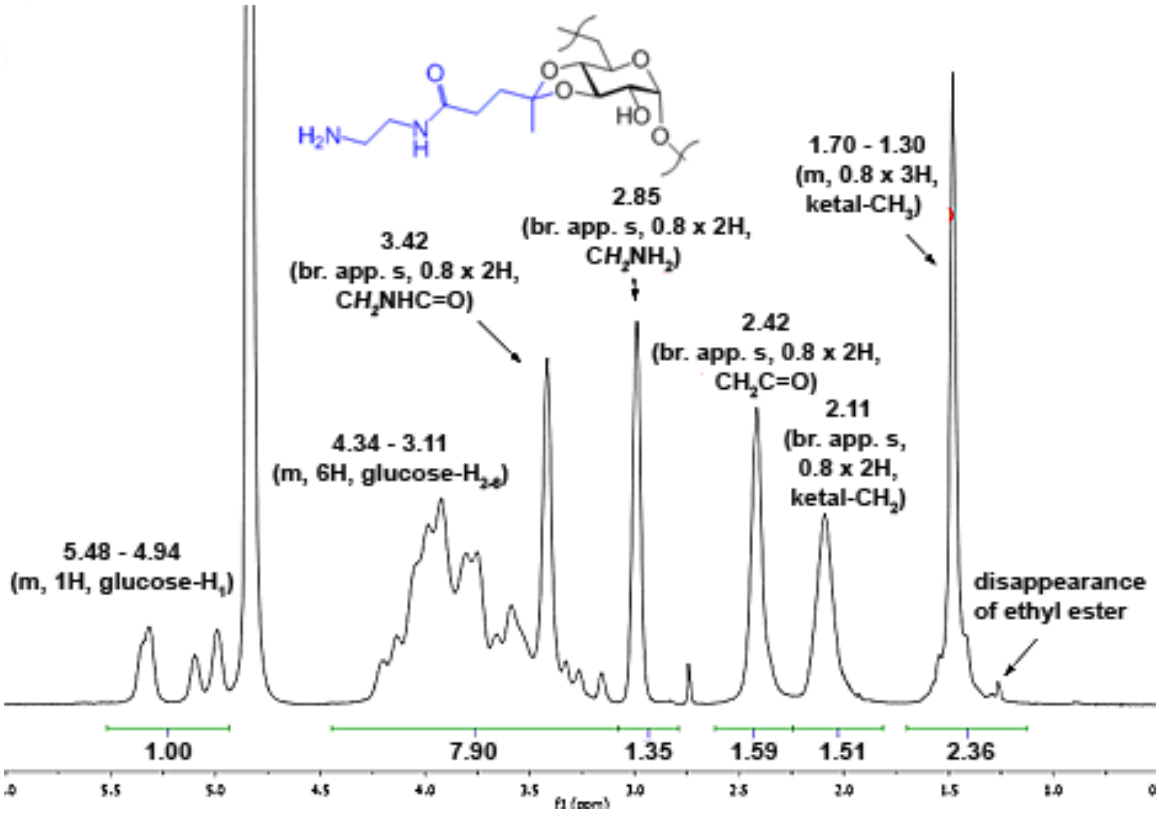

Figure 5.4. ^{1}H NMR of amine conjugation to dextran via an acetal linker. Resonance of each proton was assigned with integration to calculate the degree of substitution.

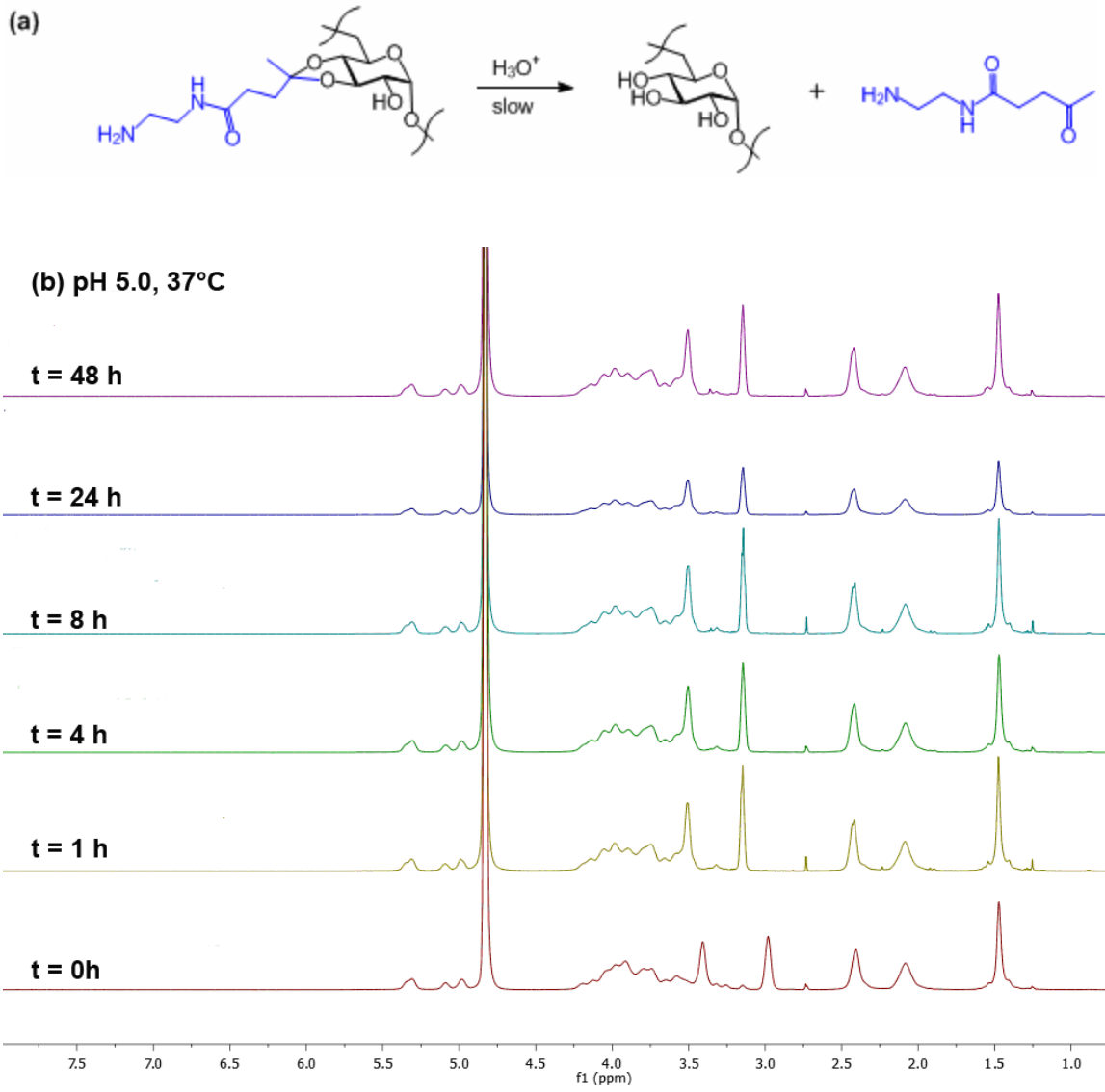
(a)
H3O+
slow
(b) pH 5.0, 37°C
t = 48 h
t = 24 h
t = 8 h
t = 4 h
t = 1 h
t = 0h
f1 (ppm)

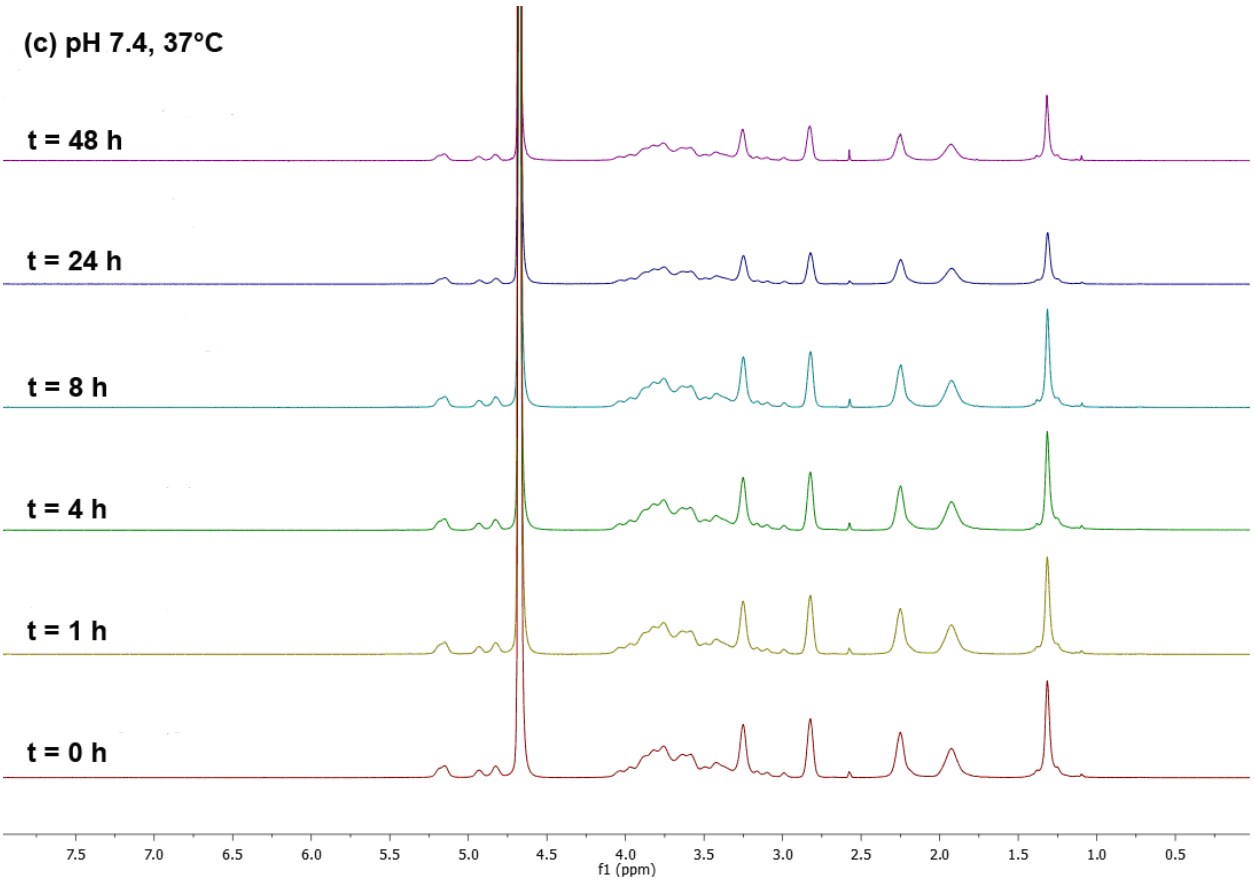

Figure 5.5. Degradation study of slow-degrading amine-dextran **9*** at 37°C. a) Scheme of the degradation reaction under acidic conditions. b) Array of ^{1}H NMR spectra of amine-dextran **9** at various incubation times (bottom to top: time = 0, 1, 4, 8, 24, 48 h) at pH 5.0. c) Array of ^{1}H NMR spectra of amine-dextran **9** at various incubation times (bottom to top: time = 0, 1, 4, 8, 24, 48 h) at pH 7.4.*For clarity, the degradation of the simplest slow-degrading amine-dextran **9** was shown. Other slow-degrading amine-dextrans degraded in roughly the same manner.

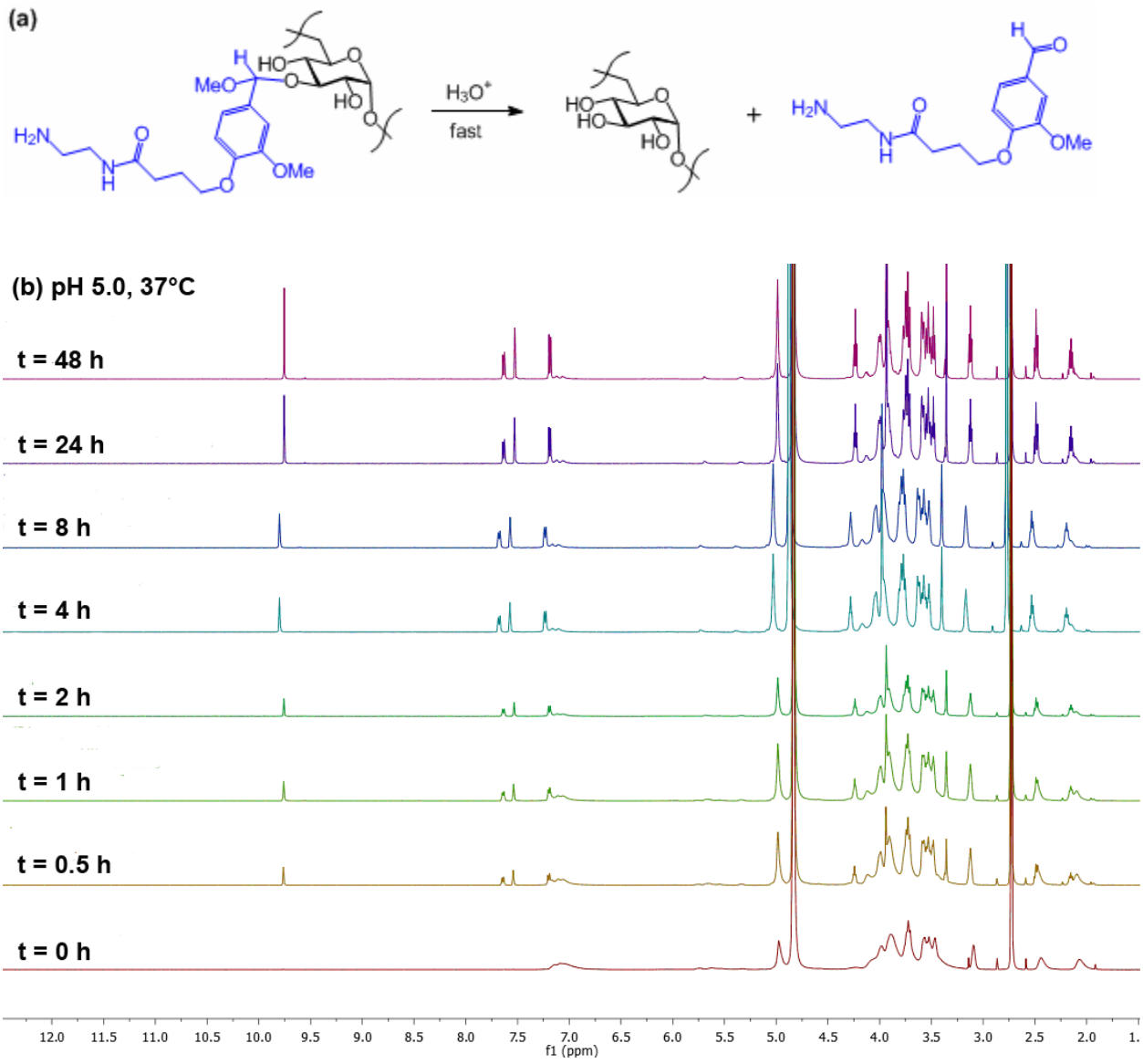
(a)
H
HO
MeO
O
HO
O
H2N
N
H
O
OMe
H3O+
fast
HO
HO
HO
O
+
H
O
H2N
N
H
O
O
OMe
(b) pH 5.0, 37°C
t = 48 h
t = 24 h
t = 8 h
t = 4 h
t = 2 h
t = 1 h
t = 0.5 h
t = 0 h
12.0 11.5 11.0 10.5 10.0 9.5 9.0 8.5 8.0 7.5 7.0 6.5 6.0 5.5 5.0 4.5 4.0 3.5 3.0 2.5 2.0 1.
f1 (ppm)

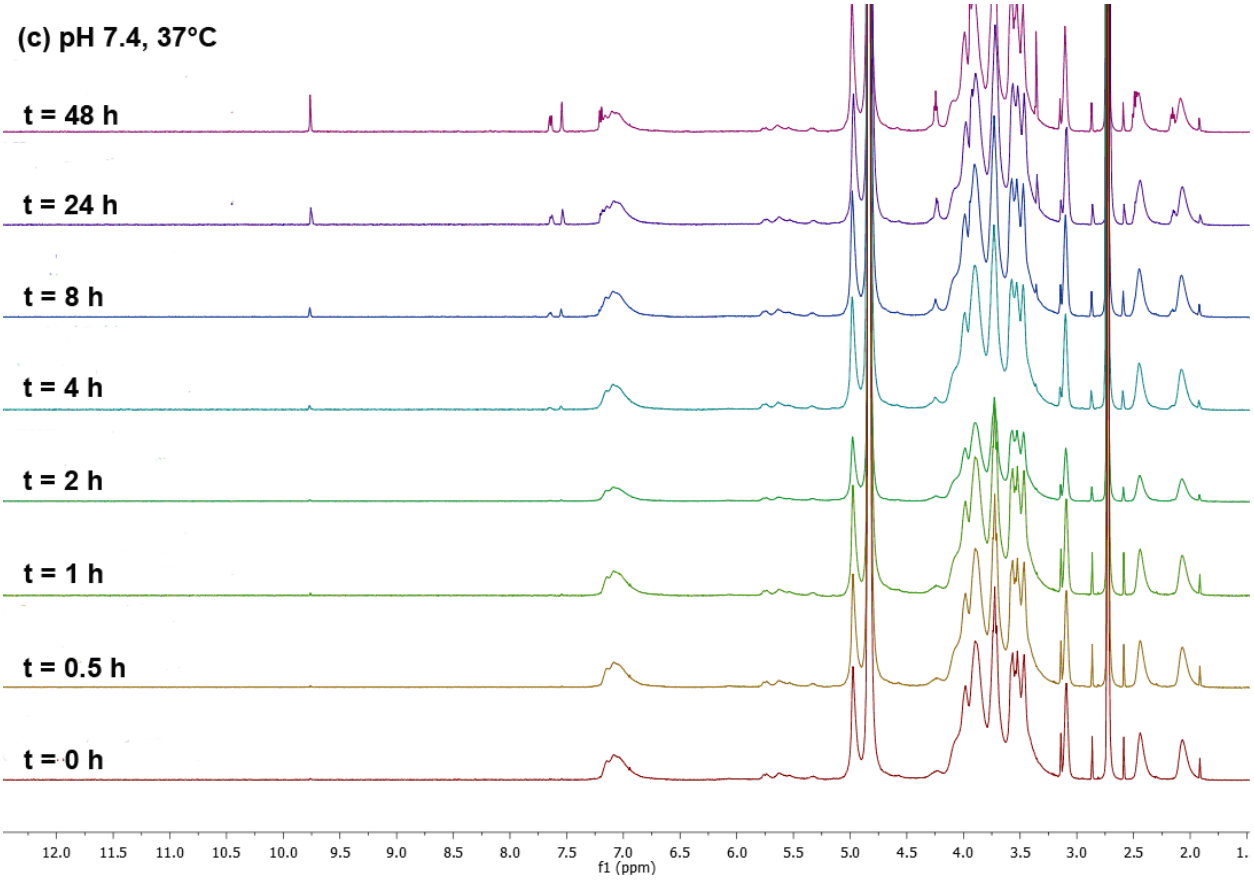

Figure 5.6. Degradation study of fast-degrading amine-dextran **15*** at 37°C. a) Scheme of the degradation reaction under acidic conditions. b) Array of ^{1}H NMR spectra of amine-dextran **15** at various incubation times (bottom to top: time = 0, 0.5, 1, 2, 4, 8, 24, 48 h) at pH 5.0. c) Array of ^{1}H NMR spectra of amine-dextran **15** at various incubation times (bottom to top: time = 0, 0.5, 1, 2, 4, 8, 24, 48 h) at pH 7.4.*For clarity, the degradation of the simplest fast-degrading amine-dextran **15** was shown. Other fast-degrading amine-dextrans degraded in roughly the same manner.

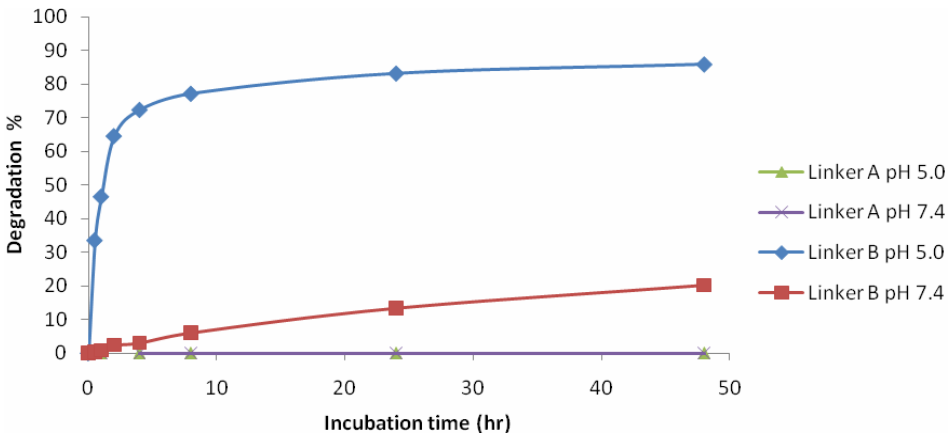

Figure 5.7. Degradation study of slow- (linker A) and fast- (linker B) degrading amine-dextrans at 37°C at pH 5.0 and pH 7.4 over a course of 48 h. Degree of degradation was calculated using integration of signature peaks in ^{1}H NMR.

This feature of these amine-dextran molecules allows us to evaluate the effects of different degradation rates (or nucleic acid release rates) while maintaining the same amine functionalities. This is of particular interest in siRNA delivery, as the release mechanism of siRNA from the carrier is still unknown. Thus, varying one structural parameter at a time may provide valuable information in understanding the status of siRNA molecules before they reach their target gene.

Complex Formation Between Amine-Dextrans and Nucleic Acid

One of the major challenges in gene delivery is the reluctant uptake of negatively charged nucleic acids by cells. Therefore, making the surface electric charge positive by complexing genetic materials with positively charged carriers has been a common strategy in gene delivery.

To see whether amine-dextrans can form stable complexes with nucleic acid, we mixed the amine-dextrans with firefly luciferase DNA at nitrogen/phosphate (N/P) ratios of 1, 10 and 100. All compounds formed firm complexes as compared with PEI-DNA complexes (Figures 5.8a and 5.8b, left panel of each trio). As expected, complexes at higher N/P ratios (10 and 100) moved further toward the negative field, indicating overall positive charge of the complexes (confirmed by zeta potential measurement using dynamic light scattering). It is also worthwhile to note that complexes formed by compounds **10** (at N/P 10 and 100) and **12** (at N/P 1, 10 and 100) showed very faint fluorescence compared to others. This is presumably due to exclusion of ethidium bromide from DNA base-pairs caused by very tight binding between the amine-dextran and DNA molecule.

Release of Nucleic Acid from the Complexes

We proposed our acetal-linked amine-dextrans could degrade under acidic conditions, therefore we studied whether the small 21-bp DNA could be released from complexes with amine-dextrans by gel electrophoresis (Figure 5.8). We incubated all complexes at pH 7.4 (Figure 5.8, middle panel of each trio) and pH 5.0 (Figure 5.8, right panel of each trio) at 37°C for 48 h before developing the gel. It is clearly shown that the slow-degrading amine-dextrans (Figure 5.8a) did not release any DNA at either pH. The fast-degrading amine-dextrans (Figure

5.8b) started to release little to partial DNA at N/P 1 at pH 7.4, leaving N/P 10 and 100 intact. In sharp contrast, most of the fast-degrading amine-dextrans released DNA completely at N/P 10, and some at N/P 100 at pH 5.0 (with the exception of compound **18** which only released DNA at N/P 1).

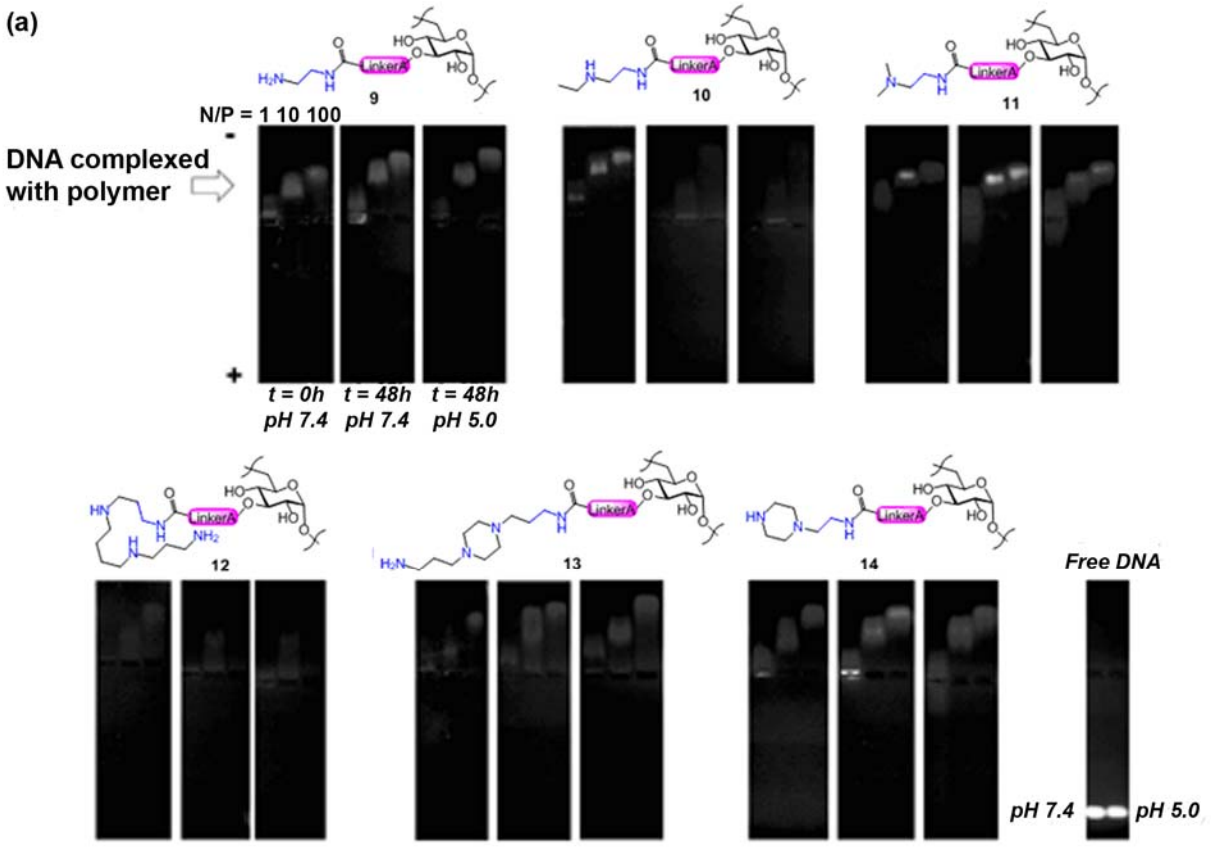

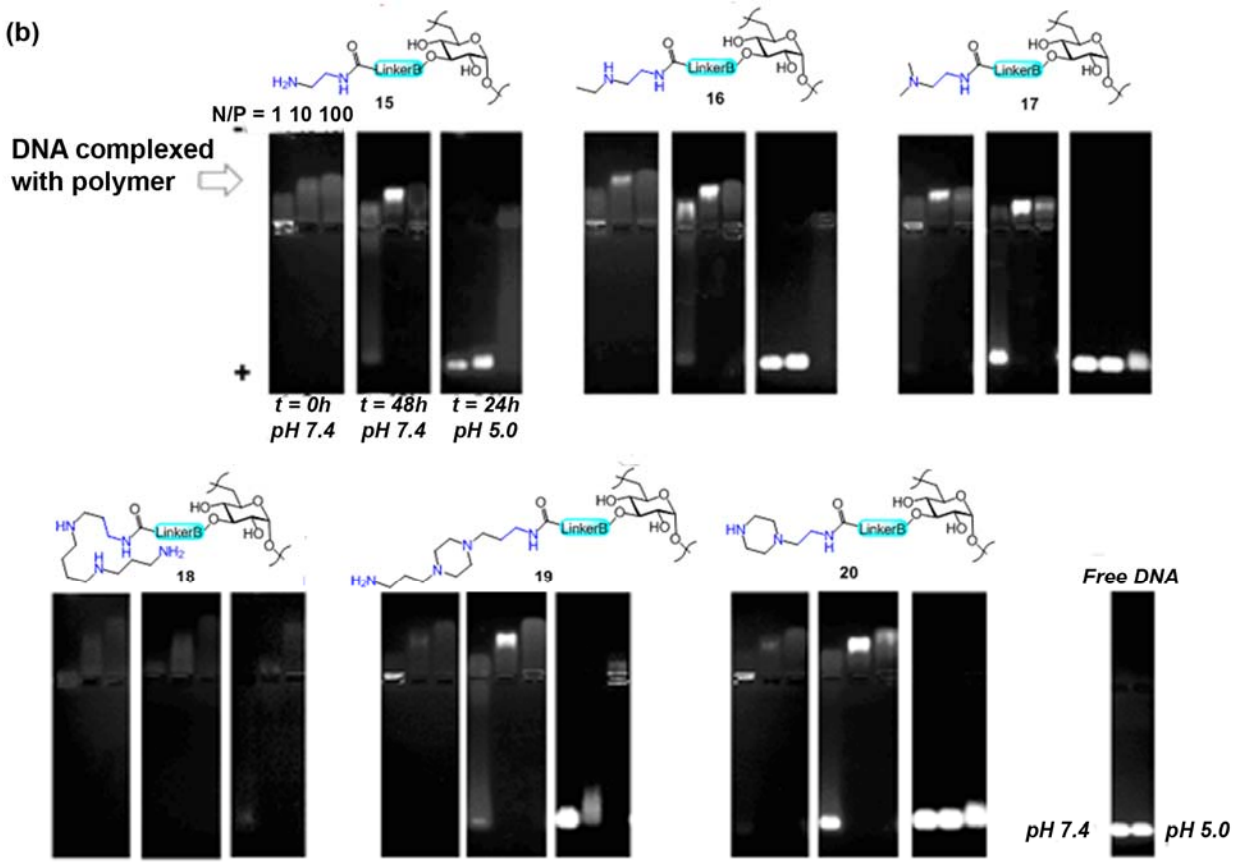

Figure 5.8. Complex formation between amine-dextrans and DNA at different N/P ratios, and release of DNA from the complexes at pH 7.4 and pH 5.0. a) Gel electrophoresis of complexes of DNA and slow-degrading amine-dextrans **9-14** at various time points. b) Gel electrophoresis of complexes of DNA and fast-degrading amine-dextrans **15-20** at various time points.

In the NMR degradation studies of all amine-dextrans, all compounds with the same acetal linker degraded in a rather similar way. Therefore, in the case of the fast-degrading amine-dextrans, the difference in DNA release was probably caused by different binding affinity of various amine-dextrans to DNA. Although not a direct measurement, the DNA release study together with amine-dextran degradation study suggested the release rate of DNA is inversely proportional to the binding energy of the complex. Thus, among all fast-degrading amine-dextrans, **18**, which released DNA the slowest, was the tightest binder to DNA.

In Vitro Delivery of siRNA by Amine-Dextrans

The promising complexation data motivated us to test the ability of the amine-dextran polymers to deliver siRNA *in vitro*. Several polymer characteristics are known to influence transfection efficiency, including molecular weight and overall charge.[27-31] In particular, we were interested in investigating the effect of the amine structure and the polymer degradation kinetics on transfection. The structure and basicity of amines present in a polymer can significantly affect the ability of a polymer to complex with nucleic acids and transfect cells, with small modifications considerably enhancing or abolishing efficacy.[32-36] Specifically, primary amines

have been shown to increase polymer binding to DNA and siRNA, while tertiary amines can enhance intracellular delivery of genetic material, presumably by buffering the endosome and increasing endosomal escape.[37-39]

To determine the extent to which the structure of the amines affects transfection efficiency in our system, we prepared a small library of amine-dextrans (**9-14**) containing only primary, only secondary, or only tertiary amines as well as amine-dextrans with mixtures of amines. The transfection efficiency of each of these polymers was tested *in vitro* in a luciferase-expressing HeLa cell line (HeLa-*luc*). In these experiments, anti-firefly luciferase siRNA was complexed with polymer at various N/P ratios and incubated with cells for 48 h. In order to exclude non-specific gene silencing by the polyplexes themselves, the cells were also incubated with polyplexes prepared using a negative control siRNA (Silencer Negative Control #1 siRNA). The luciferase-specific knockdown obtained with each polymer is shown in Figure 5.9.

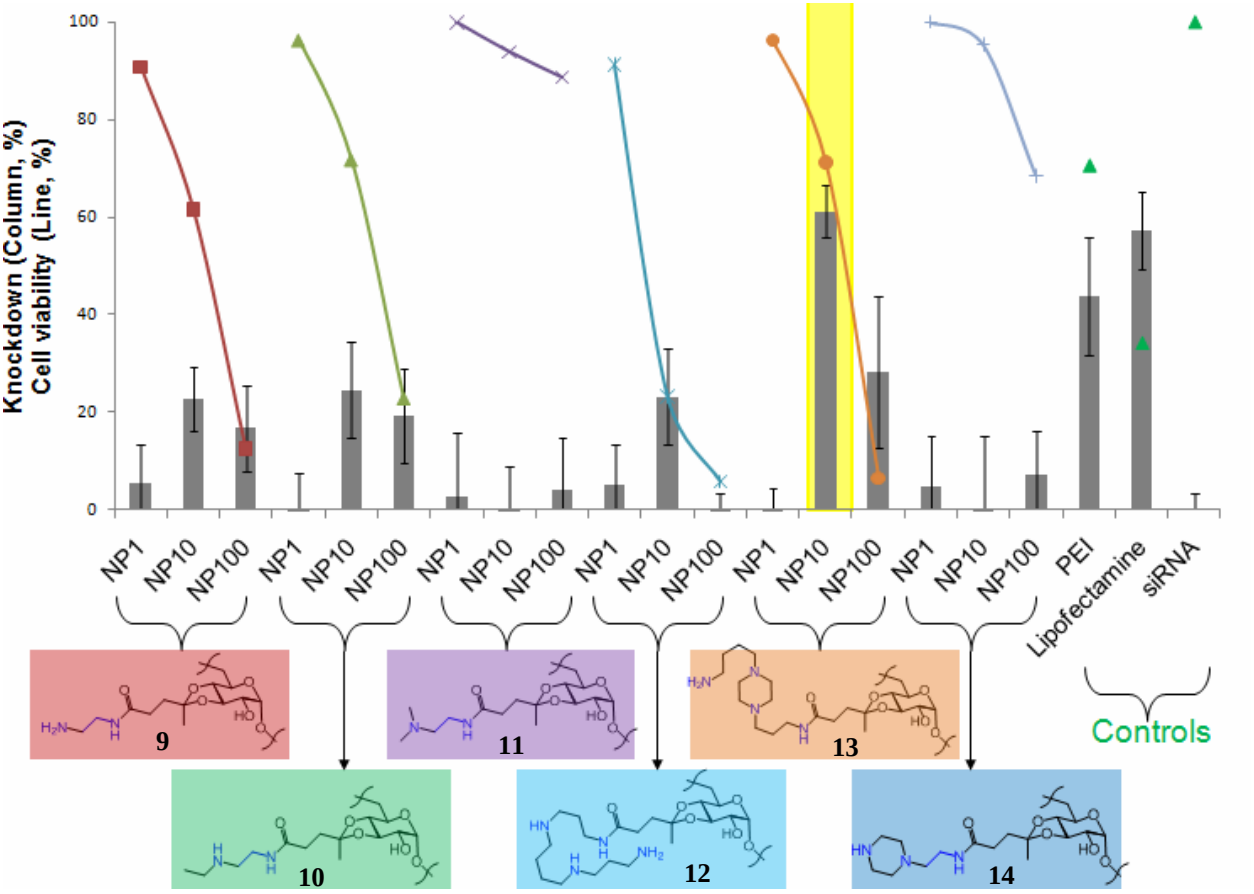

Figure 5.9. The type of amine is important for transfection efficiency. *In vitro* delivery of siRNA by amine-dextrans bearing different types of amines. HeLa-*luc* cells were treated with polymers complexed with 0.5 µg siRNA/well. Complexes were prepared at various N/P ratios to determine the optimum for transfection efficiency. Results were compared to untreated cells and the percentage knockdown of luciferase expression was calculated. Results (columns) are combined with results from a concurrently performed cytotoxicity assay (closed symbols and lines).

These results demonstrate the importance of the type of amine on overall transfection efficiency. The optimal knockdown in these experiments was obtained at an N/P ratio of 10 with the bis(aminopropyl)piperazine modified dextran (**13**), which contains a mixture of primary and tertiary amines. Other amine-dextran polymers showed minimal reduction in luciferase expression at all N/P ratios tested. Importantly, the transfection obtained with polymer **13** was better than or comparable to the levels of transfection achieved with the positive controls, PEI and Lipofectamine 2000. Cytotoxicity assays were also performed and showed that the polymers have concentration-dependent toxicity. Polymer **13** exhibited only slight cytotoxicity at the concentration necessary to achieve efficient gene silencing and this toxicity was comparable to that of PEI.

In addition to exploring the effect of amine structure on transfection efficiency, we were also interested in studying the role of polymer degradation rate on transfection. We have previously demonstrated the importance of degradation rate for both antigen presentation[23] and transfection of plasmid DNA[25]. In these prior reports, fast-degrading polymers resulted in superior performance when compared to their slower-degrading counterparts. To investigate the effect that degradation rate has on transfection efficiency with this polymer system, we prepared an additional library of amine-dextrans (**15-20**) comprising the same amine structures as the previous library but containing a fast-degrading vanillin ketal linkage in place of the slow-degrading levulinate acetal. The transfection efficiency of these polymers *in vitro* was tested using the luciferase proof-of-concept system described above. Figure 5.10 shows the highest-transfecting fast-degrading polymer (**18**) plotted alongside its slow-degrading counterpart (**12**). The fast-degrading polymer led to more efficient transfection and less toxicity than the slow-degrading polymer. In addition, this polymer mediated significantly better transfection than PEI at its optimal N/P ratio with siRNA (N/P 10). Interestingly, the other five fast-degrading amine-dextrans (**15-17**, **19**, and **20**) showed little or no knockdown, although it has been reported that rapid polymer degradation may enhance siRNA delivery by contributing to a rapid release of the siRNA inside the cytosol.[40,41]

Based on our above observations, fast release of the siRNA molecule does not necessarily lead to enhanced gene transfection, and vice versa. The efficiency of siRNA delivery results from an array of combined factors, including the binding energy of the polymer-siRNA complex, "proton sponge" strength of the amine on the polymer, and release of siRNA from the cationic polymer either by degradation of the polymer backbone or by erosion of the polymer during cytosolic trafficking.

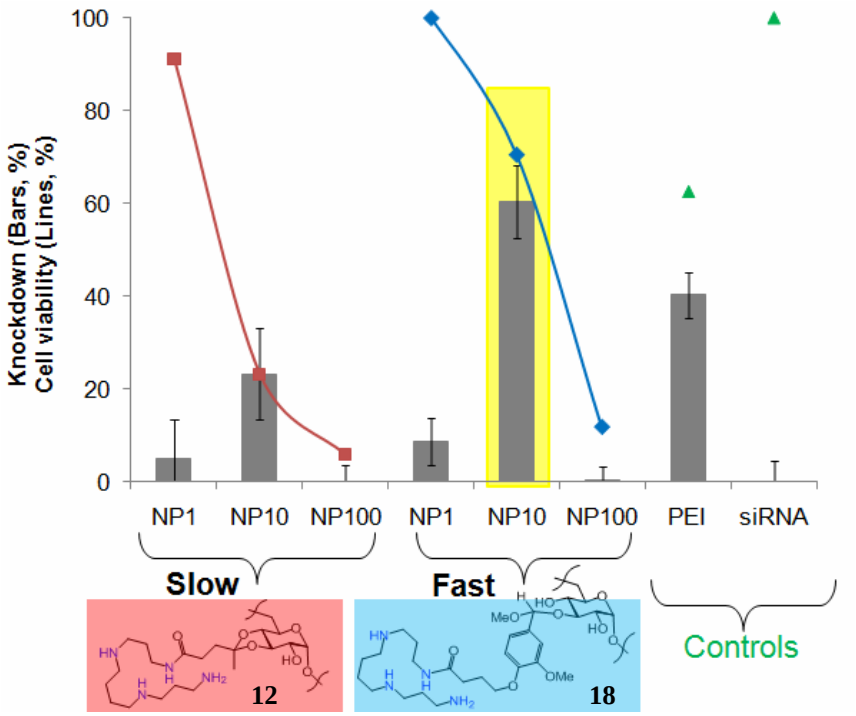

Figure 5.10. Degradation rate is important for transfection efficiency. *In vitro* delivery of siRNA by spermine-dextrans of different degradation rates (**12** and **18**). HeLa-*luc* cells were treated with polymers complexed with 0.5 µg siRNA/well. Complexes were prepared at various N/P ratios to determine the optimum for transfection efficiency. Results were compared to untreated cells and the percentage knockdown of luciferase expression was calculated. Results (columns) are combined with results from a concurrently performed cytotoxicity assay (closed symbols and lines). Fast-degrading spermine-dextran (**18**) shows superior knockdown of luciferase.

Conclusions

We have developed a new conjugation protocol for biocompatible dextran through the formation of acetals on its hydroxyl groups. The features of the acetal groups can be tuned by introducing diverse functional groups of different sizes and with varying electronic properties, therefore providing materials with tunable degradation rates that allow the cargo to be released at desired rates. We have applied this new chemistry in the development of siRNA carriers, acetal linked amine-dextrans. All amine-dextrans bound nucleic acids tightly, and we found the nucleic acid molecules could be released at different rates. Together with the different amine functionalities on the backbone, release rates of siRNA affected the effectiveness of gene silencing. These interesting findings may provide additional understanding in the search of ideal siRNA delivery systems.

Experimental Procedures

General Materials and Methods

All chemical reagents were purchased from Sigma-Aldrich (St. Louis, MO) and used as supplied, unless otherwise noted. The anti-luciferase siRNA (sense strand: 5'-CUU ACG CUG AGU ACU UCG A dTdT-3') was obtained from Dharmacon (Lafayette, CO) and Silencer Negative Control #1 siRNA was purchased from Ambion (Austin, TX). Firefly luciferase DNA (sequences: 5'-CTT ACG CTG AGT ACT TCG ATT-3' and 5'-TCG AAG TAC TCA GCG TAA GTT-3') was synthesized by Integrated DNA Technologies (IDT, Coralville, IA). Phosphate buffered saline (PBS, pH 7.4, GIBCO-10010) was purchased from Invitrogen-Gibco (Carlsbad, CA). Water (dd-H_2O) was purified to a resistance of 18 MΩ using a NANOpure purification system (Barnstead, USA). All reactions were conducted under nitrogen. Methanol used in the reactions was dried over magnesium methoxide. Other organic solvents in reactions were purified by passing through two columns of neutral alumina on a commercial push still apparatus (Glass Contour, SG Water, NH). Analytical thin layer chromatography (TLC) was performed on silica gel 60-F_{254} (Merck). Plates were visualized by ultraviolet light or charring with basic potassium permanganate solution, triphenylphosphine/ninhydrin solution or ethanolic sulfuric acid-anisaldehyde solution. Column chromatography used silica gel (SiliCycle, F60, 40-63 μm, 60 Å) and solvents were of reagent grade, and used as supplied. ^{1}H NMR spectra were recorded at 400 or 500 MHz and ^{13}C NMR spectra were recorded at 126 or 151 MHz. First order chemical shifts are reported in δ (ppm) using residual solvent signals from deuterated solvents as references. Mass spectrometry was performed under positive/negative-mode high resolution electrospray ionization (ESI) on an Orbitrap instrument by the Chemistry Mass Spectrometry Facility of the University of California, Berkeley. Fourier transform infrared spectroscopy (FT-IR) was carried out on a Varian 3100 FT-IR spectrometer (Varian, USA). Fluorescence and UV-vis absorbance measurements for microplate-based assays were obtained on a SpectraMax M3 multi-mode microplate reader (Molecular Devices, USA), usage courtesy of Professor Carolyn Bertozzi.

The synthesis of the acid-degradable linkers (**2** and **6**) is outlined in Scheme 5.1.

Scheme 5.1. Synthesis of acid-degradable linkers (**2** and **6**).

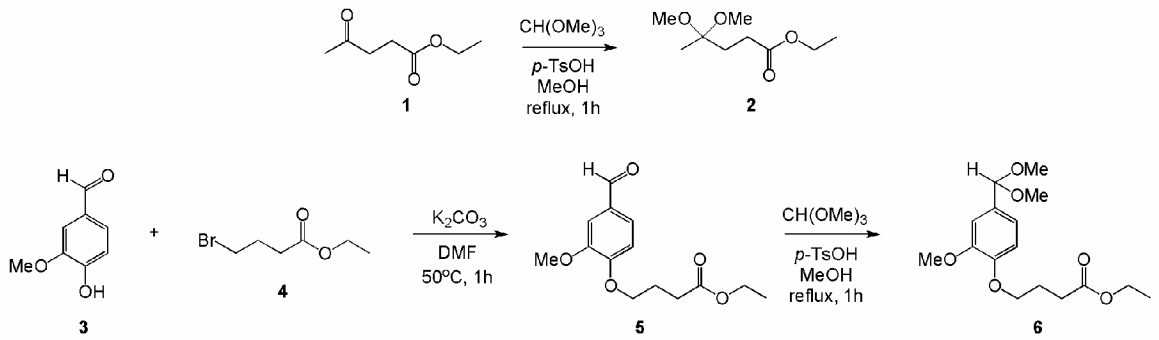

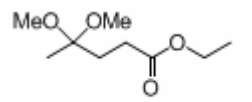

2

Synthesis of ethyl levulinate dimethyl ketal (2). Ethyl levulinate (**1**) (5.0 g, 34.7 mmol) and trimethyl orthoformate (7.6 mL, 69.4 mmol) were refluxed in anhydrous methanol (50 mL) with the presence of activated molecular sieves (4 Å, 5.0 g) and *p*-toluenesulfonic acid monohydrate (50 mg) for 1 h, then heat was removed and the reaction was quenched by addition of triethylamine. Molecular sieves were filtered off and solvents were removed by rotary evaporator. The residue was redissolved in dichloromethane (200 mL) and was washed with sodium bicarbonate solution (pH 8.0, 200 mL). The dichloromethane layer was isolated and dried over anhydrous sodium sulfate powder, the solvent was evaporated, and the residue was dried under vacuum to yield 5.8 g product as colorless oil (88% in yield, 86% in purity by NMR). The mixture of dimethyl ketal and ketone was not further separated, and was used directly in the next step synthesis. IR (cm^{-1}): 2987, 2945, 2909, 2831, 1739, 1448, 1380, 1294, 1174, 1128, 1106, 1046, 859. ^{1}H NMR (400 MHz, CD_2Cl_2): δ 4.09 (q, 2H, J = 7.1 Hz, CH_2CH$_3$), 3.14 (s, 6H, OCH$_3$), 2.30 (t, 2H, J = 7.8 Hz, CH_2C=O), 1.90 (t, 2H, J = 8.3 Hz, CH_2CH$_2$C=O), 1.23 (t, 3H, J = 7.8 Hz, CH$_2$CH_3,), 1.21 (s, 3H, CH_3C). ^{13}C NMR (126 MHz, CD_3CN): δ 174.14, 101.83, 61.11, 48.44, 32.37, 30.25, 21.21, 14.61. ESI HRMS calcd for $C_9H_{18}O_4Li$ (M + Li): 197.1360, found: 197.1360.

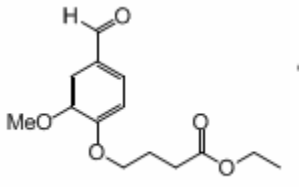

5

Synthesis of ethyl 4-(4-formyl-3-methoxy)-phenyl butyrate (5). Vanillin (**3**) (20.0 g, 0.131 mol), ethyl 4-bromobutyrate (**4**) (22.5 mL, 0.157 mol), and potassium carbonate (36.3 g, 0.263 mol) were heated at 50°C in dry DMF (200 mL) for 1 h. (Sodium hydride was not suitable for the reaction due to the formation of by-product ethyl acrylate.) Potassium carbonate was then filtered, and the DMF solution was extracted with ethyl acetate (1 L) and water (1 L) twice. The ethyl acetate layer was collected, dried over anhydrous magnesium sulfate, and removed by rotary evaporation. The residue was dried under high vacuum to obtain the pure vanillin-scented product **5** as a white powder (32.7 g, 93%). IR (KBr, cm^{-1}): 3008, 2976, 2869, 2350, 1766, 1710, 1620, 1565, 1530, 1493, 1433, 1366, 1301, 1222. ^{1}H NMR (400 MHz, $CDCl_3$): δ 9.84 (s, 1H, HC=O), 7.49 – 7.34 (m, 2H, Ar), 6.98 (d, 1H, J = 8.1 Hz, Ar), 4.34 – 3.99 (m, 4H, OCH$_2$, COOCH$_2$), 3.92 (s, 3H, OCH$_3$), 2.54 (t, 2H, J = 7.2 Hz, CH$_2$C=O), 2.20 (dddd, 2H, J = 6.8, 6.8, 6.8, 6.8 Hz, CH$_2$CH_2CH$_2$), 1.25 (t, 3H, J = 7.1 Hz, CH$_2$CH_3). ^{13}C NMR (126 MHz, $CDCl_3$): δ 191.10, 173.14, 154.02, 150.06, 130.29, 126.95, 111.73, 109.44, 68.07, 60.70, 56.17, 30.72, 24.42, 14.39. ESI HRMS calcd for $C_{14}H_{18}O_5Li$ (M + Li): 273.1309, found: 273.1310.

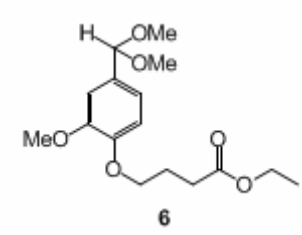

6

Synthesis of ethyl 4-(4-formyl-3-methoxy)-phenyl butyrate dimethyl acetal (6). Compound **6** was prepared in a similar way as that of compound **2** using **5** (31.7 g, 0.119 mol), trimethyl orthoformate (26.1 mL, 0.238 mol), activated molecular sieves (4 Å, 30.0 g) and *p*-toluenesulfonic acid monohydrate (300 mg) in anhydrous methanol (300 mL), to yield 35.7 g product as colorless oil (95 % in yield, 99% in purity). The mixture of dimethyl ketal and ketone was not further separated, and was used directly in the next step synthesis. IR (cm^{-1}): 3077, 2941, 2831, 2756, 1737, 1685, 1595, 1511, 1467, 1418, 1375, 1348, 1268, 1137, 1102, 864, 809. ^{1}H NMR (400 MHz, CD_3CN): δ 6.99 (d, 1H, J = 1.5 Hz, Ar), 6.95 – 6.92 (m, 2H, Ar), 5.29 (s, 1H, C*H*$(OCH_3)_2$), 4.11 (q, 2H, J = 7.1 Hz, $COOCH_2$), 4.03 (t, 2H, J = 6.3 Hz, OCH_2), 3.82 (s, 3H, $ArOCH_3$), 3.30 (s, 6H, $CH(OCH_3)_2$), 2.48 (t, 2H, J = 7.3 Hz, CH_2C=O), 2.05 (dddd, 2H, J = 7.2, 7.2, 6.4, 6.4 Hz, $CH_2CH_2CH_2$), 1.23 (t, 3H, J = 7.1 Hz, CH_2CH_3). ^{13}C NMR (151 MHz, CD_2Cl_2): δ 173.73, 150.22, 149.24, 132.21, 119.90, 113.49, 111.09, 103.99, 68.72, 61.07, 56.61, 53.35, 31.49, 25.51, 14.79. ESI HRMS calcd for $C_{16}H_{24}O_6Li$ (M + Li): 319.1727, found: 319.1730.

Polymer Synthesis

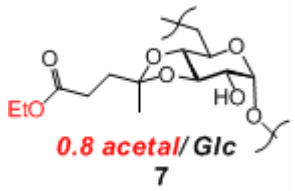

7

Synthesis of ester-functionalized dextran through slow-degrading ketal linkage (7). To a solution of dextran (MW = 35000 ~ 45000 g/mol, 500 mg, 3.09 mmol glucose residue) in anhydrous DMSO (5 mL) were added ethyl levulinate dimethyl ketal (**2**) (3.55 g, 18.5 mmol), molecular sieves (5Å, 500 mg) and *p*-toluenesulfonic acid monohydrate (8.8 mg). The reaction mixture was heated for 2 h at 50°C, and the reaction was quenched by addition of triethylamine. Molecular sieves were then filtered, and the DMSO solution was dripped into a mixture of isopropanol and hexanes (1:1, 40 mL) to obtain white precipitate, which was collected by centrifugation. The white precipitate was purified by redissolving in DMSO (4 mL) and precipitating in isopropanol and hexanes (1:1, 40 mL). After centrifuging the resulting suspension, the product was dried under vacuum to obtain a water-insoluble white powder (802 mg, 0.8 ester per glucose residue (calculated by its ^{1}H NMR, and confirmed by the ^{1}H NMR of its derivatives **9**-**14**), yield 99%). Due to the rather complex and uninterpretable ^{1}H NMR spectrum in its only solvent d_6-DMSO, the ^{1}H NMR of compound **7** was obtained in acidic D_2O (pH 2.0), where the attached ketals were cleaved to give water-soluble free dextran and ethyl levulinate (**1**). ^{1}H NMR (500 MHz, D_2O-DCl-$(CD_3)_2SO$) δ 5.22 – 4.76 (m, 1H, glucose-H_1), 3.98 (q, 0.8 x 2H, J = 7.2 Hz, $COOCH_2$), 3.90 – 3.21 (m, 6H, glucose-$H_{2\text{-}6}$), 2.73 (t, 0.8 x 2H, J = 6.3

Hz, CH_2COO), 2.42 (t, 0.8 x 2H, J = 6.3 Hz, CH_3COCH_2), 2.06 (s, 0.8 x 3H, CH_3COCH_2), 1.05 (t, 0.8 x 3H, J = 7.2 Hz, CH_2CH_3). As a reference, the ^{1}H NMR resonances of a less densely functionalized (0.5 ketal per glucose residue) water-soluble analogue **7'** is provided as follows: ^{1}H NMR (500 MHz, D_2O) δ 5.43 – 4.91 (m, 1H, glucose-H_1), 4.29 – 4.11 (m, 0.5 x 2H, $COOCH_2$), 4.17 – 3.25 (m, 6H, glucose-$H_{2\text{-}6}$), 2.56 (m, 0.5 x 2H, CH_2COO), 2.21 (m, 0.5 x 2H, ketal-CH_2), 1.68 – 1.36 (m, 0.5 x 3H, ketal-CH_3), 1.37 – 1.22 (m, 0.5 x 3H, $COOCH_2CH_3$).

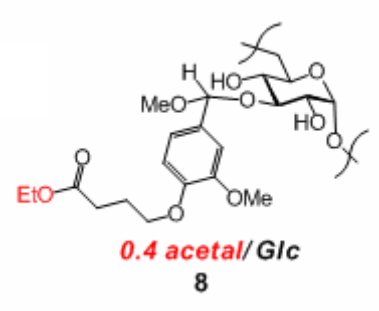

8

Synthesis of ester-functionalized dextran through fast-degrading ketal linkage (8). To a solution of dextran (MW = 35000 ~ 45000 g/mol, 2.0 g, 12.3 mmol glucose residue) in anhydrous DMSO (20 mL) were added dimethyl acetal **6** (23.1 g, 74.1 mmol), molecular sieves (5Å, 2.0 g) and *p*-toluenesulfonic acid monohydrate (35.2 mg). The reaction mixture was heated overnight at 80°C, and the reaction was quenched by addition of triethylamine. Molecular sieves were then filtered, and the DMSO solution was dripped into a mixture of isopropanol (200 mL) to obtain a white precipitate, which was collected by centrifugation. The white precipitate was purified by redissolving in DMSO (20 mL) and precipitating in isopropanol (200 mL). After centrifuging the resulting suspension, the product was dried under vacuum to obtain a water-insoluble white powder (3.35 mg, 0.4 ester per glucose residue, yield 99%). Due to the same reason as that described for compound **7**, the ^{1}H NMR of compound **8** was also obtained in acidic D_2O, and the formation of acyclic ketal was confirmed by the generation of methanol in acidic solution: ^{1}H NMR (500 MHz, D_2O-DCl-$(CD_3)_2SO$) δ 9.77 (s, 0.4 x 1H), 7.65 (dd, 0.4 x 1H, J = 8.3, 1.7 Hz, Ar), 7.51 (d, 0.4 x 1H, J = 1.7 Hz, Ar), 7.22 (d, 0.4 x 1H, J = 8.4 Hz, Ar), 5.34 – 4.90 (m, 1H, glucose-H_1), 4.24 (t, 0.4 x 2H, J = 6.1 Hz, $ArOCH_2$), 4.12 (q, 0.4 x 2H, J = 7.1 Hz, $COOCH_2$), 4.04 – 3.39 (m, 6H, glucose-$H_{2\text{-}6}$), **3.33 (s, 0.4 x 3H, CH_3OH)**, 2.55 (dd, 0.4 x 2H, J = 9.8, 4.2 Hz, CH_2C=O), 2.15 (p, 0.4 x 2H, J = 6.5 Hz, $CH_2CH_2CH_2$), 1.21 (t, 0.4 x 3H, J = 7.2 Hz, CH_2CH_3).

Synthesis of amine-dextran with tunable degradability and functionality (9-20). 9-20 were synthesized according to the general procedure described below. **7** or **8** was dissolved in anhydrous DMSO (Table 5.1), followed by addition of various amines (**A1-A6**, 40 eq. amino group per ester group). The reaction mixture was then warmed at 50°C for 2 weeks for completion. The reaction was worked up by dripping the DMSO solution into ethyl acetate (20 mL) to have the product precipitated. The suspension was centrifuged for 10 min at 10,000 x g to collect the white precipitation, which was then redissolved in DMSO (2 mL) and precipitated into ethyl acetate (20 mL) followed by centrifugation. The washing step was repeated twice, the white precipitate was collected, and the residual solvents were removed under high vacuum to give a white dry powder. The amine-dextran was then dissolved in dd-H_2O (pH 8.0) and lyophilized to get white foamy solid products. **Note:** The starting materials, **7** and **8**, were water-

insoluble, and products were water-soluble, indicating the replacement of ester groups by amine groups. ^{1}H NMR (500 MHz, D_2O) signals of each amine-dextran are listed below.

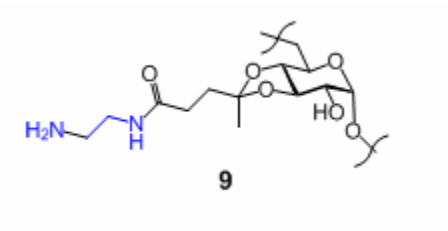

9

Compound 9. ^{1}H NMR (500 MHz, D_2O) δ 5.48 – 4.94 (m, 1H, glucose-H_1), 4.34 – 3.11 (m, 6H, glucose-$H_{2\text{-}6}$), 3.42 (br. app. s, 0.8 x 2H, C*H*$_2$NHC=O), 2.85 (br. app. s, 0.8 x 2H, C*H*$_2$NH$_2$), 2.42 (br. app. s, 0.8 x 2H, CH_2C=O), 2.11 (br. app. s, 0.8 x 2H, ketal-CH_2), 1.70 – 1.30 (m, 0.8 x 3H, ketal-CH_3).

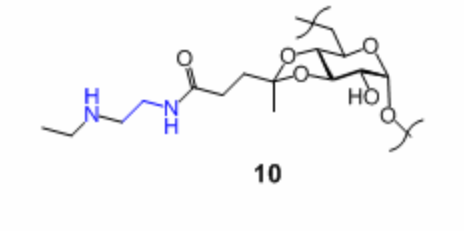

10

Compound 10. ^{1}H NMR (500 MHz, D_2O) δ 5.44 – 4.92 (m, 1H, glucose-H_1), 4.31 – 3.12 (m, 6H, glucose-$H_{2\text{-}6}$), 3.43 (br. app. s, 0.8 x 2H, C*H*$_2$NHC=O), 2.87 (br. app. s, 0.8 x 2H, C*H*$_2$NH), 2.87 (br. app. s, 0.8 x 2H, C*H*$_2$NH), 2.39 (br. app. s, 0.8 x 2H, CH_2C=O), 2.08 (br. app. s, 0.8 x 2H, ketal-CH_2), 1.63 – 1.35 (m, 0.8 x 3H, ketal-CH_3), 1.10 (br. app. s, 0.8 x 3H, NHCH$_2$C*H*$_3$).

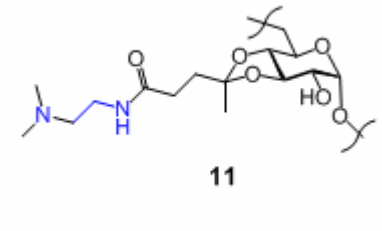

11

Compound 11. ^{1}H NMR (500 MHz, D_2O) δ 5.46 – 4.92(m, 1H, glucose-H_1), 4.30 – 3.16 (m, 6H, glucose-$H_{2\text{-}6}$), 3.46 (br. app. s, 0.8 x 2H, C*H*$_2$NHC=O), 2.89 (br. app. s, 0.8 x 2H, C*H*$_2$N), 2.57 (br. app. s, 0.8 x 6H, $(CH_3)_2$N), 2.40 (br. app. s, 0.8 x 2H, CH_2C=O), 2.07 (br. app. s, 0.8 x 2H, ketal-CH_2), 1.70 – 1.32 (m, 0.8 x 3H, ketal-CH_3).

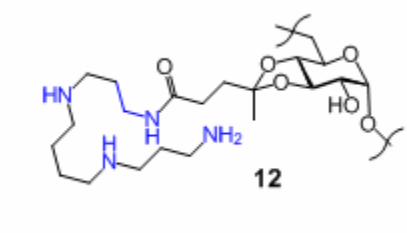

12

Compound 12. ^{1}H NMR (500 MHz, D_2O) δ 5.44 – 4.92 (m, 1H, glucose-H_1), 4.32 – 3.03 (m, 6H, glucose-$H_{2\text{-}6}$), 3.25 (br. app. s, 0.8 x 2H, CH_2NHC=O), 3.04 – 2.65 (m, 0.8 x 10H, CH_2NH, CH_2NH$_2$), 2.37 (br. app. s, 0.8 x 2H, CH$_2$C=O), 2.08 (br. app. s, 0.8 x 2H, ketal-CH$_2$), 1.88 (br. app. s, 0.8 x 2H, NHCH$_2$CH_2CH$_2$NHC=O), 1.80 (br. app. s, 0.8 x 2H, NHCH$_2$CH_2CH$_2$NH$_2$), 1.65 (br. app. s, 0.8 x 4H, NHCH$_2$CH_2CH_2CH$_2$NH), 1.65 – 1.30 (m, 0.8 x 3H, ketal-CH$_3$).

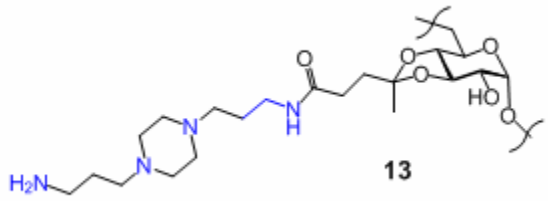

13

Compound 13. ^{1}H NMR (500 MHz, D_2O) δ 5.42 – 4.89 (m, 1H, glucose-H_1), 4.31 – 3.24 (m, 6H, glucose-$H_{2\text{-}6}$), 3.20 (app. br. s, 0.8 x 2H, CH_2NHC=O), 3.11 – 2.14 (m, 0.8 x 16H, CH_2N, CH_2NH$_2$, CH$_2$C=O), 2.07 (br. app. s, 0.8 x 2H, ketal-CH$_2$), 1.86 – 1.75 (m, 0.8 x 2H, NCH$_2$CH_2CH$_2$NHC=O), 1.68 (br. app. s, 0.8 x 2H, NCH$_2$CH_2CH$_2$NH$_2$), 1.57 – 1.27 (m, 0.8 x 3H, ketal-CH$_3$).

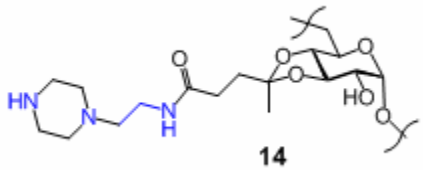

14

Compound 14. ^{11}H NMR (500 MHz, D_2O) δ 5.40 – 4.92 (m, 1H, glucose-H_1), 4.29 – 3.18 (m, 6H, glucose-$H_{2\text{-}6}$), 3.37 (m, 0.8 x 2H, CH_2NHC=O), 3.09 (br. app. s, 0.8 x 4H, NHCH_2CH$_2$N), 2.70 (br. app. s, 0.8 x 4H, NHCH$_2$CH_2N), 2.60 (br. app. s, 0.8 x 2H, NCH_2CH$_2$NHC=O), 2.38 (br. app. s, 0.8 x 2H, CH$_2$C=O), 2.08 (br. app. s, 0.8 x 2H, ketal-CH$_2$), 1.65 – 1.30 (m, 0.8 x 3H, ketal-CH$_3$).

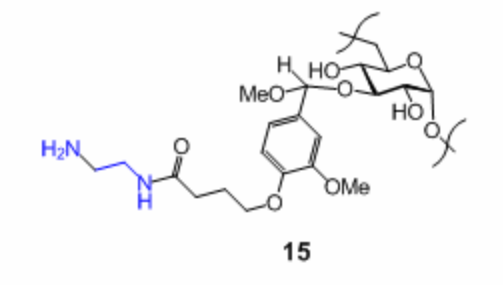

15

Compound 15. ^{1}H NMR (500 MHz, D_2O) δ 7.28 – 6.69 (m, 0.4 x 3H, Ar), 6.17 – 5.41 (m, 0.4 x 1H, acetal-H), 5.40 – 4.90 (m, 1H, glucose-H_1), 4.36 – 3.18 (m, 6H, glucose-$H_{2\text{-}6}$; 0.4 x 2H, $ArOCH_2$; 0.4 x 3H, $ArOCH_3$; 0.4 x 2H, $CH_2NHC{=}O$; 0.4 x 3H, acetal-OCH_3), 3.09 (br. app. s, 0.4 x 2H, CH_2NH_2), 2.35 (br. app. s, 0.4 x 2H, $CH_2C{=}O$), 2.07 (br. app. s, 0.4 x 2H, $ArOCH_2CH_2$).

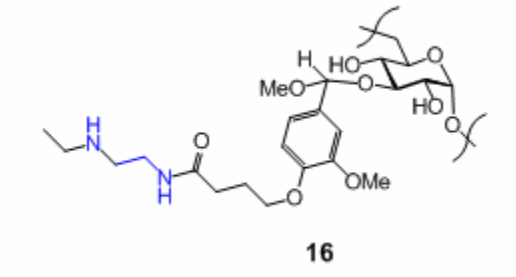

16

Compound 16. ^{1}H NMR (500 MHz, D_2O) δ 7.24 – 6.75 (m, 0.4 x 3H, Ar), 6.12 – 5.43 (m, 0.4 x 1H, acetal-H), 5.38 – 4.92 (m, 1H, glucose-H_1), 4.37 – 3.32 (m, 6H, glucose-$H_{2\text{-}6}$; 0.4 x 2H, $ArOCH_2$; 0.4 x 3H, $ArOCH_3$; 0.4 x 2H, $CH_2NHC{=}O$; 0.4 x 3H, acetal-OCH_3), 3.17 – 2.99 (m, 0.4 x 4H, CH_2NH), 2.48 (br. app. s, 0.4 x 2H, $CH_2C{=}O$), 2.08 (br. app. s, 0.4 x 2H, $ArOCH_2CH_2$), 1.37 – 1.11 (br. app. s, 0.4 x 3H, $NHCH_2CH_3$).

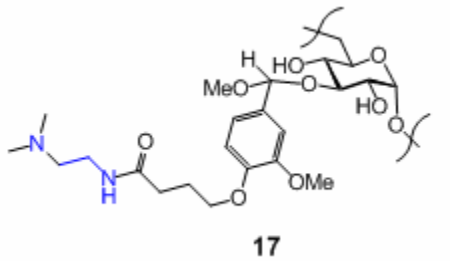

17

Compound 17. ^{1}H NMR (500 MHz, D_2O) δ 7.28 – 6.65 (m, 0.4 x 3H, Ar), 6.22 – 5.42 (m, 0.4 x 1H, acetal-H), 5.39 – 4.90 (m, 1H, glucose-H_1), 4.38 – 3.20 (m, 6H, glucose-$H_{2\text{-}6}$; 0.4 x 2H, $ArOCH_2$; 0.4 x 3H, $ArOCH_3$; 0.4 x 3H, acetal-OCH_3, 0.4 x 2H, $CH_2NHC{=}O$), 3.11 (br. app. s, 0.4 x 2H, CH_2N), 2.77 (br. app. d, 0.4 x 6H, $(CH_3)_2N$), 2.45 (br. app. s, 0.4 x 2H, $CH_2C{=}O$), 2.08 (br. app. s, 0.4 x 2H, $ArOCH_2CH_2$).

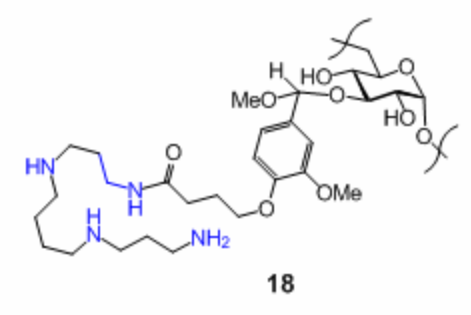

18

Compound 18. ^{1}H NMR (500 MHz, D_2O) δ 7.31 – 6.63 (m, 0.4 x 3H, Ar), 6.22 – 5.44 (m, 0.4 x 1H, acetal-H), 5.38 – 4.91 (m, 1H, glucose-H_1), 4.40 – 3.06 (m, 6H, glucose-$H_{2\text{-}6}$; 0.4 x 2H, $ArOCH_2$; 0.4 x 3H, $ArOCH_3$; 0.4 x 3H, acetal-OCH_3, 0.4 x 2H, $CH_2NHC{=}O$), 3.07 – 2.77 (m, 0.4 x 10H, CH_2NH, CH_2NH_2), 2.43 (br. app. s, 0.4 x 2H, $CH_2C{=}O$), 2.07 (br. app. s, 0.4 x 2H, $ArOCH_2CH_2$), 1.97 – 1.86 (m, 0.4 x 2H, $NHCH_2CH_2CH_2NHC{=}O$), 1.80 (br. app. s, 0.4 x 2H, $NHCH_2CH_2CH_2NH_2$), 1.74 – 1.45 (m, 0.4 x 4H, $NHCH_2CH_2CH_2CH_2NH$).

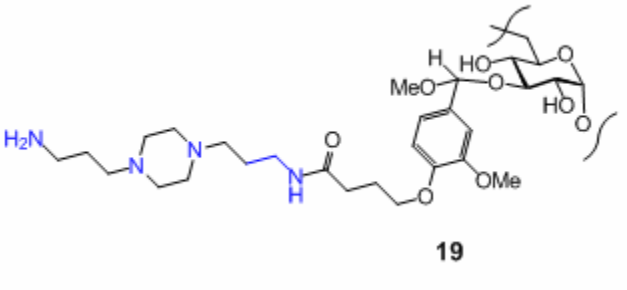

19

Compound 19. ^{1}H NMR (500 MHz, D_2O) δ 7.31 – 6.69 (m, 0.4 x 3H, Ar), 6.14 – 5.44 (m, 0.4 x 1H, acetal-H), 5.39 – 4.94 (m, 1H, glucose-H_1), 4.40 – 3.24 (m, 6H, glucose-$H_{2\text{-}6}$; 0.4 x 2H, $ArOCH_2$; 0.4 x 3H, $ArOCH_3$; 0.4 x 3H, acetal-OCH_3), 3.17 (0.4 x 2H, $CH_2NHC{=}O$), 3.03 (br. app. s, 0.4 x 2H, CH_2NH_2), 2.62 – 2.17 (m, 0.4 x 12H, CH_2N; 0.4 x 2H, $CH_2C{=}O$), 2.08 (br. app. s, 0.4 x 2H, $ArOCH_2CH_2$), 1.87 (br. app. s, 0.4 x 2H, $NCH_2CH_2CH_2NHC{=}O$), 1.68 (br. app. s, 0.4 x 2H, $NCH_2CH_2CH_2NH_2$).

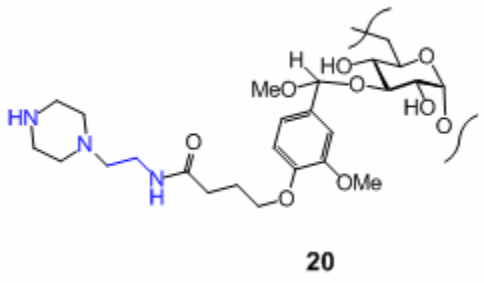

20

Compound 20. ^{1}H NMR (500 MHz, D_2O) δ 7.35 – 6.70 (m, 0.4 x 3H, Ar), 6.23 – 5.43 (m, 0.4 x 1H, acetal-H), 5.23 – 4.92 (m, 1H, glucose-H_1), 4.37 – 2.98 (m, 6H, glucose-$H_{2\text{-}6}$; 0.4 x 2H, $ArOCH_2$; 0.4 x 3H, $ArOCH_3$; 0.4 x 3H, acetal-OCH_3, 0.4 x 2H, $CH_2NHC{=}O$), 2.89 – 2.21 (m, 0.4 x 10H, CH_2NH, CH_2N; 0.4 x 2H, $CH_2C{=}O$), 2.07 (br. app. s, 0.4 x 2H, $ArOCH_2CH_2$).

Table 5.1. Reaction details to obtain amine-dextrans (9-20).

Product ID	*Reaction*			*Product*		
	Starting material	DMSO	Amine[a]	Yield	Amine/Glucose[b]	Amino N/mg[c]
9	**7** (50 mg, 0.150 mmol ester)	0.5 mL	**A1** 201 μL	45 mg (87%)	0.8	2.92 μmol
10	**7** (50 mg, 0.150 mmol ester)	0.5 mL	**A2** 632 μL	42 mg (75%)	0.8	2.70 μmol
11	**7** (50 mg, 0.150 mmol ester)	0.5 mL	**A3** 656 μL	40 mg (72%)	0.8	2.70 μmol
12	**7** (50 mg, 0.150 mmol ester)	0.5 mL	**A4** 647 μL	65 mg (89%)	0.8	6.18 μmol
13	**7** (50 mg, 0.150 mmol ester)	0.5 mL	**A5** 618 μL	63 mg (87%)	0.8	6.21 μmol
14	**7** (50 mg, 0.150 mmol ester)	0.5 mL	**A6** 786 μL	60 mg (97%)	0.8	4.85 μmol
15	**8** (200 mg, 0.292 mmol ester)	2.0 mL	**A1** 195 μL	180 mg (88%)	0.4	0.77 μmol
16	**8** (200 mg, 0.292 mmol ester)	2.0 mL	**A2** 614 μL	185 mg (87%)	0.4	0.75 μmol
17	**8** (200 mg, 0.292 mmol ester)	2.0 mL	**A3** 637 μL	176 mg (83%)	0.4	0.75 μmol
18	**8** (200 mg, 0.292 mmol ester)	2.0 mL	**A4** 629 μL	201 mg (82%)	0.4	2.08 μmol
19	**8** (200 mg, 0.292 mmol ester)	2.0 mL	**A5** 601 μL	214 mg (79%)	0.4	2.09 μmol
20	**8** (200 mg, 0.292 mmol ester)	2.0 mL	**A6** 765 μL	205 mg (91%)	0.4	1.46 μmol

[a]Amine structures are listed in Figure 5.3.
[b]Amine per glucose residue means the entire amine structure (not counting each amino group) per glucose. The value was determined by ^{1}H NMR.
[c]Amine nitrogen per mg counts each amino nitrogen in the entire amine-dextran molecule.

Polymer Characterization

Gel electrophoresis. To study the binding of amine-dextran to short fragments of nucleic acids, a solution of firefly luciferase DNA (0.5 μg/μL, 10 μL) in PBS buffer (pH 7.4) was mixed well with a polymer solution (10 μL in PBS buffer) to give nitrogen (of polymer)/phosphate (of DNA) ratios of 100, 10 and 1. The solution was mixed for 20 min to allow the complex to form, and loaded to a gel (0.5 g agarose, 50 mL tris-acetate-EDTA buffer, 1 drop of ethidium bromide solution (GeneChoice, final concentration 0.5 μg/mL)). The gel was developed for 40 min (100 V, 3.0 A, 300 W), visualized under UV at 254 nm, and digital images were collected with an EpiChemi II Darkroom unit fitted with a CCD camera (UVP, Upland, CA), usage courtesy of Professor Carolyn Bertozzi. In the DNA release study, a solution of firefly luciferase DNA (1 μg/μL, 5 μL) in PBS buffer (pH 7.4) was mixed well with a polymer solution (5 μL in PBS buffer) to give nitrogen (of polymer)/phosphate (of DNA) ratios of 100, 10 and 1. The solution was mixed for 20 min, and pH was adjusted to 5.0 by addition of acetate buffer (10 μL, 150 mM, pH 4.98). The mixture was incubated at 37°C for 24 h or 48 h before loading to the agarose gel.

NMR study of cleavage of amines from amine-dextran conjugates
Amine-dextran (**9-20**, 2 mg) was dissolved in either deuterated phosphate buffer (700 μL, 30 mM, pH 7.4) or deuterated acetate buffer (700 μL, 30 mM, pH 5.0), the solution was kept at 37°C, and ^{1}H NMR was acquired at desired time points. Integrations of relevant resonances were compared and data was plotted using Microsoft Excel 2007.

Studies Performed with Polymers

Cell Lines and Culture. HeLa cell line stably expressing firefly luciferase (HeLa-*luc*) were a kind gift of Dr. Chris Contag. HeLa-*luc* cells were maintained in Dulbecco's Modified Eagle's Medium (DMEM) supplemented with 10% (v/v) fetal bovine serum (FBS), 1% GlutaMAX, and 500 μg/mL Zeocin (all from Invitrogen except the serum, which was from Hyclone (Logan, UT)). Cell incubations were performed in a water-jacketed 37°C/5% CO_2 incubator.

***In Vitro* siRNA Transfection Assay.** HeLa-*luc* cells were seeded (15,000 cells/well) into each well of a 96-well clear tissue culture plate (Costar, Corning, NY) and allowed to attach overnight in growth medium. Growth medium was composed of DMEM (with phenol red), 10% FBS, and 1% GlutaMAX. The polymer/siRNA ratio was expressed as the nitrogen/phosphate (N/P) ratio, where N represents moles of amine on the polymer and P represents moles of phosphate on siRNA. Cells were transfected with 0.5 μg of siRNA complexed with polymer at various N/P ratios to determine the optimum for transfection efficiency. In order to exclude non-specific gene silencing by the polyplexes themselves, the cells were also incubated with polyplexes prepared using a negative control siRNA (Silencer Negative Control #1 siRNA).

Working dilutions of each polymer were prepared (at concentrations necessary to yield the different N/P ratios) in PBS (pH 7.4). Polymer solutions (50 μL) were mixed with siRNA solutions (50 μL of 100 μg/mL siRNA in PBS) and incubated for 20 min at rt to allow for complex formation. The complex solutions were then diluted with 900 μL of medium (either FBS-free DMEM or 10% FBS-containing DMEM). Existing medium was replaced with 100 μl of each polymer/siRNA sample in triplicate wells. In the case of experiments without serum, the medium was replaced 4 h after polyplex addition with fresh serum-containing (10% FBS) growth medium. The cells were allowed to grow for a total of 48 h before being analyzed for gene expression. Lipofectamine 2000 (Invitrogen, Carlsbad, CA) was used as a positive control for siRNA delivery and was prepared according to the manufacturer's instructions. Complexes containing equivalent doses of siRNA to polyplexes were prepared by mixing Lipofectamine 2000 and siRNA (3.8:1 ratio). As negative controls, both equivalent doses of free siRNA in medium and medium alone were used.

After 48 h, the plate was centrifuged (1200 x g, 5 min) and the medium was replaced with DPBS (100 μL/well). The cells were centrifuged (1200 x g, 5 min) once more, the buffer was replaced with Glo Lysis Buffer (120 μL/well, Promega, Madison, WI), and the plate was vortexed at rt for 20 min. Samples from each well (100 μL) were transferred to the wells of a white 96-well tissue culture plate (Corning, Lowell, MA). Steady-Glo luciferase assay reagent (Promega) was reconstituted according to the manufacturer's instructions and injected into each well in series (100 μL/well) using a GloMax 96 microplate luminometer (Promega). After a 10 s post-injection delay, each well was read with a 2 s integration time.

Total Protein Assay. Cells treated identically and in parallel with transfection assays were tested on a second 96-well plate. After washing, the cells were lysed with M-PER Mammalian Protein Extraction Reagent (50 μL/well, Pierce, Rockford, IL) by incubating for 10 min at rt. PBS (50 μL/well) was then added, and the plate was briefly vortexed. Samples from each well (50 μL) were transferred to a black 96-well plate (Corning) already containing PBS (100 μL/well). A solution of 3 mg/mL fluorescamine in acetone (50 μL) was added to each well and mixed well using a multi-channel pipette. After 5 min, fluorescence was measured using a SpectraMax M3 multi-mode microplate reader (ex. 400 nm, em. 460 nm). Protein concentrations were determined using bovine serum albumin as a standard. Relative light units (RLU) from the luminometer were normalized to the total mass of cellular protein. The resulting data (RLU/mg of protein) are given as a mean ± standard deviation of three independent measurements. Percentage knockdown was calculated by comparison of treated cells to untreated cells. The data was compared to the knockdown of cells treated with polymers complexed with control siRNA or control siRNA/Lipofectamine complexes.

Viability Assay. Cells treated identically and in parallel with transfection assays were tested on a third 96-well plate. A 3.0 mg/mL solution of MTT (3-(4,5-dimethyl-2-thiazolyl)-2,5-diphenyl-2H-tetrazolium bromide) in medium (40 μL) was added directly to each well, and the plate was incubated for an additional 30 min. The medium was then replaced with DMSO (200 μL/well), 100 μL of which was transferred to another clear-bottom 96-well assay plate (Pro-Bind, Falcon) containing 100 μL DMSO and 25 μL of glycine buffer (0.1 M glycine, 0.1 M NaCl, pH 10.5) per well. The absorbances at 570 nm were measured using a SpectraMax M3 multi-mode microplate reader (Molecular Devices). Cell viability was normalized to the absorbance measured from untreated cells. Data are represented as a mean ± standard deviation of three measurements.

References

(1) Kamath, R. S.; Ahringer, J. *Methods (Amsterdam, Neth.)* **2003**, *30*, 313-321.
(2) Bumcrot, D.; Manoharan, M.; Koteliansky, V.; Sah, D. W. Y. *Nat. Chem. Biol.* **2006**, *2*, 711-719.
(3) Hebert, C. G.; Valdes, J. J.; Bentley, W. E. *Curr. Opin. Biotechnol.* **2008**, *19*, 500-505.
(4) Falschlehner, C.; Steinbrink, S.; Erdmann, G.; Boutros, M. *Biotechnol. J.* **2010**, *5*, 368-376.
(5) Pecot, C. V.; Calin, G. A.; Coleman, R. L.; Lopez-Berestein, G.; Sood, A. K. *Nat. Rev. Cancer* **2011**, *11*, 59-67.
(6) Whitehead, K. A.; Langer, R.; Anderson, D. G. *Nat. Rev. Drug Discovery* **2009**, *8*, 129-138.
(7) Huang, C.; Li, M.; Chen, C.; Yao, Q. *Expert Opin. Ther. Targets* **2008**, *12*, 637-645.
(8) Lares, M. R.; Rossi, J. J.; Ouellet, D. L. *Trends Biotechnol.* **2010**, *28*, 570-579.
(9) Devroe, E.; Silver, P. A. *Expert Opin. Biol. Ther.* **2004**, *4*, 319-327.
(10) Zhu, L.; Mahato, R. I. *Expert Opin. Drug Delivery* **2010**, *7*, 1209-1226.
(11) Thomas, C. E.; Ehrhardt, A.; Kay, M. A. *Nat. Rev. Genet.* **2003**, *4*, 346-358.
(12) Chau, Y.; Dang, N. M.; Tan, F. E.; Langer, R. *J. Pharm. Sci.* **2006**, *95*, 542-551.
(13) Hosseinkhani, H.; Azzam, T.; Tabata, Y.; Domb, A. J. *Gene Ther.* **2004**, *11*, 194-203.
(14) Heinze, T.; Liebert, T.; Heublein, B.; Hornig, S. *Adv. Polym. Sci.* **2006**, *205*, 199-291.
(15) Baldwin, A. D.; Kiick, K. L. *Biopolymers* **2010**, *94*, 128-140.
(16) Wuts, P. G. M.; Greene, T. W. *Greene's Protective Groups in Organic Synthesis*; 4th ed.; John Wiley & Sons, Inc.: Hoboken, NJ, 2007.
(17) Mellman, I.; Fuchs, R.; Helenius, A. *Annu. Rev. Biochem.* **1986**, *55*, 663-700.
(18) Standley, S. M.; Kwon, Y. J.; Murthy, N.; Kunisawa, J.; Shastri, N.; Guillaudeu, S. J.; Lau, L.; Fréchet, J. M. J. *Bioconjugate Chem.* **2004**, *15*, 1281-1288.
(19) Bachelder, E. M.; Beaudette, T. T.; Broaders, K. E.; Paramonov, S. E.; Dashe, J.; Fréchet, J. M. J. *Mol. Pharmaceutics* **2008**, *5*, 876-884.
(20) Paramonov, S. E.; Bachelder, E. M.; Beaudette, T. T.; Standley, S. M.; Lee, C. C.; Dashe, J.; Fréchet, J. M. J. *Bioconjugate Chem.* **2008**, *19*, 911-919.
(21) Murthy, N.; Xu, M.; Schuck, S.; Kunisawa, J.; Shastri, N.; Fréchet, J. M. J. *Proc. Natl. Acad. Sci. U.S.A.* **2003**, *100*, 4995-5000.
(22) Jain, R.; Standley, S. M.; Fréchet, J. M. J. *Macromolecules* **2007**, *40*, 452-457.
(23) Broaders, K. E.; Cohen, J. A.; Beaudette, T. T.; Bachelder, E. M.; Fréchet, J. M. J. *Proc. Natl. Acad. Sci. U. S. A.* **2009**, *106*, 5497-5502.
(24) Bachelder, E. M.; Beaudette, T. T.; Broaders, K. E.; Dashe, J.; Fréchet, J. M. J. *J. Am. Chem. Soc.* **2008**, *130*, 10494-10495.
(25) Cohen, J. A.; Beaudette, T. T.; Cohen, J. L.; Broaders, K. E.; Bachelder, E. M.; Fréchet, J. M. J. *Adv. Mater. (Weinheim, Ger.)* **2010**, *22*, 3593-3597.
(26) Bachelder, E. M.; Beaudette, T. T.; Broaders, K. E.; Fréchet, J. M. J.; Albrecht, M. T.; Mateczun, A. J.; Ainslie, K. M.; Pesce, J. T.; Keane-Myers, A. M. *Mol. Pharmaceutics* **2010**, *7*, 826-835.
(27) Godbey, W. T.; Wu, K. K.; Mikos, A. G. *J. Biomed. Mater. Res., Part A* **1999**, *45*, 268-275.
(28) Grayson, A. C. R.; Doody, A. M.; Putnam, D. *Pharm. Res.* **2006**, *23*, 1868-1876.

(29) Liu, X.; Howard, K. A.; Dong, M.; Anderson, M. Ø.; Rahbek, U. L.; Johnsen, M. G.; Hansen, O. C.; Besenbacher, F.; Kjems, J. *Biomaterials* **2007**, *28*, 1280-1288.
(30) Shim, M. S.; Kwon, Y. J. *J. Controlled Release* **2009**, *133*, 206-213.
(31) Ren, Y.; Jiang, X.; Pan, D.; Mao, H.-Q. *Biomacromolecules* **2010**, *11*, 3432-3439.
(32) Reineke, T. M.; Davis, M. E. *Bioconjugate Chem.* **2003**, *14*, 255-261.
(33) Bhise, N. S.; Gray, R. S.; Sunshine, J. C.; Htet, S.; Ewald, A. J.; Green, J. J. *Biomaterials* **2010**, *31*, 8088-8096.
(34) Akinc, A.; Zumbuehl, A.; Goldberg, M.; Leshchiner, E. S.; Busini, V.; Hossain, N.; Bacallado, S. A.; Nguyen, D. N.; Fuller, J. E.; Alvarez, R.; Borodovsky, A.; Borland, T.; Constien, R.; de Fougerolles, A.; Dorkin, J. R.; Jayaprakash, K. N.; Jayaraman, M.; John, M.; Koteliansky, V.; Manoharan, M.; Nechev, L. V.; Qin, J.; Racie, T.; Raitcheva, D.; Rajeev, K. G.; Sah, D. W. Y.; Soutschek, J.; Toudjarska, I.; Vornlocher, H.-P.; Zimmerman, T. S.; Langer, R.; Anderson, D. G. *Nat. Biotechnol.* **2008**, *26*, 561-569.
(35) Tamura, A.; Oishi, M.; Nagasaki, Y. *J. Controlled Release* **2010**, *146*, 378-387.
(36) Wang, J.; Gao, S.-J.; Zhang, P.-C.; Wang, S.; Mao, H.-Q.; Leong, K. W. *Gene Ther.* **2004**, *11*, 1001-1010.
(37) Wong, S. Y.; Sood, N.; Putnam, D. *Mol. Ther.* **2009**, *17*, 480-490.
(38) Zhang, K.; Fang, H.; Wang, Z.; Li, Z.; Taylor, J.-S. A.; Wooley, K. L. *Biomaterials* **2010**, *31*, 1805-1813.
(39) Ou, M.; Wang, X.-L.; Xu, R.; Chang, C.-W.; Bull, D. A.; Kim, S. W. *Bioconjugate Chem.* **2008**, *19*, 626-633.
(40) Nguyen, J.; Steele, T. W. J.; Merkel, O.; Reul, R.; Kissel, T. *J. Controlled Release* **2008**, *132*, 243-251.
(41) Shim, M. S.; Kwon, Y. J. *Bioconjugate Chem.* **2009**, *20*, 488-499.